

HYDROGEOLOGIC CHARACTERIZATION OF A NEWLY CONSTRUCTED
SALINE-SODIC CLAY OVERBURDEN HILL

A Thesis

Submitted to the College of Graduate Studies and Research

In Partial Fulfillment of the Requirements

For the Degree of Master of Science

in the Department of Civil and Geological Engineering

University of Saskatchewan

Saskatoon, Canada

By

Denise E. Chapman

© Copyright Denise E. Chapman, September 2008. All rights reserved.

PERMISSION TO USE

In presenting this thesis in partial fulfillment of the requirements for a Postgraduate degree from the University of Saskatchewan, I agree that the Libraries of this University may make it freely available for inspection. I further agree that the permission for copying of this thesis in any manner, in whole or in part, for scholarly purposes may be granted by the professor or professors who supervised my thesis work or, in their absence, by the Head of the Department or the Dean of the College in which my thesis work was done. It is understood that any copying or publication or use of this thesis or parts thereof for financial gain shall not be allowed without my written permission. It is also understood that due recognition shall be given to me and the University of Saskatchewan in any scholarly use which may be made of any material in my thesis.

DISCLAIMER

Reference in this thesis to any specific commercial products, process, or service by trade name, trademark, manufacturer, or otherwise, does not constitute or imply its endorsement, recommendation, or favoring by the University of Saskatchewan. The views and opinions of the author expressed herein do not state or reflect those of the University of Saskatchewan, and shall not be used for advertising or product endorsement purposes.

Requests for permission to copy or to make other use of material in this thesis in whole or part should be addressed to:

Head of the Department of Civil and Geological Engineering,
University of Saskatchewan
Saskatoon, Saskatchewan S7N 0W0
Canada

ABSTRACT

Syncrude Canada Ltd (Syncrude) Mildred Lake operation is the largest producer of crude oil from oil sands mining in Canada. A saline-sodic clay-shale overburden known as the Clearwater Formation (K_c) must be removed in order to access the oil-bearing McMurray Formation (K_m). The potential concerns associated with the reclamation of overburden structures include shale weathering and salt release and migration, resulting in salinization of groundwater, surface water, and reclamation soil covers. South Bison Hill (SBH) is one example of a K_c overburden structure located at the Syncrude Mildred Lake Operation. The general objective of this study is to develop a preliminary conceptual/interpretative model of the hydrogeology of the newly reclaimed SBH at the Syncrude mine site.

A number of tasks were undertaken to meet this general objective. The first, and most important aspect of this study was to develop a geological model of SBH including pile geometry and depositional history of the hill. Secondly, to gain an understanding of the field conditions, a program was carried out over 2002 and 2003 to obtain pile physical characteristics. The geological model revealed that there are four main geological sections of SBH of different materials using different construction methods. The field data were used to verify the geological model, which illustrated the differences in hydraulic conductivities and geochemical signatures between the different sections.

All information was used to develop a simple steady-state numerical seepage model of SBH to be used as a tool to investigate the response of the water levels of SBH to variations in the model parameters. The model illustrated that groundwater flow is largely controlled by a more permeable section on the south side of SBH and an unstructured K_c fill at the base of the pile. A sensitivity analysis was conducted on the model changing the flux into the pile, the permeability of the materials, and most importantly the head value of the tailings facility located on the north side both showing to be influential on the elevation of the water table through SBH.

ACKNOWLEDGEMENTS

There are a number of people that need to be thanked for helping me throughout this journey. I would like to thank my supervisor Dr. Lee Barbour for his guidance, patience, and all the memorable hikes around the '30 Dump'. Thank you Syncrude Canada Ltd. for providing funding and equipment for my program. I would like to acknowledge Clara Qualizza Syncrude Canada Ltd. who always showed such enthusiasm and limitless support for myself and every other grad student that was fortunate enough to be able to work with Clara. Special thanks to Gord McKenna and Grey Kampala who were so helpful and generous, giving me their time and their knowledge of the '30 Dump'. Thank you Mike McKinnon at Syncrude Research, for analysing all water samples. Also thank you to Sophie Kessler and Heather Rogers who for all of their help, in particular collecting field data. Thank you to O'Kane Consultants for being so generous with allowing me time and use of their computer resources in order for me to complete my work. Thank you Laura Reifferscheid for all of your support and advice, you definitely helped keep me going!

Lastly, and most importantly, thank you to my family. My family was always there to lend help when I required some time and to give me encouragement when I needed it. To my husband Bryce, thank you for always being my rock I couldn't have completed this without you. To my children Addison and Owen, this is a testament to never give up on anything you do and more importantly never give up on yourself!

TABLE OF CONTENTS

CHAPTER 1	INTRODUCTION	1
1.1	Description of the Problem	1
1.2	Site Description.....	3
1.3	Research Objectives.....	4
1.4	Organization of Thesis.....	5
CHAPTER 2	BACKGROUND INFORMATION	6
2.1	Introduction	6
2.2	Hydrogeology and Reclamation	6
2.3	Geology of Syncrude Leases	7
2.3.1	Clearwater Formation.....	9
2.3.2	Summary of Clearwater Formation Properties.....	11
2.4	In situ Testing of Hydraulic Conductivity.....	12
2.4.1	Interpretation of Piezometer Recovery Data	14
2.4.2	Hydraulic Conductivity of Formations at Syncrude Mildred Lake Operation..	16
2.5	Summary.....	16
CHAPTER 3	MATERIALS AND METHODS	18
3.1	Introduction	18
3.2	Geological Reconstruction.....	18
3.3	Piezometer Network	19
3.3.1	2003 Drill Program for Additional Standpipe Piezometers	22
3.4	Water Level Monitoring.....	26
3.5	Rising Head Tests and Water Quality Sampling	26
3.6	Deep In situ Moisture Measurement.....	27
3.7	Seepage Rates	28
3.8	Summary.....	28
CHAPTER 4	PRESENTATION OF RESULTS AND DISCUSSION	30
4.1	Introduction	30
4.2	Description of the Construction of South Bison Hill.....	30
4.2.1	Construction Methods and Geology.....	30
4.2.2	Topography	35
4.3	Piezometer Water Level Measurements	36
4.3.1	Bills Lake; Surface Elevation 325 m (Location A)	37
4.3.2	Peat Pond – Surface Elevation 328 (Location B).....	38
4.3.3	S1 Dump – Surface Elevation 340 m (Location C)	40
4.3.4	Top South Side of SBH – Surface Elevation 350 m (Location D)	42
4.3.5	Top North Side of SBH – Surface Elevation 350 m (Location E).....	44
4.3.6	Bottom Slope Nest - 330 m Bench (Location F).....	47
4.3.7	Northwest Nest – 319.5 m Bench (Location G).....	49
4.3.8	North Nest – Surface Elevation 316.5 (Location H)	51
4.3.9	2003 Installation – Surface Elevation 320 m (Location I).....	53
4.3.10	2003 Installation – Surface Elevation 320 m (Location J).....	55

4.3.11	Key Trends of SBH Water Levels.....	58
4.4	In Situ Hydraulic Conductivity Tests	61
4.4.1	Summary of Measured and Collected Hydraulic conductivity Data for K _c Materials	64
4.5	Piezometer Water Chemistry.....	65
4.5.1	In Situ Chemistry of Syncrude Lease Areas	65
4.5.2	SBH Solids Chemistry	66
4.5.3	General Observations from SBH Standpipe Chemistry	68
4.5.4	Summary - Piezometer Water Chemistry.....	70
4.6	Investigation of Potential Flow Systems on SBH.....	70
4.7	In situ Moisture and Density using Neutron Probe	73
4.8	Seepage Indicators and Measured Seepage Rates.....	77
4.8.1	Seepage Stream Flow Rates	79
4.9	Summary.....	82
CHAPTER 5	CONCEPTUAL FLOW MODEL	85
5.1	Introduction	85
5.2	Purpose and Approach.....	85
5.3	Development of the Model Area	86
5.4	Boundary Conditions and Simulation Scenarios	88
5.4.1	Model Inputs and Assumptions	88
5.4.2	Steady State Analysis	88
5.4.3	Lift Construction.....	95
5.4.4	Model Limitations	97
5.5	Three Dimesional Modelling Program	98
5.6	Summary.....	98
CHAPTER 6	SUMMARY AND RECOMMENDATIONS FOR FUTURE RESEARCH	100
6.1	Conclusions	100
6.1.1	General Flow Patterns.....	101
6.1.2	Conceptual Model Results	102
6.2	Recommendations for Future Research.....	103
REFERENCES	105

List of Tables

Table 2.1 Geotechnical properties of <i>in situ</i> and rehandled overburden materials (Lord and Isaac, 1989)	12
Table 2.2 Hydraulic Conductivity values compiled for use in 1998 regional groundwater model (Synchrude, 2005)	16
Table 3.1 Details of piezometers installed in 1999 as part of initial hydrogeologic study at SBH	19
Table 3.1 Summary of additional boreholes drilled for the SBH drilling program, August 2003....	25
Table 4.1 <i>In situ</i> K of SBH materials organized by installation in S1 dump, limestone base, screen elevation below 320 m, and screen elevation above 320 m.....	63
Table 4.2 Summary of K values for SBH materials.	64
Table 4.3 Summary of standpipe chemistry.....	69
Table 4.4 Summary of piezometer characteristics showing perched water table conditions.	71
Table 4.5 Summary of piezometer characteristics installed around Peat Pond and Bill's Lake shallow wetlands.	72
Table 4.6 Summary of piezometer characteristics located at contact limestone base of SBH. ...	72
Table 4.7 Summary of piezometer characteristics in <i>in situ</i> K_m material.	73
Table 4.8 Summary of piezometer characteristics of piezometers showing artesian conditions in K_c fill.....	73
Table 4.9 Summary of different 'zones' as measured by density probe in deep access tube.....	75
Table 4.10 Measured and calculated values for K_c properties (Lord and Isaac,1989).	75
Table 5.1 <i>In situ</i> K values used in the SBH numerical model.	86
Table A1 Completion Details for South Bison Hill Piezometers.....	111
Table B.1 Major ion chemistry from South Bison Hill piezometers in 2002	116
Table B.2 Major ion chemistry from South Bison Hill piezometers in 2003	117
Table B.3 Major ion chemistry from Synchrude Lease Formations (Reszat, 2002)	118
Table B.4 Major ion chemistry anerobic solids chemistry from South Bison Hill neutron access tube installation (Wall, 2004)	119
Table B.5 Major ion chemistry oxidized solids chemistry from South Bison Hill neutron access tube installation (Wall, 2004)	120

List of Figures

Figure 1.1	Location of Syncrude Canada Ltd. Mildred Lake Operation.	2
Figure 1.2	South Bison Hill (SBH) looking south.	4
Figure 2.1	Cross section of regional geology of northeastern Athabasca oil sands region (Conly <i>et al.</i> , 2002).	8
Figure 2.2	Lithostratigraphy of Clearwater Formation found in Syncrude mining areas (from Isaac <i>et al.</i> , 1982).	10
Figure 2.1	Hvorslev piezometer geometry (Freeze and Cherry 1979).	15
Figure 3.1	Aerial photograph showing standpipe piezometer nests on SBH.	21
Figure 4.1	Plan-view drawing of as-built of SBH area in 1991 (left) and in 2001 (right).	31
Figure 4.2	Cross-section of SBH along 50200E (looking west) illustrating timeline and general construction materials for each stage (3x Vertical Exaggeration).	32
Figure 4.3	Cross-section of SBH along 50200E (looking west) illustrating construction technique for each stage (3x vertical exaggeration).	33
Figure 4.4	Cross-section showing piezometer nest at Bill's Lake (location A) on June 9, 2004.	37
Figure 4.5	Water level measurements for piezometer nest and pond water level at Bill's Lake.	38
Figure 4.6	Cross section showing water levels measured at piezometer nest at Peat Pond on June 9, 2004.	39
Figure 4.7	Water level readings from piezometers installed at Peat Pond.	40
Figure 4.8	Cross section showing water levels measured at piezometer nest on the S1 dump on June 9, 2004.	41
Figure 4.9	Water level readings for piezometers installed on the S1 Dump.	42
Figure 4.10	Cross-section showing water levels measured at piezometer nest on the located on the top south side of SBH (location D) on June 9, 2004.	43
Figure 4.11	Water level readings for piezometer nest installed on south top side of SBH.	44
Figure 4.12	Cross-section showing water levels measured at piezometer nest on the located on the top south side of SBH (location E) on June 9, 2004.	45
Figure 4.13	Water level readings from Location E nest located at north central portion of SBH.	46
Figure 4.14	WIP water level elevation compared to water level response of SP8A.	47
Figure 4.15	Piezometer nest at location F at surface elevation 330 m.	48
Figure 4.16	Piezometer nest at location F at surface elevation 330 m.	49
Figure 4.17	Cross-section of piezometer nest at location G at surface elevation on 319.5 m.	50

Figure 4.18 Water levels in piezometer nest at location G at surface elevation on 319.5 m.	51
Figure 4.19 Cross-sections of piezometer nest at location H (Figure 3.1) at a surface elevation of 317 m.	52
Figure 4.20 Water levels of piezometer nest at location H (Figure 3.1) at a surface elevation of 317 m.	53
Figure 4.21 Cross-sections of piezometers located at Location I (Figure 3.1) at surface elevation 320 m.	54
Figure 4.22 Water levels of piezometers located at location I (Figure 3.1) at surface elevation 320 m.	55
Figure 4.23 Cross-section of piezometers located at location J (Figure 3.1) at surface elevation 320 m.	56
Figure 4.24 Water levels of piezometers located at Location J (Figure 3.1) at surface elevation 320 m.	57
Figure 4.25 Photograph of SP4-2 showing ice protruding from standpipe November 2003.	57
Figure 4.26 Cross-section showing piezometers installed at the contact of Devonian limestone and K_c fill of SBH in relation to water level of WIP.	59
Figure 4.27 Water levels measured in piezometers installed in the Devonian limestone base and WIP water level elevation.	59
Figure 4.28 Cross-section of piezometers installed closest to lean oil sands pillar located north side of SBH.	60
Figure 4.29 Cross-section of piezometers installed closest to lean oil sands pillar located north side of SBH.	60
Figure 4.30 Graph of normalized head recovery versus time for SP011730-15 in 2002.	62
Figure 4.31 Frequency distribution of hydraulic conductivity values for fill materials below 320 m elevation.	64
Figure 4.32 Piper plot showing 'zones' of <i>in situ</i> formation standpipe chemistry (Reszat, 2002).	66
Figure 4.33 Piper plot showing 'zones' of oxidized and anaerobic shale and till samples from Wall (2004).	67
Figure 4.34 SBH standpipe chemistry (shown in symbols) compared to oxidized and anaerobic solid sample analysis (shown by shaded areas).	69
Figure 4.35 Volumetric water content measured with the neutron probe for October 2002 to August 2005.	74
Figure 4.36 Dry bulk density profile measured with the neutron probe for October 2005.	74
Figure 4.37 Range of placement saturation and volumetric water content compared to conditions measured at SBH in 2005.	76
Figure 4.38 Subsidence with changes in volumetric water content and saturation at SBH.	77

Figure 4.39. North side of SBH showing vegetation.....	78
Figure 4.40 South side of SBH showing lush varying vegetation.....	78
Figure 4.41 Seepage stream observed on South side of SBH.....	79
Figure 4.41 Flow rates measured from inlet and outlet pipes on south side of SBH in 2002 and 2003.....	80
Figure 4.42 S1 heads versus location (N-S) for various recharge rates using Dupuit analysis. ...	82
Figure 5.1 Model mesh through Section 50200 E used for the SBH steady-state seepage analysis.....	87
Figure 5.2 SBH steady-state seepage analysis for 0.4 mm/yr flux value.....	89
Figure 5.3 SBH steady-state seepage analysis for 4 mm/yr flux value.....	89
Figure 5.4 SBH steady-state seepage analysis for 8 mm/yr flux value.....	90
Figure 5.5 SBH steady-state seepage analysis for 20 mm/yr flux value.....	90
Figure 5.6 SBH steady-state seepage analysis for 8 mm/yr flux value and increasing S1 K value to 1.7×10^{-7} m/s.....	93
Figure 5.7 SBH steady-state seepage analysis for 8 mm/yr flux value and decreasing flux value to 0.8 mm/yr (2.8×10^{-11} m/s) over S1 dump surface.....	94
Figure 5.8 Steady state SEEP/W results increasing K value of upper Fill 1 materials to 1.7 $\times 10^{-9}$ m/s.....	96
Figure 5.9 Steady state SEEP/W results for increase in WIP to 315 m.....	96
Figure B1 – Plan view of area as of June 30, 1991.....	104
Figure B2 Section along 49344 E looking west.....	105
Figure B3 June 1991 topographic map showing section 49657E looking west.....	106
Figure B4 June 1991 topographic map showing section 49675 E looking west.....	107
Figure B5 June 1991 topographic map showing section 50425 E looking west.....	108
Figure B6 August 2002 topographic map showing section 49344 E looking west.....	109
Figure B7 August 2002 topographic map showing section 49675 E looking west.....	110
Figure B8 August 2002 topographic map showing section 50070 E looking west.....	111
Figure B9 August 2002 topographic map showing section 50200 E looking west.....	112
Figure B10 August 2002 topographic map showing section 50425 E looking west.....	113
Figure B11 August 2002 topographic map showing section 50765 E looking west.....	114
Figure D2 Permeability test for SP999904 in 2002 (Location D).....	122
Figure D3 Permeability test for SP999904 in 2003 (Location D).....	123
Figure D4 Permeability test for SP999907 in 2002 (Location E).....	123
Figure D5 Permeability test for SP011730-10 in 2002 (Location C).....	124

Figure D6	Permeability test for SP011730-12 in 2003 (Location C)	124
Figure D7	Permeability test for SP11730-14 in 2002 (Location G)	125
Figure D8	Permeability test for SP11730-15 in 2002 (Location G)	125
Figure D9	Permeability test for SP011730-16 in 2002 (Location G)	126
Figure D10	Permeability test for SP011730-16 in 2003 (Location G)	126
Figure D11	Permeability test for SP9999019 in 2003 (Location F)	127
Figure D12	Permeability test for SP9999019 in 2003 (Location F)	127
Figure D13	Permeability test for SP011730-20 in 2002 (Location F)	128
Figure D14	Permeability test for SP011730-20 in 2003 (Location F)	128
Figure D15	Permeability test for SP9999124 in 2002 (Location B)	129
Figure D16	Permeability test for SP9999124 in 2003 (Location B)	129
Figure D17	Permeability test for SP9999125 in 2002 (Location B)	130
Figure D18	Permeability test for SP9999125 in 2003 (Location B)	130
Figure D19	Permeability test for SP99990126 in 2002 (Location A)	131
Figure D20	Permeability test for SP99990126 in 2003 (Location A)	131
Figure D21	Permeability test for SP9999127 in 2002 (Location A)	132
Figure D22	Permeability test for SP9999127 in 2003 (Location A)	132
Figure D23	Permeability test for SP9999128 in 2002 (Location A)	133
Figure D24	Permeability test for SP9999128 in 2003 (Location A)	133
Figure D25	Permeability test for SP99990145 in 2002 (Location B)	134
Figure D26	Permeability test for SP99990145 in 2003 (Location B)	134

CHAPTER 1

INTRODUCTION

Alberta's oil sands contain over 170 billion barrels of oil, recoverable with today's current technology, making Canada second only to Saudi Arabia as the top oil resource country in the world (InfoMine, 2006). The Athabasca oil sands, located in the Athabasca basin of north eastern Alberta, Canada, is one of the most extensive shallow oil sands deposits in the world estimated to be twice the size of Lake Ontario (Syn crude, 2007). This deposit covers approximately 40,000 km² and contains over a trillion barrels of bitumen. Surface mining in this area is the primary method of recovery and is used to retrieve oil sand that is located under a maximum depth of 75 m of overburden. Surface mining is estimated to recover only 18% of the deposit with the remaining 82% extracted through *in situ* methods.

The production of oil sands can be loosely categorized into three main activities namely mining, extraction, and upgrading, each process having the potential to affect the environment in different ways. Environmental issues related to extraction and upgrading include air quality and the disposal of mine tailings and wastewater. Land disturbance is the primary environmental issue related to surface mining and can occur during exploration, site preparation, and active mining. Post-mining issues include land productivity and stability, surface and groundwater quality, and final land use. As the world's energy demands increase, fossil fuel suppliers are striving to create a balance between meeting these demands and conserving the environment. One way in which they can minimize the environmental impact of their extraction operations is through reclamation and environmental restoration.

1.1 Description of the Problem

The Syncrude Canada Ltd (Syn crude) Mildred Lake operation is located 40 km north of Ft. McMurray, AB (Fig. 1.1). This particular mine has the largest production of crude oil from oil sands, providing approximately 15% of Canada's energy requirements. Syncrude is the project operator of a joint venture among project owners Canadian Oil Sands Limited Partnership, Canadian Oil Sands Ltd., Conoco Phillips Oilsands Partnership II, Imperial Oil Resources, Mocal Energy Ltd., Murphy Oil Company Ltd., Nexen Inc., and Petro-Canada Oil and Gas. In addition to mining of oil sands, Syncrude operates a utilities plant, a bitumen extraction plant, and an

upgrading facility that produces Syncrude Sweet Blend (SSB), a value-added light sweet crude oil for domestic consumption and export. As of 2006, Syncrude had a cumulative crude oil production of 1.6 billion barrels while creating approximately 19,160 ha of land disturbance - 4,357 ha of which has been reclaimed. (Syncrude, 2007)



Figure 1.1 Location of Syncrude Canada Ltd. Mildred Lake Operation.

The oil-bearing formation is accessed by the removal of overburden, consisting of organic and glacial material, followed by removal of a deposit known as the Clearwater Formation (K_c). The K_c overburden consists of saline-sodic Cretaceous clay-shales. A detailed description of the background geology of the Syncrude lease areas is provided in Chapter 2. Shale overburden stripping at the Mildred Lake Operation generates approximately 120,000 m³ per day (40 million m³ per year) of this material. The surface organic and glacial materials are stockpiled so that they can be used for future reclamation. The K_c overburden is used as 'fill' placed in mined-out pits or onto the land surface as upland structures.

Overburden structures will account for about 80 km² of Syncrude's final landscape and half the oil sands mines in the region will have similar structures composed of comparable materials (McKenna, 2002). Potential concerns associated with the reclamation of structures comprised of saline-sodic overburden include shale weathering and salt release which may result in salt migration and salinization of groundwater, reclamation soils, and surface water.

1.2 Site Description

The Syncrude Mildred Lake Mine is located in the mixed-wood ecoregion in a northern temperate climate which is classified as being semi-arid, with an annual precipitation of 450 mm (approximately 30% as snow) and an annual potential evaporation of approximately 700 mm, with cold winters and moderate summers (McKenna, 2002). South Bison Hill (SBH) is one of six overburden piles constructed in the South Hills area at the southern edge of the Syncrude mine lease. Mining in this area commenced in 1977 and continued until 1997. South Bison Hill is the amalgamation of two overburden piles, operationally known as the S1 and the SW30 overburden hills. The S1 overburden hill was constructed on the surface and the SW30 was constructed in-pit. In total, SBH is approximately 2 km (E-W) by 1 km (N-S) and is comprised of fill materials approximately 50 m deep. A 'pillar' of lean oil sand situated in the northern edge of SBH was deemed uneconomic to mine and consequently was left in the mined-out pit and covered with overburden fill materials. A natural wetland known as Beaver Creek Reservoir is located to the south side of SBH and the north side of SBH is bounded by a mined out pit filled with mature fine tailings known as the West In Pit (Figure 1.2). SBH was reclaimed using different soil cover prescriptions, as determined by approved reclamation practises during time of placement, with final cover placement occurring in 2001. The final design of the top of the pile incorporated slopes and swales to create a free draining surface using a series of small watersheds. A description of the geological lithology, construction history, and topography of SBH can be found in Chapter 4, Section 4.2.

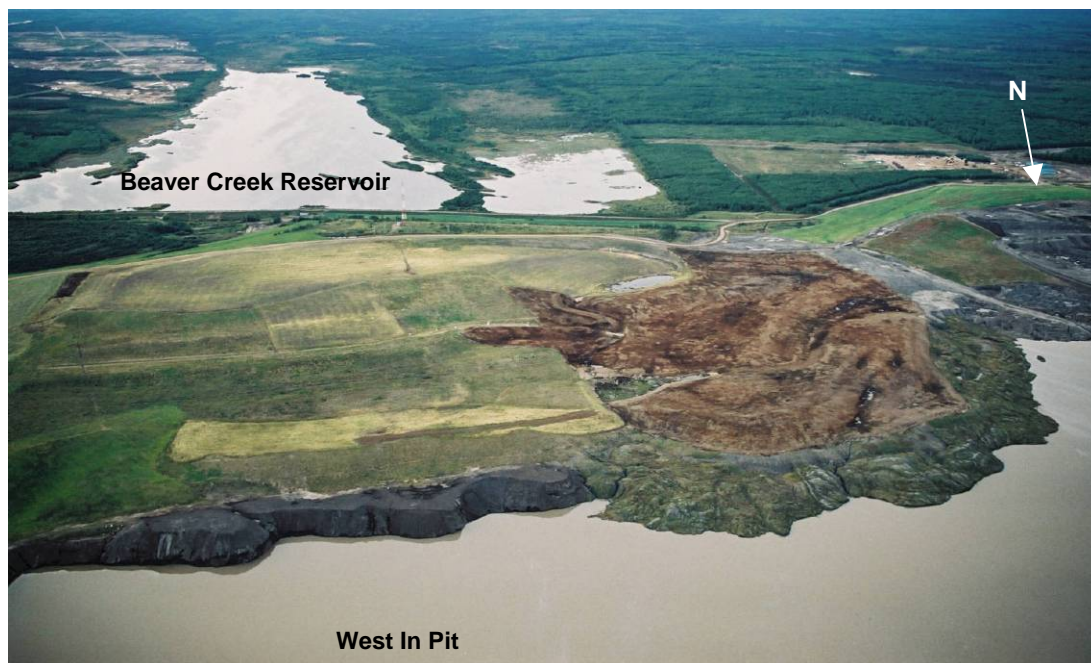


Figure 1.2 South Bison Hill (SBH) looking south.

1.3 Research Objectives

The groundwater flow system of a reclaimed landform constructed of saline-sodic K_c overburden is important to understand in order to determine the impact of shale weathering and the associated release of water and salts to uplands, wetlands, and groundwater systems. A completely new hydrogeologic system is forming within reclaimed overburden piles and the interaction of this system with surface soils and water bodies with respect to moisture and salt fluxes must be understood. In addition to salt release and transport, the behaviour of the groundwater system will also influence the structure's geotechnical stability. In the past, only small independent perched systems at the surface of these overburden landforms were expected, and the deep groundwater systems was not a primary reclamation concern because it was assumed that the low hydraulic conductivity of the shale would prevent excess pore pressures developing deep in the piles.

SBH is expected to develop a groundwater flow system because of the changes in the shale overburden properties as a result of mining disturbance. The development of SBH is the result of removing the geology, and hence the existing hydrogeology, from an area and then placing it in a highly disturbed state into another area which will ultimately alter material properties, including hydraulic conductivity of the shale. The general objective of this study is to develop a conceptual/interpretative model of the hydrogeology of a SBH, a newly reclaimed landform

composed of saline sodic overburden, at the Syncrude mine site. The methodology to achieve this objective will include:

- Development of a geologic model of SBH (geometry and depositional history) by analysis of aerial photos, maps, and mining records;
- Mapping the distribution of hydraulic head within SBH with time using transects of existing standpipe piezometers to gain an understanding of direction of groundwater flow, changes in hydraulic gradients, and identify discharge and recharge areas;
- Measurement of *in situ* hydraulic conductivity using the existing piezometer network to help to verify geological differences and to determine flow rates; ;
- Obtaining groundwater samples for major ion chemistry to validate consistency in construction materials and locate potential flow patterns;
- Installation and monitoring of additional piezometers to obtain hydrogeologic information near the north and south groundwater discharge areas; and
- Collection of any supplemental information regarding the groundwater flow movement within the overburden pile to support data collected during the research program.

Based on this information, a simple steady state two-dimensional conceptual/numerical model of the groundwater flow system of the overburden hill will be developed. This model will be used to investigate the fate of the water table as the water levels in the West In Pit begin to rise in response to mine closure activities.

1.4 Organization of Thesis

This thesis is comprised of the following six chapters. Chapter 2 provides a brief literature review looking at reclamation efforts on shale landforms, an overview of the background geology of the region and *in situ* properties of the materials. This chapter also outlines methods of measuring hydraulic conductivity through the use of *in situ* test methods. Chapter 3 provides an overview of the materials and methods used for the hydrogeologic investigation. Chapter 4 presents the data and develops a conceptual model of South Bison Hill. Chapter 5 illustrates this conceptual model using a two-dimensional numerical groundwater flow mode and Chapter 6 provides conclusions and future recommendations arrived at from this study.

CHAPTER 2

BACKGROUND INFORMATION

2.1 Introduction

A hydrogeologic investigation of any site involves interpreting information and observations regarding the interaction of soil and water as obtained from past and present conditions to predict the future behaviour of the groundwater system (Domenico and Schwartz, 1998). Hydrogeologic studies not only include groundwater supply and geotechnical investigations, but characterization of waste disposal sites, and evaluation of soil drainage for agriculture (Hendry, 1982). In the mining industry, hydrogeologic investigations are used primarily in exploration and in land reclamation.

2.2 Hydrogeology and Reclamation

Reclamation is a means of returning land that has been highly disturbed back to a productive state, but successful reclamation does require various engineering, environmental, and ecological problems be overcome. A unique aspect of large scale surface mining, such as that conducted in the oil sands, is that the entire pre-existing, hydrogeologic system is completely disturbed and will have to re-establish itself as an entirely new hydrogeologic system, subject to new geologic and boundary conditions. Large-scale reclamation can impact the regional flow system to such an extent that regional water levels change and groundwater flow patterns are modified. Jiao (2000) provides a summary of engineering and ecological examples that can be associated with rising groundwater levels and altering flow patterns along a coastline near Hong Kong due to reclamation for the purpose of urban development. Re-establishment of the groundwater regime following reclamation is a slow unsteady process due to changes in storage as placed overburden material re-saturates or consolidates, with the concomitant changes in hydraulic conductivity that accompany these processes (Jiao *et al.*, 2001).

Research on the reclamation of saline/sodic overburden has been conducted in the coal mining areas in the Northern Great Plains region of Canada and the USA. The most notable soil properties affected by rehandling of this type of overburden are water infiltration/retention and

the sodicity/mobility of soluble salts (Oddie and Bailey, 1988). Oddie and Bailey (1988) summarize how rehandled saline sodic overburden can disperse upon exposure to freshwater which causes a reduction in pore size, restricting the movement of air and water. A reduction in hydraulic conductivity at the spoil contact can result in perched water table conditions, aiding in the mobilization of salts. Mobilized salts can migrate to the overlying topsoil or be discharged into surface water bodies. Oddie and Bailey (1988), Merrill et al. (1985), Barth and Martin (1984), and Boese (2003) all examine how different thickness of top soil covers can improve reclamation over saline-sodic mine spoil. While these studies provide support for the depths of covers required to provide a suitable growth medium for the establishment of surface vegetation on saline sodic spoil material, there is limited knowledge of the deep hydrogeologic flow system that develops within structures of this type. Syncrude's current reclamation strategy for overburden landforms constructed of saline sodic overburden is to develop landscapes that include a vegetated uplands and isolated wetlands. Once regrading is completed, the overburden landforms are required be capped with 0.20 m of peat overlying 0.30 m of glacial till over 0.50 m of non-sodic soil (Boese, 2003).

2.3 Geology of Syncrude Leases

The regional geology of the Athabasca oil sand region has been studied extensively for exploration and development purposes (Flach, 1984). The Cretaceous McMurray Formation (K_m) in northeastern Alberta is one of the largest viscous bitumen deposits in the world contained within a quartz sandstone, commonly referred to as 'oil sands'. This formation was deposited approximately 130 million years ago in a tidal environment and sediments originated from successive deposition in fluvial, estuarine tidal conditions where tidal flats developed without strong waves (Wedage *et al.*, 1998). The McMurray Formation is underlain by shales and limestones of the Devonian Waterways Formation of the Beaverhill Lake Group and overlain by shales and sandstones of the Cretaceous Clearwater Formation. Overlying the Clearwater Formation is the Grand Rapids Formation that consists primarily of sandstone. A layer of spatially variable Quaternary deposits consisting of glacial, glacial-fluvial, and glacial lacustrine sediments are found above the Grand Rapids Formation. Figure 2.1 provides a cross-section of the oil sand area in northeastern Alberta (Conly *et al.*, 2002).

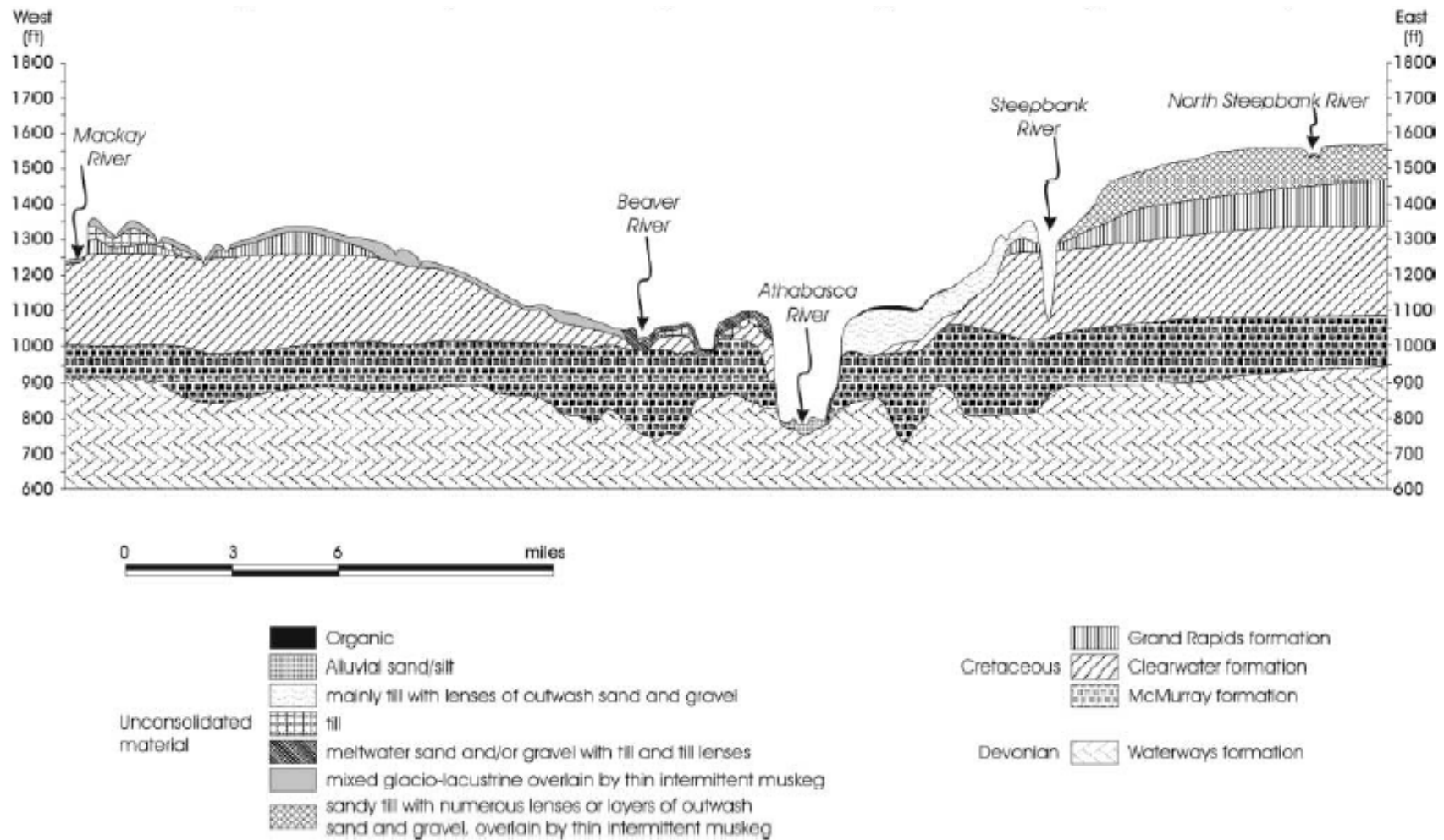


Figure 2.1 Cross section of regional geology of northeastern Athabasca oil sands region (Conly *et al.*, 2002).

Particular emphasis has been placed on the characterization of the geology of the oil-bearing McMurray Formation as it is the main focus of the economic development, particularly in recent years. This deposit can vary in thickness from over 150 m to zero where it pinches out at the western edge of the formation. The oil bearing formation can be found within 75 m of the surface in the areas north of Fort McMurray which has allowed surface mining to be used for extraction of the bitumen (Conly *et al.*, 2002). The texture of this formation is variable, ranging from shale, interbedded shale, sandstone, and bitumen impregnated sands. The McMurray Formation has been informally divided into three stratigraphic layers known as the Lower, Middle, and Upper McMurray based on depositional history. Each layer has some consistent features such as grain size and the presence or absence of fossils, however; the subdivisions have not been formalized because the units are not typically mappable (Gingras and Rokosh, 2004). Even though the oil sands are virtually uncemented, the bitumen found within the pore spaces is immobile at *in situ* temperatures and behaves more like a solid rather than a liquid (Conly *et al.*, 2002). Detailed descriptions of the geology of the McMurray Formation are provided by Hein and Cotterill (2006), Gringras and Rokosh (2004), Wightman *et al.* (1995), and Mossop (1980).

2.3.1 Clearwater Formation

The major overburden material that must be removed in order to gain access to the McMurray Formation is the Clearwater Formation (K_c). This is also the primary fill within the SBH. This formation is a widespread and somewhat uniform deposit containing uncemented clay-shales, clay-silts, and fine-grained sands with several thin indurated sandstones. The mine development plan is based on accurate knowledge of overburden material properties. The K_c has been found to contain fairly consistent signatures within its profile. Syncrude has used geophysical logs, core examination, and engineering and geologic tests to separate the K_c into seven subdivisions (Figure 2.2). These subdivisions are informal classifications given by Syncrude based on borehole logging responses that were characteristic of each division and only apply to Syncrude Leases (Isaac *et al.*, 1982). The following paragraphs provide a brief description of the characteristics of each division of K_c starting from the first unit overlying the K_m to the material surface.

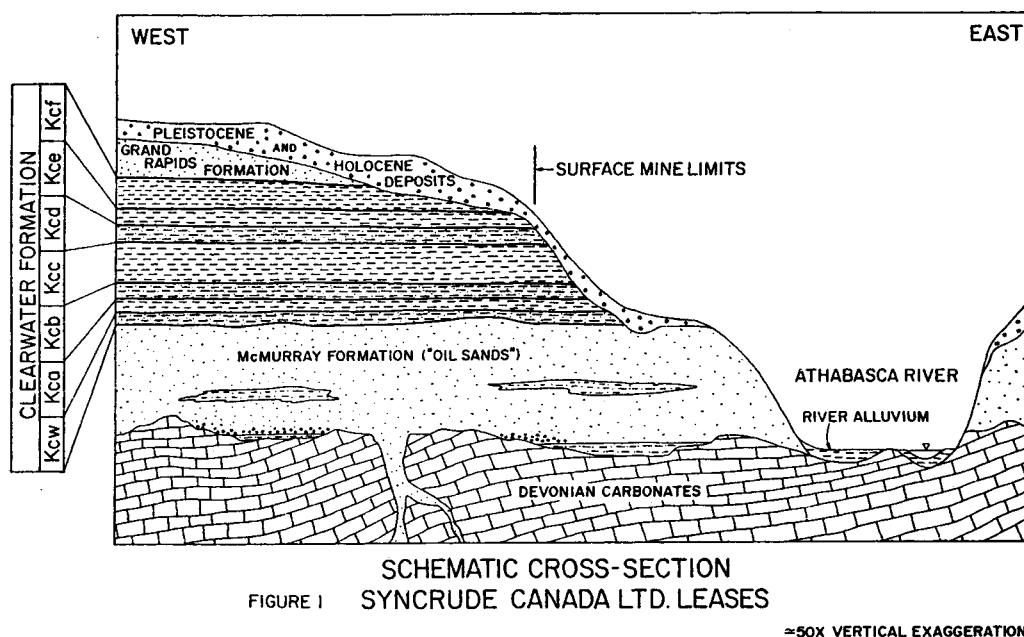


Figure 2.2 Lithostratigraphy of Clearwater Formation found in Syncrude mining areas (from Isaac *et al.*, 1982).

2.3.1.1 Wabiskaw Member

The Wabiskaw Member (K_{cw}) overlies the K_m formation with a thickness ranging from 3 to 5 m. This member is classified as being shallow-marine glauconitic interbedded fine grained sand with minor clay shale generally becoming more fine-grained moving upwards, ranging from bitumen saturated fine grained sand to silty clays. There is a small amount of bitumen stored within the K_{cw} layer, but is minor compared to K_m . Features include a mineral consisting of a dull green iron potassium silicate occurring in greensand with thick grey colored fissured clay shale (Wedage *et al.*, 1998). The mean clay content of K_{cw} is 23%. It is assumed that this is the original clay mineralogy, unaltered because of low temperatures and restricted groundwater flow due to low permeability. Because of the low permeability and high porosities, there is a high ability of the clay minerals within the K_{cw} to retain water during burial. This is particularly true for the smectite contained within this division.

2.3.1.2 K_{ca} Unit

The K_{ca} unit is found directly above the K_{cw} formation and ranges in thickness of 3 to 5 m. The K_{ca} member is a weak, highly plastic unit which is conducive to weakening by glaciotectionic deformation. This unit is dark grey clay silt in the lower portion to silty clay in the upper portion. This layer contains one laterally discontinuous siltstone. This unit is thinly laminated with some churned bedding in the silty zones. Mean clay content is approximately 50% (5% chlorite, 45% illite, 5% kaolinite and 45% smectite).

2.3.1.3 K_{cb} Unit

The K_{cb} unit overlies the K_{ca} unit and is approximately 4.5 to 6 m thick. This has a high clay content (60%) which is predominantly smectite, with a low bulk density (2.1 g/cm^3). This layer is interesting in that conventional gamma ray analysis would interpret this layer to be composed of silt size material due to the low potassium concentrations present in the smectite.

2.3.1.4 K_{cc} Unit

The K_{cc} unit is the thickest Clearwater Formation unit varying from 21 to 23 m thick. This unit consists of a light grey clay silt, with one low density zone, and six siltstone layers. This unit is well graded (1% sand / 61% silt / 38% clay) although there is considerable variation in grain sizes. This unit is found to have natural gravimetric moisture contents ranging from 18% to 27%, which correspond to *in situ* porosities of 36% to 50%. These porosity values are considered high when taking into account a stress pre-load of at least 15 MPa due to ice.

2.3.1.5 K_{cd} Unit

The thickness of K_{cd} ranges from approximately 9 to 13 m. This unit is the uppermost unit that will be surface mined. The K_{cd} unit is a glauconitic silty sand to clayey silt containing several siltstones. The mean natural gravimetric moisture content is approximately 20% corresponding to a porosity of about 40%. There have been two additional units identified however, these occur in areas of thick overburden where it is unlikely that surface mining will occur.

2.3.1.6 Pleistocene Formations

The mean thickness of Pleistocene formations in the Syncrude lease area is approximately 10 m. The major deposits are till, glaciolacustrine clays and silts, glaciofluvial sands, gravels, and organic deposits. These deposits are found overlying the upper McMurray or Clearwater Formation deposits, depending on the amount of glacial fluvial erosion.

2.3.2 Summary of Clearwater Formation Properties

In general, the overall mean sand / silt / clay contents of the K_c Formation is 6.5% sand, 53.0% silt, and 40.5% clay. Throughout the formation, there are subtle changes in clay mineralogy suggesting slightly different origins for the different units. Bulk density values as determined by geophysical bulk density logging show values greater than 2.4 g/cm^3 , indicative of well cemented siltstones, values lower than 2.3 g/cm^3 indicative of uncemented strata, and values less than 2.1 g/cm^3 indicative of low density shales usually high in smectite (Isaac *et al.*, 1982). A study conducted by Lord and Issac (1989) looked at the geotechnical

properties of dredged overburden that was transported in lump form and deposited in a number of study cells. A summary of the geotechnical properties of both *in situ* and rehandled Pleistocene and Clearwater formation materials are found in Table 2.1. It is interesting to note that the gravimetric moisture content between the *in situ* and rehandled K_c remains fairly consistent, even though there is a shift in the dry density. This suggests that rehandling K_c materials causes a decrease in volumetric moisture content and degree of saturation during mining activities

Table 2.1
Geotechnical properties of *in situ* and rehandled overburden materials
(Lord and Isaac, 1989)

Geotechnical Property	<i>In situ</i> Lacustrine Clay	<i>In situ</i> Till	Rehandled Clay-Till	<i>In situ</i> Clearwater	Rehandled Clearwater
Clay content (%)	18	NA	NA	11 - 40	43 - 64
Liquid limit (Yo)	29 - 45	21 - 24	-	37 - 53	64 - 79
Plastic limit (Yo)	12 - 26	10 - 11	-	18 - 25	22 - 28
Plasticity index	17 - 19	10 - 14	-	12 - 33	30 - 51
Gravimetric Moisture Content	16 - 32	11	14 - 19	16 - 25	17 - 25
SPT N (blows/305 mm)	14 - 29	14 - 84	11	15 - 75	17
Dry Density (kg/m ³)	1410 - 1710	1730 - 2040	1746 - 1889	1760 - 1780	1375 - 1645
Bulk Density (kg/m ³)	1860 - 2030	1950 - 2300	2074 - 2156	2070 - 2100	1700 - 2000

2.4 *In situ* Testing of Hydraulic Conductivity

The most important hydrogeologic properties of a soil are the ability to store and to transmit water. Aquifer hydraulic properties include hydraulic conductivity (both horizontal and vertical), storage coefficient (e.g. compressibility) and specific yield. Techniques such as that of a slug test, also known as bail tests, falling/rising head tests, or response tests, are commonly used to measure the *in situ* hydraulic conductivity in the immediate area of a small-diameter monitoring well. These tests involve an instantaneous change in the piezometer water level. The *in situ* hydraulic conductivity is then determined by observing the recovery in the piezometer water level with time. The recovery is then analysed using the appropriate analysis method. Slug tests have been recommended as a primary method of determining hydraulic conductivity, with laboratory tests used to supplement the field tests (Herzog and Morse, 1986).

The advantages to using rising head test include: obtaining *in situ* estimates while avoiding laboratory errors caused by sample disturbance or sample size, procedural simplicity and interpretation and cost effectiveness. (Freeze and Cherry 1979; van der Kamp 2000; Shaw and Hendry 1998; Hendry 1982). Herzog and Morse (1986) completed a study comparing laboratory and field hydraulic conductivity tests in fine-grained deposits from a waste disposal site in southern Illinois. Their test results showed consistency between laboratory tests and field tests, however; laboratory methods produced lower values of hydraulic conductivity by at least an order of magnitude compared to field methods. The differences in values were attributed to the small sample population and the destruction of the original structure of the materials, including any fractures present. However, the slug test method is only as effective as the piezometer and its installation. Incorrect installation methods can result in cross contamination, false piezometric levels, drawdowns, and incorrect hydraulic gradients, hydraulic conductivity, and groundwater seepage velocities computed from erroneous values of hydraulic heads (Chapuis and Sabourin, 1989) as a result of hydraulic short-circuiting. Other reasons why bail or slug tests may not provide accurate *in situ* hydraulic conductivity data are summarised by Wisconsin Department of Natural Resources (1993) as follows:

- Only the part of the aquifer immediately adjacent to the screen is evaluated;
- Only the uppermost part of the aquifer is tested in water table wells;
- Only a small part of the aquifer is tested when using piezometers since the screen and gravel pack are relatively short (2 to 3 m);
- The wells must be adequately developed to yield meaningful results;
- Results may be inaccurate depending if the well has intercepted a fracture, or has been installed to miss flow that may be occurring in secondary porosity channels.
- Highly permeable aquifers often yield artificially low results with this type of testing since the rate of induced flow/outflow from the aquifer is not instantaneous; and
- In the situation of the filter pack being less permeable than the surrounding formation, this type of test would yield a false result because it is only testing the filter pack. A screen slot size that is too low would yield the same result.

The main inadequacy of slug and / or bail tests is that the results are highly dependent on the effectiveness of the screened interval in allowing the free flow of water. Low measured values of hydraulic conductivity can be caused by corroded or clogged intake. Conversely, high measured values of hydraulic conductivity can be caused by creating a coarse medium around the intake by surging or backwashing prior to commencing the test (Freeze and Cherry, 1979).

2.4.1 Interpretation of Piezometer Recovery Data

A number of methods have been used to determine *in situ* aquifer parameters from slug or bail tests. A description of the following analysis methods can be found in Freeze and Cherry (1979) and Fetter (1994).

In general, most types of analyses assume that the aquifer is homogeneous and isotropic. The Cooper-Bredehoeft-Papadopoulos Method (1967) is used to determine the transmissivity (T) and storativity (S) of a confined aquifer that is completely penetrated by an open borehole or a well screen. This method considers the compressibility of water and the soil matrix. A value of K can then be calculated by dividing the transmissivity (T) by the thickness of the aquifer (b). The water level in the standpipe or well is changed with the addition or removal water, or by lowering a slug into the well. The ratio of measured head to initial head is monitored as a function of time. The results are plotted and matched to type curves to find values for T and S. Some limitations associated with this method include the difficulties in selecting the correct curve to use in the analyses, the applicability of the determined parameters to only the soil immediately surrounding the test hole, and the validity of the assumption of full aquifer penetration.

The Bower and Rice method (Bower and Rice, 1976) can be performed in partially or fully penetrating wells in boreholes or in screened wells. This method can be used in the case of both unconfined and confined aquifers providing that the top of the screened layer is some distance below the confining layer. A full description of this method can be found in Fetter (1994). Herzog and Morse (1986) found this method to be appropriate for tests conducted in moderate to low hydraulic conductivity soil as the test takes less than a day to run, is not affected by seasonal fluctuations, and barometric fluctuations are minimized.

The most widely used method for measuring *in situ* hydraulic conductivity was developed by Hvorslev (1951). The Hvorslev method is generally used for piezometers installed at a specific depth to monitor head and groundwater quality (Fetter, 1994) and is widely used as a way of interpreting piezometer field recovery data for both confined and unconfined aquifers (Freeze and Cherry 1979; van der Kamp 2000; Shaw and Hendry 1998; Hendry 1982). This method was initially used assuming that the aquifer was homogeneous, isotropic, and that both the water and the soil were incompressible.

The basis for this analysis is the concept that the rate of inflow (q) at the piezometer tip at any time t, is proportional to the hydraulic conductivity (K) and the unrecovered head difference (H-h) (Freeze and Cherry 1979). Based on this and Figure 2.1, we can derive the relationship given in Equation 2.1:

$$q(t) = \pi r^2 \frac{dh}{dt} = FK(H - h) \quad [2.1]$$

and smearing effects can be minimized by appropriate piezometer installation techniques (van der Kamp 2000).

2.4.2 Hydraulic Conductivity of Formations at Syncrude Mildred Lake Operation

Syncrude has conducted hydraulic conductivity testing at various locations on the Mildred Lake site for investigation and calibration of three-dimensional geological modeling. A compilation of the hydraulic conductivity values used in a 1998 regional flow model is found in Table 2.2

Table 2.2
Hydraulic Conductivity values compiled for use in 1998 regional groundwater model
(Syncrude, 2005)

	K_{\min} (m/s)	K_{\max} (m/s)	K_{geomean} (m/s)	Comment
Clearwater Formation				
Regional	1.0×10^{-9}	1.0×10^{-6}	1.5×10^{-7}	From drill stem tests
Mildred Lake	1.0×10^{-13}	1.0×10^{-10}		Summary of historical sources
Lean Oil Sand				
Regional	1.0×10^{-10}	1.0×10^{-5}		Summary of historical sources
Mildred Lake			3.0×10^{-7}	Calibrated 3D flow model
Mildred Lake			8.0×10^{-9}	Vertical hydraulic conductivity, calibrated 3D flow model
Aurora North			2.0×10^{-10}	Aurora pumping tests
Upper Devonian (limestone)				
Regional	1.1×10^{-11}	1.0×10^{-7}	3.2×10^{-10}	1992 Summary of historical sources
Mildred Lake			1×10^{-10}	1992 Calibrated flow model
Mildred Lake	7.0×10^{-10}	1.10×10^{-7}		1997 Slug tests

2.5 Summary

Past research in the reclamation of saline sodic mine spoils has been largely focused on establishing a successful near surface medium for vegetative growth with limited research into the impact of the reclamation on the deep hydrogeologic system that develops. South Bison Hill (SBH) at the Syncrude Canada Ltd., Mildred Lake operation, located north of Fort McMurray, Alberta is a reclaimed landform constructed of overburden consisting primarily of Cretaceous Clearwater Formation (K_c) from oil sands mining. In the Syncrude mining lease area this formation is estimated to be 75 m thick. Syncrude has informally divided the K_c into different units based on differing *in situ* material properties. The *in situ* material properties will be compared to properties measured at SBH during the field program to help to understand and predict the flow patterns within SBH. Slug or bail tests conducted in the field are a practical method of estimating hydraulic conductivity using standpoint piezometers. The type of analysis used to determine hydraulic conductivity depends on the type of aquifer

and well. The reliability of results depends on piezometer construction methods, sufficient well development, proper test design, and appropriate analysis procedures.

CHAPTER 3

MATERIALS AND METHODS

3.1 *Introduction*

The development of a conceptual model of a hydrogeologic system relies on four general types of information: topography, geology, hydraulics (e.g. hydraulic heads and hydraulic conductivity) and chemistry (Freeze and Cherry 1979). This same type of information had to be collected to develop a conceptual hydrogeologic model of South Bison Hill (SBH). The main task included characterization of the geology and topography of the newly constructed landscape. Since SBH was an overburden dump area, an investigation of company records was necessary to obtain information on the re-constructed geological stratigraphy of this area. An initial piezometer network was installed in the overburden hill. A field program using this piezometer network was undertaken to measure standpipe piezometer water levels, conduct *in situ* hydraulic conductivity tests, and obtain water samples. Piezometers were installed late in 2003 to try to supplement the existing network. An access tube for measurement of volumetric water content using a neutron moisture gauge was installed in 2003 to a depth of 20 m. Field reconnaissance was also utilized to identify any areas of groundwater discharge based on the presence of springs, salinity or similar chemical precipitates and phreatophytes.

3.2 *Geological Reconstruction*

One of the most important controls on hydrogeologic systems is the lithology, stratigraphy, and structure of the geologic formations (Freeze and Cherry, 1979). Since the SBH was operationally an overburden dump, a complete detailed summary fill placement during hill construction did not exist. The geological stratigraphy of the hill was put together by a comprehensive investigation of topographic maps, air photos, haul records, and personal communication with site engineers, hydrogeologists, and operators (McKenna, G., geotechnical engineer, R. Cameron, geotechnical engineer and G. Kampala, hydrogeologist, personal communication, 2002). The hill had to be conceptually 'reconstructed' over time using the site maps and air photos. Haul records were used to determine the types and origins of the materials. Drilling logs from exploration boreholes and standpipe piezometers installed on SBH (Section 3.3) were also used to verify the types of materials used at

different locations in the hill. Physical properties for the fill materials were obtained from records of material testing undertaken by Syncrude. All data was organized to develop a conceptual geological model of SBH.

3.3 Piezometer Network

Groundwater investigation at the SBH began initially with the installation of two piezometer nests installed at two shallow wetlands, Bill's Lake (Location A, Fig. 3.1) and Peat Pond (Location B, Fig. 3.1). The piezometer installations were completed by Syncrude in the fall of 1999 using a mud rotary rig operated by Layne Christensen Company (Layne). A total of seven standpipes were installed at this time, three at the Bill's Lake location and four at the Peat Pond location. The installation was a part of a pilot project initiated by Syncrude to investigate 'time zero' conditions following hill construction and to get an estimate of the costs and challenges involved in drilling overburden sites. The seven piezometers were installed at three different target depths: shallow (~5 m), medium (10 – 20 m), and deep (~ 40 m). Drilling was found to be routine. From the initial water level readings, it was concluded that SBH contained more free water and was more permeable than expected. (McKenna, personal communication 2000) The piezometers were bailed and a rising head test was completed on five of seven piezometers in the spring of 2000. Details of the piezometers installed in 1999 are found in Table 3.1

Table 3.1
Details of piezometers installed in 1999 as part of initial hydrogeologic study at SBH

Peizometer ID	Approx. Midpoint Elev. of Screen (m)	Elevation of Ground Surface (m)	Materials	K (m/s)
SP990123	315.1	327.6	K _{ca} ; Dry / hard dark grey shale	N/A*
SP099124	323.6	326.9	N/A	2.5 x 10 ⁻⁸
SP099125	317.6	327.21	N/A	2.1 x 10 ⁻⁹
SP099126	311.9	325.8	K _{cw} /K _{cc} /K _{cd} ; Dry to moist; med to fine grain silty sand with glauconitic shale/dark brown to black	
SP099127	321.1	324.9	N/A	2.5 x 10 ⁻⁸
SP099128	316.9	325.4	N/A	1.8 x 10 ⁻⁸
SP099145	288.5	328.4	N/A	N/A

N/A – Data not available

As a result of these findings, an additional 25 piezometers were installed in the spring of 2000 to investigate whether a groundwater regime was developing or whether the measured piezometric surfaces were influenced by the nearby water bodies. Six locations along a north/south transect through the centre of the hill were selected with depths depending on



Figure 3.1 Aerial photograph showing standpipe piezometer nests on SBH.

the anticipated lithology of the hill as controlled by construction and varying basal geology. (The locations of all piezometer nests are denoted by letters are in Figure 3.1).

All piezometers installed at this time consisted of 5.08 cm OD (2") schedule 80 PVC pipe with threaded fittings. The screen consisted of 2 mm PVC slotted screen with a sand pack of standard frac sand was around the screen. A bentonite seal, consisting of bentonite pellets at some locations and a grout mixture at others, was placed above the sand pack to the ground surface. Completion details of the piezometers at each nest are found in Appendix A.

3.3.1 2003 Drill Program for Additional Standpipe Piezometers

The existing piezometer network gave a general idea of the groundwater flow regime; however, it was decided that the network needed to be supplemented at specific locations and depths. Syncrude approved thirteen additional piezometers and installation began in August 2003 using a mud rotary rig operated by Layne, the same contract drilling company that installed the previous piezometers. The first installation of the new network took place on the top of the hill (350 masl) on the eastern corner (Location K, Fig. 3.1). A nest of piezometers at depths of 10 m, 30 m and 80 m were to be installed at this location. The 80 m pipe was to reach the undisturbed basal material at the base of the pile.

The 10 m and 30 m pipes were installed without difficulty with the same materials (pipe, screen, and sand) as used in the previous installations. Samples of cuttings were collected from the drilling mud every 1.5 m depth using a strainer and the bottom 3 m of the borehole was cored. The cuttings were rinsed so that the borehole profile could be logged. The 10 m and 30 m holes were completed with standpipe piezometers. The 90 m hole was attempted, but drilling could not advance past the 30 m depth. The driller was of the opinion that the hole squeezed off and as a result there was a loss of mud circulation and the piezometer could not be completed.

There were additional concerns with the 10 m and 30 m piezometers installed at this location. The holes were not grouted immediately following installation and the pipes were not air lifted to clean the standpipes. A grout truck was taken back to this location the day after installation but the clay overburden had squeezed in around the pipe and the grout hose was not able to reach the bentonite layer just above the sand pack, thus compromising the integrity of the piezometer. It was deemed that these two pipes would not provide reliable data. The next location was located on the 320 m elevation bench (Location I, Fig.3.1) and a nest of three piezometers was to be installed at depths of 10, 30 and 60 m. The 10 m hole was drilled without problems and samples were collected in the manner outlined above. Prior to the standpipe installation, it was suggested that a grout hose be directly attached onto the pipe to insure that the grout would

completely seal the hole. The grout hose was attached onto the pipe and the annulus was grouted with a 5:1 bentonite-cement mixture. The driller attempted to pull the hose immediately after grout placement and the standpipe was pulled out of the ground approximately 0.3 m. This makes the integrity of the sand pack questionable and data from this standpipe must be closely monitored. A 30 m hole was drilled the following day with no problems and grouted immediately. Both the 10 m and the 30 m holes were air lifted by the drill rig to clear out any excess mud. During drilling of the 60 m hole the operator was once again unable to drill below a depth of 30 m due to what was felt to be a loss of circulation as a result of the hole squeezing in.

The rig was moved directly east of the last location but still on the 320 m bench (Location J, Fig.1). Piezometers were installed at depths of 10 and 30 m without problems. This location seemed quite wet and had noticeably different materials, having mostly Clearwater Wabisaw member (K_{cw}) containing more sandy materials than at the previous locations. Water levels in both of these pipes recovered quite rapidly. A deep hole was not attempted at this location because arrangements were being made to get a hammer rig to finish the deep locations. A hammer rig from Beck Drilling and Environmental Services Ltd. was brought in to complete the deep wells and redo the holes that were not completed properly at the first location (Location K, Fig. 3.1). The hammer rig used solid 13 cm casing that was simply pounded into the ground. Samples could not be obtained using this method of drilling. The 10 m hole at the location on the top of SBH was completed successfully. A 40 m hole was attempted however a fuel line broke delaying the program a day. The rig was repaired and continued until approximately 30 m when the hammer hit something extremely hard. The driller commented that the bit might have been hitting metal as judged by the reaction of the hammer.

The top of SBH was quite wet and the reclamation material that was placed in the fall of 2002 was extremely soft. When the rig tried to pull the pipe out of the ground, the back end sank easily into the surface. Lumber planks were placed under the back of the rig in order to provide support however due to soft soil conditions the lumber sank into the ground. A further 2 m of lumber was pushed into the ground without sufficient support being given to the back end of the rig. Rig mats were then brought in to provide additional support. A rig mat was obtained from Syncrude and had to be drug to the top of the hill and placed into position with a Cat. The single rig mat did not provide enough support for the rig and bent as a result. It was concluded that the pipe would have to stay in the ground until frost provided a stable surface layer. The rig was moved out of the area for fear of hitting anything out of the ordinary, in what was thought to be an old landfill site, and was set up using two rig mats placed on either side to support both tracks as well as the out riggers.

The drilling method was also a matter of debate. In clay materials, straight hammering did not seem to be the best option. The driller from Beck suggested using reverse air circulation (RC) to aid in the installations. This method uses double walled casing and air is pushed down the sides with the aid of an external compressor. Cuttings are then blown back through the centre pipe as hammering advances the casing. The cuttings are then collected in a cyclone where they can be gathered for sample analysis. The cuttings could be used for moisture contents because fluid was not involved in this drilling method. The RC method was approved and the program was put on hold for five days while new required drill pipe was transported.

The RC pipe arrived five days later and it took a complete day to set up the rig, two rig mats and a compressor rented from a company in Ft. McMurray. The location for this 80 m hole was changed to be approximately 100 m west of the previous location on the top of the hill in attempt to avoid the debris that may have been causing problems in the previous location. Drilling was accomplished with composite samples taken every 1.5 m until a depth of about 30 m. The top portion of the hole was becoming extremely tight and the driller decided that it would be best to pull out for fear of getting the pipe stuck. The Syncrude supervisor decided that the drilling should move to a different location since the top was extremely wet at this time and the likelihood of running into the same difficulty pulling up the pipe was very high.

The next location was on the 320 m bench (Location I, Fig. 1) where the deep hole had been attempted by Layne. A 60 m deep hole was attempted at this location to try and reach the base of the pit. Drilling and sampling took place to a depth of 30 m but the rig could not go past this depth because of a hard obstruction. The rig was then moved to the 320 m bench (Location J, Fig. 3.1) where two piezometers had previously been installed at depths of 10 m and 30 m (elev. 310 m and 290 m) and a 60 m deep hole was attempted. Once again, the hole could not be advanced past a depth of 30 m. Cuttings were collected up to this depth and were later used to measure moisture content. A summary of holes drilled in order of date of installation can be seen in Table 3.1 and piezometer completion details from the piezometers installed in 2003 are also included in Appendix A.

Table 3.1
Summary of additional boreholes drilled for the SBH drilling program, August 2003

Hole I.D.	Installation Date	Rig Type	Total Depth (m, elevation)		Piezometer Installed	Comments
2-1	Aug 21/03	Wet Rotary	10	340	Yes	Piezometer not useable because hole was not grouted properly.
2-2	Aug 21/03	Wet Rotary	30	320	Yes	Piezometer not useable because hole was not grouted properly.
2-3	Aug 22/03	Wet Rotary	30	320	No	Hole was to be 80 m but rig could not go past 30 m depth. Hole was squeezed or circulation was lost.
1-1	Aug 22/03	Wet Rotary	10	310	Yes	Piezometer was grouted but grout hose when grout hose was attempted to be pulled out, pipe came out as well; may have to watch.
1-2	Aug 24/03	Wet Rotary	30	290	Yes	Installed with no problems.
1-3	Aug 24/03	Wet Rotary	30	290	No	Hole was to be 60 m deep; could not get past 30 m because hole was squeezed or circulation was lost
4-1	Aug 24/03	Wet Rotary	10	310	Yes	Installed with no problems. Recovery was fast; water levels rose to ground surface level.
4-2	Aug 25/03	Wet Rotary	30	290	Yes	Installed with no problems, Water level rose to top of piezometer stick up; may have had influence of surface water.
2-4	Sept 17/03	Hammer	10	340	Yes	Complete with no problems.
2-5	Sept 19/03	Hammer	30	320	No	Attempted to a depth of 40 m but hit an extremely hard material. Problem pulling pipe out of ground because of extremely wet surface conditions.
2-6	Oct 1/03	Hammer/Reverse Air Circulation	30	320	No	Hole became extremely tight at this depth and driller pulled out for fear of losing pipe.
1-4	Oct 2/03	Hammer/Reverse Air Circulation	30	310	No	Hit hard material and could not go further.
4-3	Oct 3/03	Hammer/Reverse Air Circulation	30	310	No	Hit hard material and could not go further.

The August 2003 drilling program was not successful in completing the proposed installations. The maximum depth that could be reached using three different types of drilling methods was 30 m, even though the holes were attempted at different locations and elevations. Drilling depths greater than 30 m could not be reached in the initial 2003 installations. The problems experienced with the installations in 2003 in comparison to the installations conducted in previous

years may indicate that the material properties are changing. A drill program using alternative methods is still being considered by Syncrude in order to reach depths below 30 m.

The sodic clay shale that comprises this overburden landform and the wet conditions of the surface materials were the biggest challenges that had to be overcome for successful piezometer installation. Future drilling programs should be undertaken during winter months when the ground is frozen and therefore stable and when damage to reclamation would be less severe. Even though less than half of the proposed number of new piezometers were successfully installed, and none reached a depth past 320 m elevation, it was felt that the existing piezometers would still provide sufficient information regarding hydraulic conductivity and water quality to allow a preliminary interpretation of the hydrogeology to be completed.

3.4 Water Level Monitoring

Syncrude personnel were responsible for monthly water level measurements since the piezometers were installed in 1999. The University of Saskatchewan took over the measurements during the summer of 2002. Water levels were measured from the top of the piezometer casing using a standard Solinst® Model 101 Electronic Water Level Meter following the same monthly schedule as used previously up until the fall of 2004. Syncrude staff has since resumed their monthly schedule of water level reading.

3.5 Rising Head Tests and Water Quality Sampling

Rising head tests for hydraulic conductivity were performed on selected piezometers. Of the 31 existing pipes installed on SBH, 19 contained sufficient water for the rising head tests. The remaining pipes were generally less than 10 m deep and were dry or contained very small depths of water. These tests were conducted in August 2002 and June 2003 and followed ASTM standard D 4044-96 (ASTM 1996a). It was found that the water in a number of the piezometers were frozen in the early part of June 2003 so testing was completed as the pipes thawed. All tests were completed by July 9, 2003.

Water was removed manually from the pipes using 1L polyethylene Single Sample Bailers from Rice Engineering & Operating Ltd. The volume of water removed was dictated by the height of the water column originally in the pipe and by the amount needed to be taken in order to obtain a representative water quality sample. Samples for water quality were taken following guidelines found in ASTM standards D5903-96 (ASTM 1996b) and D4448-85a (92) (ASTM 1996c). As water was removed, the temperature and electrical conductivity was monitored using an YSI 600 Multi Parameter Water Quality Monitor probe connected to with an YSI 610 Terminal datalogger

from the Department of Civil and Geological Engineering Environmental Lab at the University of Saskatchewan. This probe measured temperature, conductivity, dissolved oxygen, percent oxygen saturation and pH. The pH was not monitored in the field since the pH sensor on this particular probe was out of commission. Once the temperature and conductivity stabilized, a sample was collected in a clean plastic bottle and was placed in cooler containing ice packs so as to keep them as close to ground temperature as possible. The samples were taken at the end of each day to the lab at the Syncrude Environmental Complex where they were filtered through a 0.45-micron filter and sent to Syncrude Research Labs in Edmonton where they were analysed for major cations and anions. A sample from the standpipe SP011730-12 located on the S1 section could not be sampled in 2002 due to a small blockage in the standpipe at a depth of 15 m. Water levels could be measured previously using the electronic water level meter, therefore the obstruction in the pipe may be caused by an irregularity in the pipe. A smaller polyethylene bailer (200 ml volume; 0.75" OD compared to 1.5" OD sampler used for all other samples) manufactured by RICE environmental technologies was used in 2003 and was able to bypass the obstructed section to obtain a water sample.

The rising head test was initiated immediately following collection of the water sample. As the bailer was taken out of the pipe containing the sample, the water level reader was placed back into the monitoring well and the water levels at various time intervals were recorded. Water levels were taken for up to four hours on the first day of the test and then at least once daily for approximately a week. Monthly measurements resumed for the remainder of the year.

3.6 *Deep In situ Moisture Measurement*

A neutron access tube was installed to a depth of 20 m below surface at the top of SBH in August 2002 to investigate changes in *in situ* volumetric water content deep in the pile over time. The access tube was installed in August 2002. Because of the depth of installation, standard material for the access tube such aluminum or galvanized steel (Bell, 1987) could not be used. Rather, carbon steel rods were used and were installed using a hammerhead drill rig supplied by Beck Drilling Co. Details of the access tube installation and the development of a calibration curve for the carbon steel access can be found in Wall (2004).

The first set of neutron counts were taken on October 2002 using a CPN Model 503 DR Hydroprobe. Readings continued to be taken bi-weekly through the summers of 2003, 2004, and 2005. Neutron counts were converted to volumetric water content using the material specific calibration curves developed for carbon steel. One measurement of *in situ* density was completed using a Troxler Model 3430 nuclear moisture/density gauge in October 2005.

3.7 Seepage Rates

A complete reconnaissance of the perimeter of SBH, particularly focusing on the north and south faces of the hill, was made on several occasions during the summer of 2002 and 2003. The base of both the north and south faces of SBH were observed for any indication of groundwater seepage on the slope faces which may have included a wet sheen or a wet zone on the slope, distinct changes in slope vegetation, daylighting groundwater seepage at the soil layer boundaries or at changes in the slope angle (Washington Department of Ecology, 2006). Vegetation can be a key ecological indicator of groundwater seepage and the associated groundwater chemistry and the chemical composition of the water can favour the growth of certain species. Cattail plants have been used as freshwater indicators in saline environments (Swanson *et al.*, 1984) acid-tolerant water lily species can indicate discharge of acidic groundwater (Klijn and Witte, 1999), and a study conducted in North Dakota showed that wild barley was dominant in low saline seepage areas, while Kochia was the dominant species in high saline seepage areas (Seelig, 2000). Wilson (1971) provides an extensive review of vegetation indicators of terrain conditions in Saskatchewan from a geotechnical engineering standpoint.

It was noticed that there was a small ditch running parallel to the main drainage ditch at the bottom of the south side of the hill that contained water for most of the year. The location of the small ditch can be seen in Figure 3.1. At certain points along this small drainage ditch, it appeared that there was a stream of rusty orange colored water meeting with a spring of clear water indicating that there may be seepage occurring from the base of the hill. A large pipe conveyed collected drainage water from the area west of South Bison Hill beneath the mine access road to the south side of South Bison Hill. A second pipe transfers this water and any water discharging along the south side of South Bison Hill to a sump located on the east side of the hill. The discharge rate through these two pipes was measured on a regular basis starting early July 2002 and samples of water were collected for chemical analyses. The difference between the flow rates was taken to be an estimate of the net groundwater discharge into the ditch. The water sample was handled in a similar manner to those from the piezometers. The measurements were quite sporadic throughout the two years of observation and thus these measurements were used as observations only.

3.8 Summary

This chapter has outlined the materials and methods used to collect the data required to develop a conceptual model of the hydrogeology of SBH. A thorough investigation of company records and field logs were used to develop a geological model of the hill. A field program was

undertaken during the summer of 2002 and 2003 to access information to determine physical characteristics of the SBH and to verify the geological model. The field program used existing standpipe piezometers to collect *in situ* hydraulic conductivity values and samples for water quality analysis. A drilling program was attempted in 2003, but only completed 6 of 13 proposed standpipes. Drilling for the six standpipes that were installed was unable to reach depths greater than 30 m. The problems with the drilling program in 2003 as compared to the drilling program in 1999 may indicate that the SBH material properties are changing with time.

CHAPTER 4

PRESENTATION OF RESULTS AND DISCUSSION

4.1 Introduction

This chapter presents and discusses data from the research program outlined in Chapter 3 as well as relevant data collected from related research programs. A detailed description of the geological stratigraphy of the hill built from topographic maps, air photos, haul records and personal communication is included. Water level data, measured *in situ* hydraulic conductivity, and water samples from standpipe piezometers are used to define groundwater flow patterns, material characteristics at each piezometer nest, and to verify the geological model. The results will be used to create a conceptual model of the hydrogeologic system developing in this newly constructed overburden hill.

4.2 Description of the Construction of South Bison Hill

4.2.1 Construction Methods and Geology

The SBH was constructed in an exhausted open pit over the period from 1980 to 1996. Fill placement can be separated in two phases based on elevation: below 320 m elevation and above 320 m elevation. This fill placement took place in roughly four stages over the years with final reclamation taking place in the summer of 2002. The final landform is estimated to cover an area of 85 ha with a volume of approximately 100 million cubic metres of K_c fill (McKenna, 2002). One of the main geologic features of the overburden hill is a pillar of lean oil sand, known as the SW Island, at what is currently the north side of SBH. The lean oil sand pillar is irregularly shaped, approximately 40 m high, 600 m (east-west), with an average width (north-south) of 300 m. Figure 4.1 shows the as-built topographic maps for the end of 1991 and ten years later in 2001. Figure 4.2 is a cross-section through section 50200 E (looking west) on which the chronology of the construction of the main segments of the hill is summarized. Figure 4.3 shows the same cross-section illustrating the construction method used to build each section.

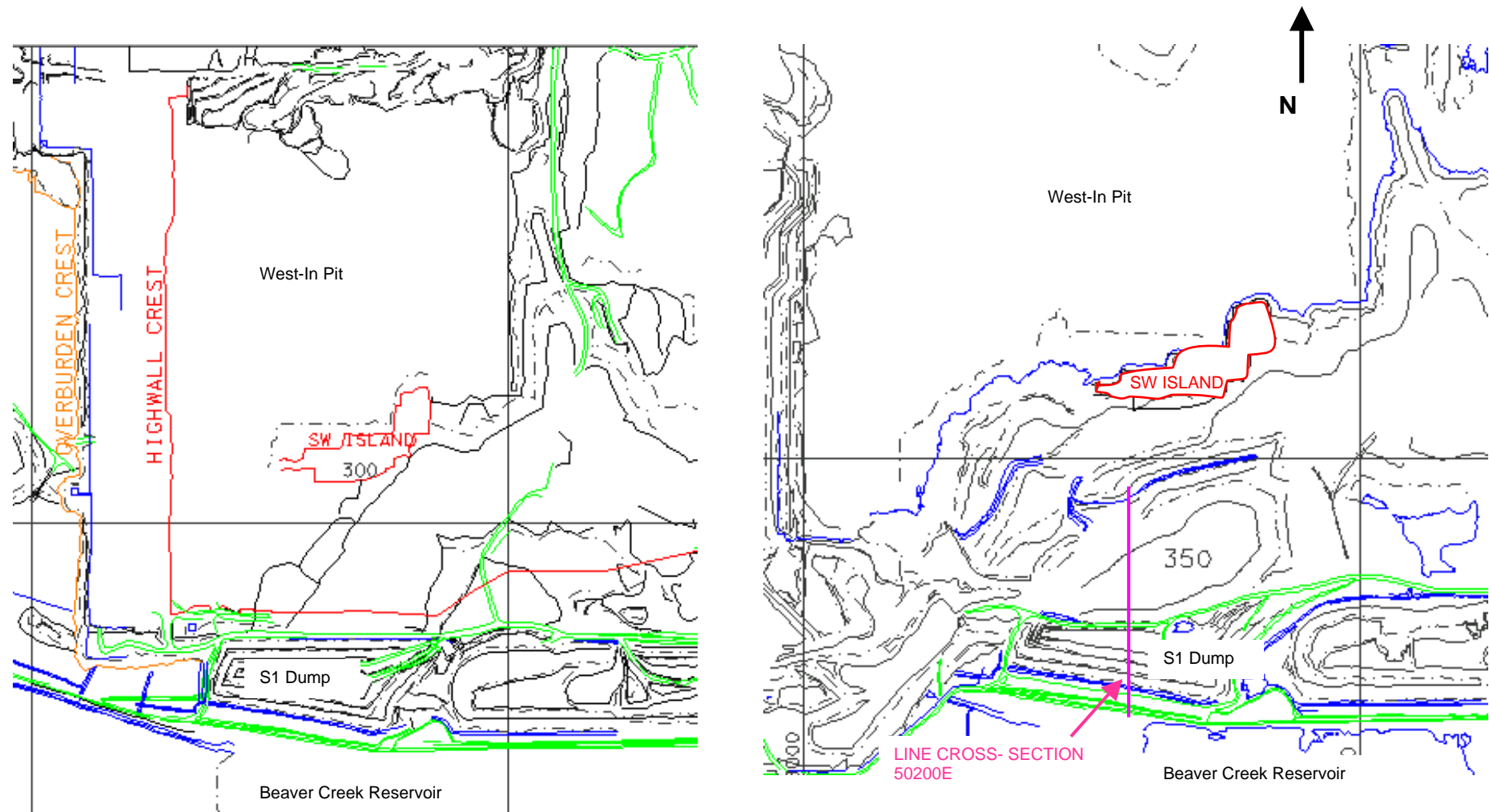


Figure 4.1 Plan-view drawing of as-built of SBH area in 1991 (left) and in 2001 (right).

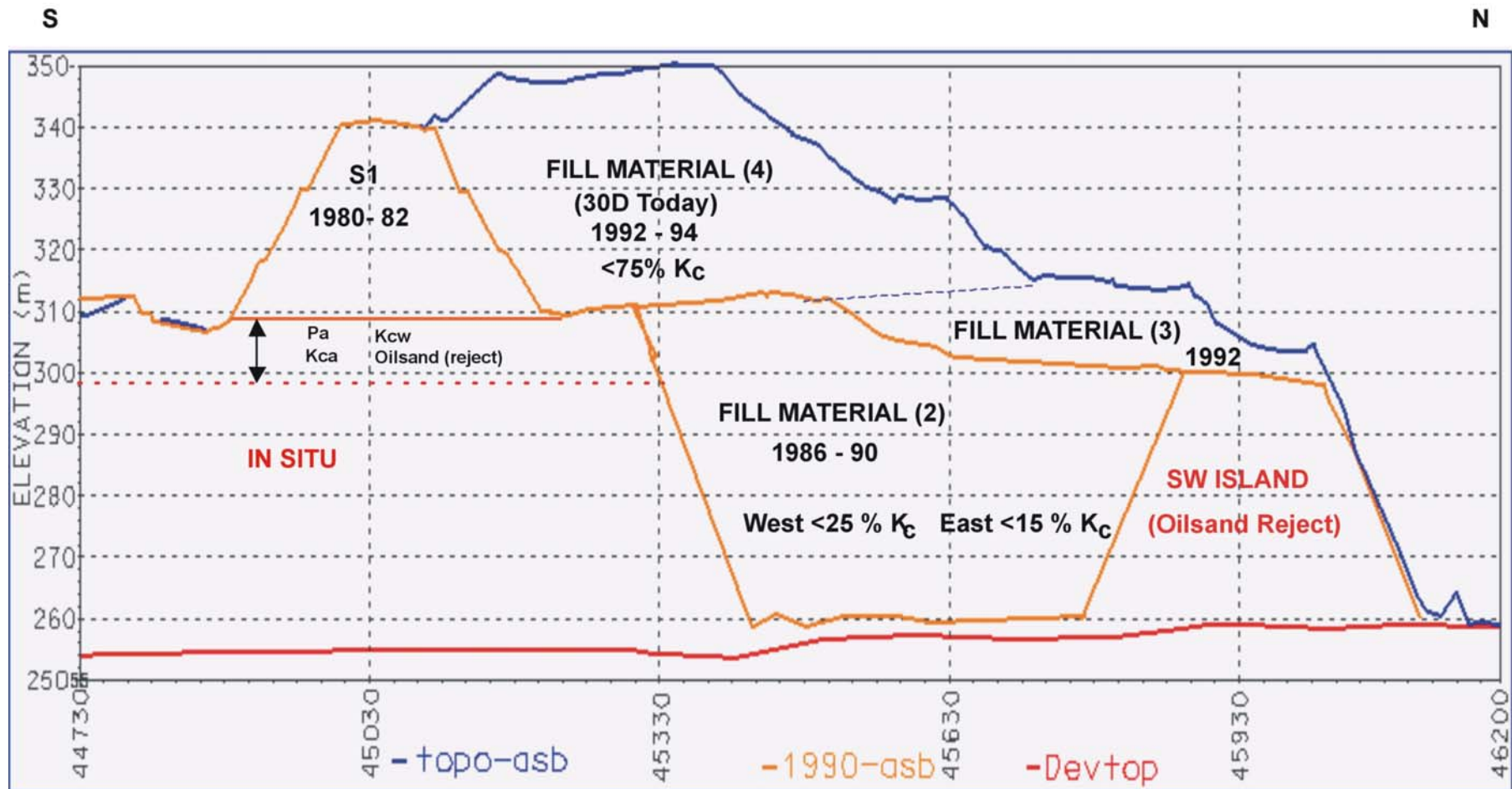


Figure 4.2 Cross-section of SBH along 50200E (looking west) illustrating timeline and general construction materials for each stage (3x Vertical Exaggeration).

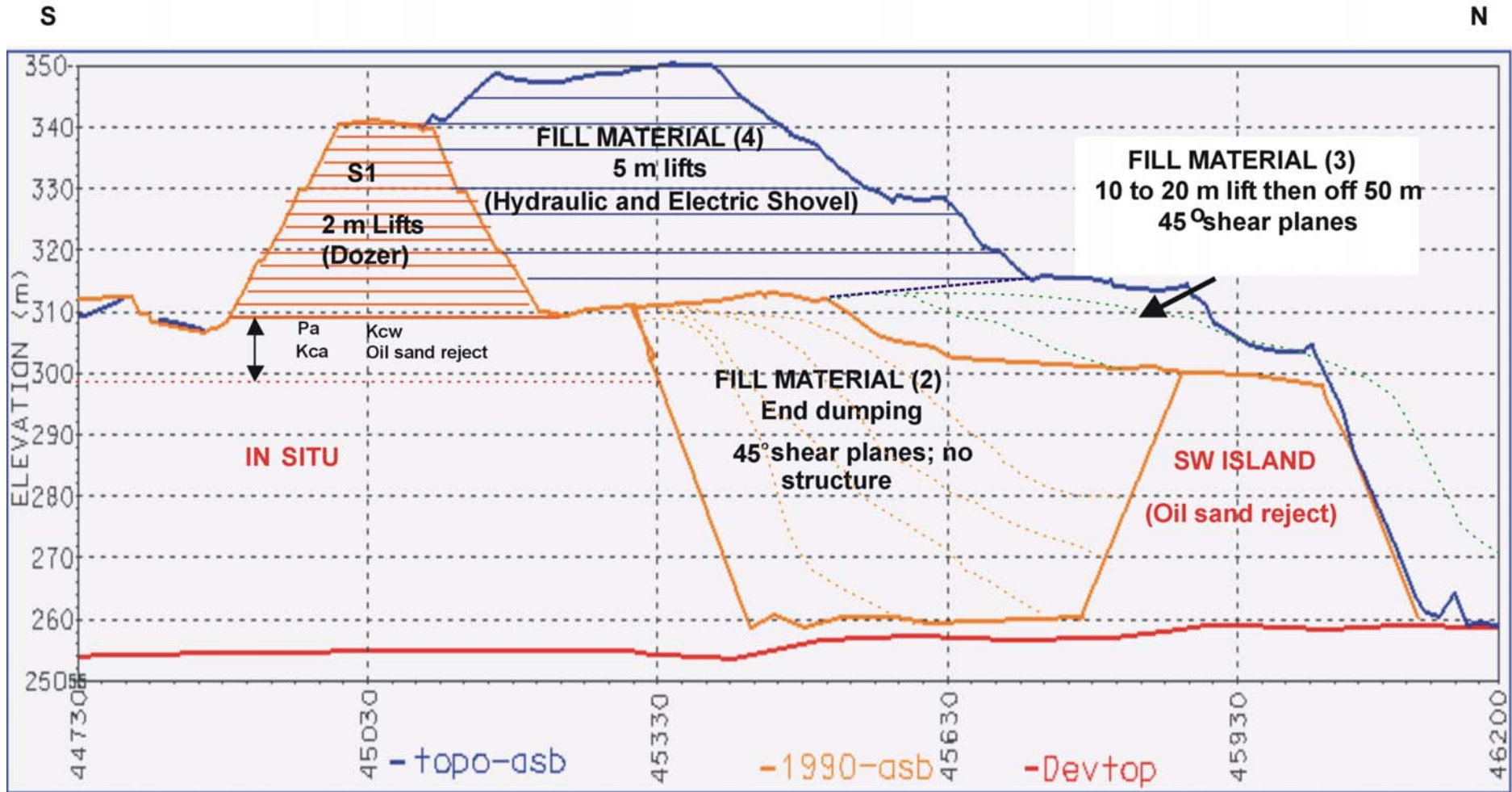


Figure 4.3 Cross-section of SBH along 50200E (looking west) illustrating construction technique for each stage (3x vertical exaggeration).

The first stage of construction is a surface dump known as the S1 dump. The S1 dump consists of mostly P_g and P_l tills with less than 10 percent K_c clays. The S1 dump has the highest percentage of glacial material as compared to the other sections of the hill because overburden was being hauled from a different section of the mine when S1 was being constructed. This portion of the dump was built in 2 m lifts by flattening formed benches with the use of dozers. With this method of placement it is likely that the values hydraulic conductivity in the vertical direction (K_v) are at least an order of magnitude lower than hydraulic conductivity in the horizontal direction (K_h) due to presence of distinct lifts and compaction horizons. The ratio of K_v/K_h for 2 m lift construction was estimated to be 10:1 based on field pit studies done by Syncrude (Lussier *et al.*, 2000 and Strueby, 1996).

The second stage of construction (Fill 2) consisted of 50 m end dumped fill. 'End dumped fill' in the case of the SBH construction refers to fill materials that were dumped or pushed off the ledge into the pit and did not receive additional compaction. The second stage of construction took place from 1986 to 1990. Fill 2 generally consists of a mixture of glacial materials combined with K_{ca} and K_{cw} with some lean oil sand (Syncrude 1999). The fill during this stage extended from the bottom of the pit, at approximately 260 m elevation to 320 m elevation. This type of construction results in an area where a distinct structure cannot be defined. It is estimated that layering may exist along angle of repose depositional slopes. These may provide the fill with an inclined, anisotropic, distribution of hydraulic conductivity and the layering may also provide potential shear planes and promote differential settlement.

The fill materials for the second stage of construction originated from overburden stripped from the southwest quadrant of Base Mine. The proportion of Clearwater Formation (K_c) in this fill is variable since the overburden became thicker as mining moved west. As a result, the east side of the dump has less than 15 percent K_c clays and the K_c proportion was greater than 25 percent on the west side of the pit.

The third stage of construction (Fill 3) was placed starting in 1992 and ending in 1994. The material in this area contains less than 40 percent K_c . The fill was placed as 10 to 20 m thick piles that were pushed off the bench and allowed to fall 40 to 50 m into the pit, resulting in an 'end-dumped' structure similar to that described above for Fill 2.

Construction of the final section (Fill 4) started in 1995 and was completed in 1996. Material of this section consists of a random mixture of materials with approximately 75 per cent being K_c (mostly K_{ca} , K_{cb} , and K_{cc}) and the remaining materials being K_m (low-grade oil sands) and small amounts of glacial tills. The section was constructed from approximately 320 m to 350 m elevation occurred at a time when most of the fill material that was considered to be "better" (e.g.

glacial material, K_{cw} , and lean oil sands) was salvaged for a dam construction project in a different area of the mine. A large portion of the material on the 320 m bench contains significant amounts of K_c either placed, or spilled from haul trucks (Syncrude 1999).

The Fill 4 materials are extremely variable with observations of cobblestones and boulders, known locally as siltstones (masses ranging from 1 kg to 100 tons), mixed randomly in the hill and accounting for approximately 1 to 5 percent by volume (Syncrude 1999). Heterogeneity within this fill can also be attributed to the type of equipment used during excavation. Mining was accomplished by both electric and hydraulic shovels during this time. This is significant in that the teeth on both the top and bottom of the hydraulic shovel resulted in a greater amount of material mixing as compared to the electric shovel.

The Fill 4 section was constructed in 5 m lifts. This type of construction is estimated to produce a hydraulic conductivity profile that was likely more variable than that noted for the 2 m lift construction. The top 2 m of each 5 m lift was found to be far denser than the bottom 3 m as a result of equipment traffic, with $K_v:K_h$ ratios of approximately 100:1 (Lussier *et al.*, 2000 and Strueby, 1996). In addition, a majority of hill construction was carried out during winter months and it is likely that layers of snow were trapped between layers. This may alter material properties by producing zones of increased saturation. McKenna (2002) sampled the surface of SBH materials just prior to capping to investigate the main index properties. The results showed that material at the surface was at its natural moisture content ranging from 9 to 21% gravimetric moisture content.

4.2.2 Topography

SBH received very little engineering design with minimal control of material placement and compaction (McKenna, 2002). The only design specifications that were controlled were the limitations on the overall slope angles, as this area was operationally known as a 'landform grading area'. The local topographic relief of SBH varies approximately 90 m from the base of the WIP (~260 m elevation) to the surface of the pile (~350 m elevation). After final construction, the slopes were pushed by dozers to 5V:1H or flatter. The final design of the top surface of SBH was bowl-shaped and incorporated slopes that were sculpted into shallow swales and ridges to create a free draining surface using a series of small watersheds. Consequently, the top surface received more compaction from truck and machinery traffic as compared to the rest of the dump. The deep flow system of SBH is expected to closely follow the topography. Small independent systems are also likely to develop as a result of the low permeability shale, designed channels and wetlands, and microtopography that has developed over time.

The methods of material placement left much of the material within SBH loose and fissured. This was expected to result in several meters of long-term subsidence, which was factored into the surface contour design. The hill is noted soon after placement to be moderately jointed due to the gaps between the large lumps and cracks caused by traffic and subsidence. Long-term subsidence on SBH is expected to be spatially and temporally irregular due to the overall variability in materials and construction techniques (McKenna, 2002). From studies conducted by Syncrude (Lussier *et al.*, 2000 and Strueby, 1996) the introduction of water of different chemistry may also affect the hydraulic conductivity of these types of clays. Any amount of meteoric water added to the system may also cause differential settlement and increased variability in material properties. It is important to realize that SBH was not fully vegetated until 2002 (different sections of SBH were reclaimed at different times) and therefore different amounts of meteoric water may have infiltrated and been stored within SBH over the years. This may lead to additional internal variability as a result of wetting, subsidence, and internal erosion or piping. The north side of SBH has not been fully reclaimed since the mature fine tailings storage facility, known as West In Pit (WIP) is eventually going to rise to a final elevation of approximately 310 m and be capped with an additional 5 m of fresh water prior to site closure when it will be known as Base Mine Lake (Syncrude, 1999). The elevation of WIP establishes an important total head boundary condition along the north side of the SBH hydrogeological system.

4.3 Piezometer Water Level Measurements

Water level measurements have been taken monthly at each of the seven piezometer nests since installation, depending upon accessibility. Two new piezometer nests installed in the summer of 2003 have been monitored regularly since installation. Each piezometer nest on SBH was designed to contain a 'shallow', 'mid', and 'deep' piezometer installed at depths that take into account any geological features that may be present at each location. Two sets of rising head tests (summer of 2002 and 2003) were performed on all piezometers that contained a sufficient amount of water for *in situ* hydraulic conductivity measurements.

Two figures are included for each piezometer nest location. A cross-section illustrates the geologic materials at each location along with the elevation of the bottom of the screen and the measured water level in each piezometer as of June 2004. A second figure shows water level measurements from 2000 to 2004. Any dry piezometers are represented in the figures by a small dashed line having no label markers. The elevation of each intake screen is provided in the brackets next to the piezometer designation in the figure legend.

4.3.1 Bills Lake; Surface Elevation 325 m (Location A)

Figure 4.4 shows an illustration of the cross section through the piezometer nest located on the south shore of a shallow wetland known as Bill's Lake, which has a surface elevation of approximately 325 m. All three piezometers at this location were installed along a north-south line in K_c fill material, which was constructed in 5 m lifts. Figure 4.4 illustrates the piezometer location, the elevation of the piezometer tips, and the piezometer water levels measured on June 9, 2004 relative to the measured pond elevation on that day. The closest piezometer to the pond SP99990127 (SP 127) is at a depth of approximately 5 m, followed by SP99990128 (SP128) at a depth of 10 m below surface, and SP99990126 (SP126) at a depth of 15 m below surface.

The water level in Bill's Lake has been measured manually using a staff gauge during non-frozen periods since 2000. In 2002, a pressure transducer/datalogger was placed in the pond by a research group from the University of Alberta to automatically record pond water levels. Readings from the pressure transducer were compared to manual readings and were found to be in agreement. In 2003, the pressure transducer for measuring the pond level was not operational for most of the season. The pond water levels shown are manual readings supplemented with pressure transducer readings where manual readings were not available, with the exception of 2003 where only manual readings were available.

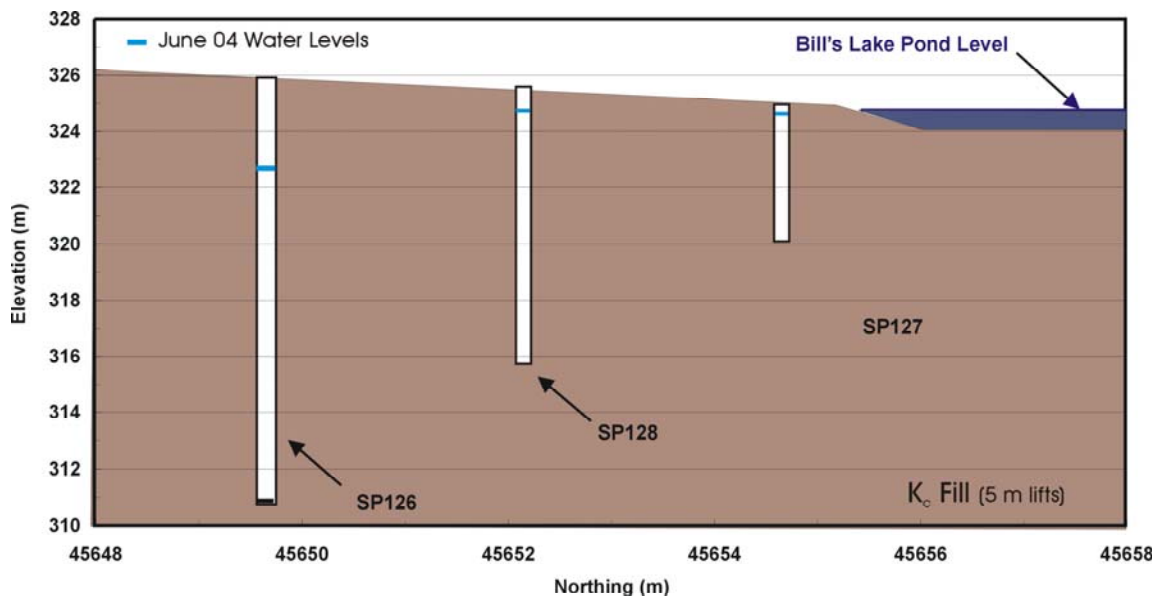


Figure 4.4 Cross-section showing piezometer nest at Bill's Lake (location A) on June 9, 2004.

Figure 4.5 shows the piezometer water level readings and pond level from March 2000 to June 2004. It appears from this figure, as though the water levels in this nest may be influenced by

the pond level, following seasonal fluctuations. This is especially apparent in the closest piezometer to the pond SP 127. Bill's Lake is largely recharged by surface snowmelt runoff and pond levels drop during the summer months. In 2000 and 2001, the level of Bill's Lake and the SP127 water level are approximately equal. During seasonal high water levels in the spring, the gradient suggests recharge from the pond into the shallow groundwater system. As the season progresses in each of these years the pond level drops and the piezometer levels rise suggesting the gradient reverses back towards the pond. This suggests that a localized flow system may develop near the pond which alternates between a recharge and discharge condition over the course of the year (Fetter, 1994). Piezometers SP128 and SP126 seem to follow the same general pattern, although for the majority of the monitoring period, the gradient directs water away from the pond indicating that it is a recharge area.

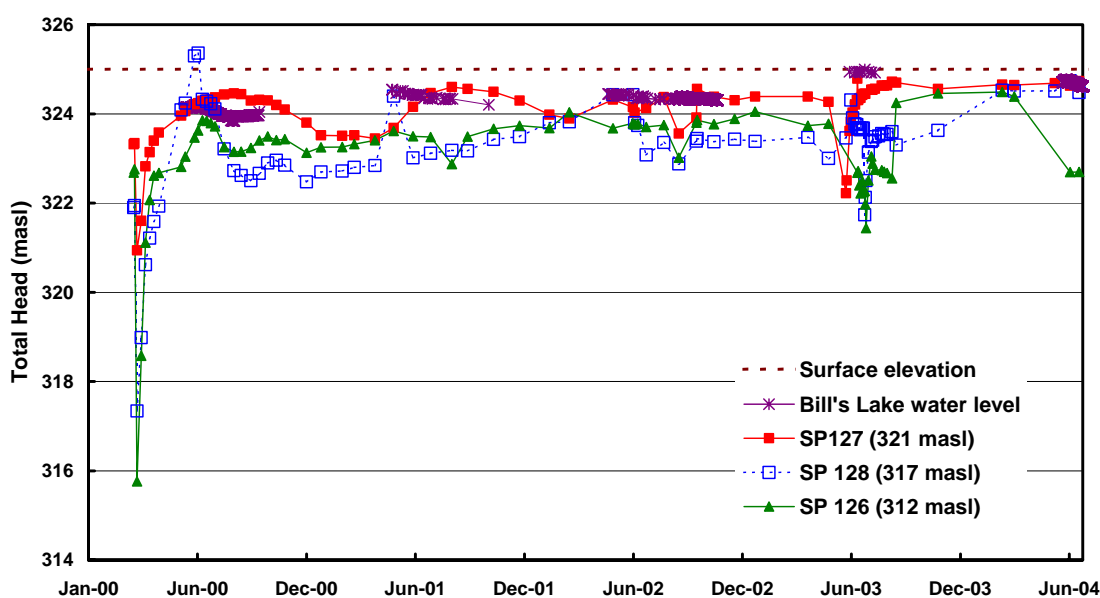


Figure 4.5 Water level measurements for piezometer nest and pond water level at Bill's Lake.

4.3.2 Peat Pond – Surface Elevation 328 (Location B)

The piezometers located on the south side of Peat Pond are shown in the cross-section provided in Figure 4.6. This pond is the first constructed wetland in the oil sands region and was the second nest of the piezometers installed in 1999. This nest consists of four piezometers aligned in a north-south orientation. This area of SBH was constructed of end-dumped fill. The deepest piezometer SP9990145 (SP145), at a depth of approximately 40 m below ground surface, is installed in lean oil sand that has not been mined. Piezometer SP09990123 (SP123), at a depth of approximately 13 m below surface, has contained an insignificant amount of water (<20 cm from the bottom of the pipe) since installation and has shown an increase in water level

of approximately one meter over the four-year measurement period, although the water level remains below the top of the screen. SP123 was one of the few piezometers that had a detailed borehole log. The drill logs described the materials in which this standpipe was installed as hard, dry K_{ca} material. SP99990124 (SP124), at a depth of approximately 5 m below surface, and SP99990125 (SP125), at a depth of approximately 10 m below the surface were installed in similar K_c material according to cross-sections found in Appendix B provided by Syncrude.

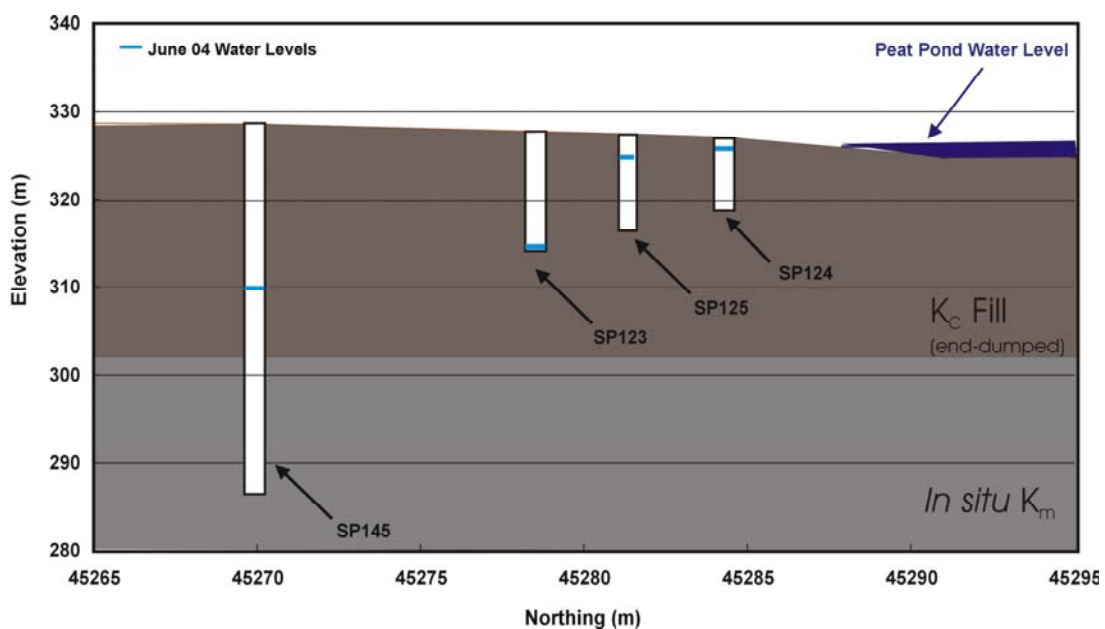


Figure 4.6 Cross section showing water levels measured at piezometer nest at Peat Pond on June 9, 2004.

Peat Pond water levels were measured using the same methods as those used at Bill's Lake. Manual readings using a staff gauge are presented for 2000. During 2001, the pond was being recontoured and additional reclamation material was being placed, consequently, the pond water levels were not measured. Pressure transducer readings began in 2002 and showed good agreement with the manual water level measurements. Pressure transducer readings are shown for the years 2002, 2003, and 2004.

Figure 4.7 shows the piezometer water level measurements since installation to the end of June 2004 with measured pond elevation. At the beginning of monitoring, SP125 had a larger head than that of SP124. This likely meant that when the pond was first developing, it was acting as a discharge area with recharge water from upslope. Over the 2000 season, SP125 water level gradually drops off. Water then moved down and away from Peat Pond indicating that the pond is now acting as a recharge area. This behaviour continues until the spring of 2003 where SP125 water levels recover to almost the same elevation as SP124. In 2001, the pond was recontoured as the top of SBH, inlet channel, and the area surrounding the pond was reclaimed.

Throughout reclamation of the pond and surrounding area, there was minimal water in the pond and water levels in the piezometers stayed relatively stable. In the spring of 2003, it was noticed that the outlet channel was blocking flow through Peat Pond allowing the surface water elevation to rise approximately 1.2 m, which is reflected by water levels in SP125 increasing by almost 7 m. The pond still remains a recharge area even with the change in the piezometer water levels. The deepest piezometer SP145 does not show the same trend as the other standpipes, reflective of a separate flow system. The water level of SP145 has decreased over the three years of monitoring indicating that draining of the *in situ* materials may be occurring or possibly a decrease in the hydraulic conductivity of the K_c materials is occurring reducing the amount of percolation to the underlying materials. The dry piezometer at this nest, SP123, show some evidence of perched water table conditions in the 5 m layered portion of SBH.

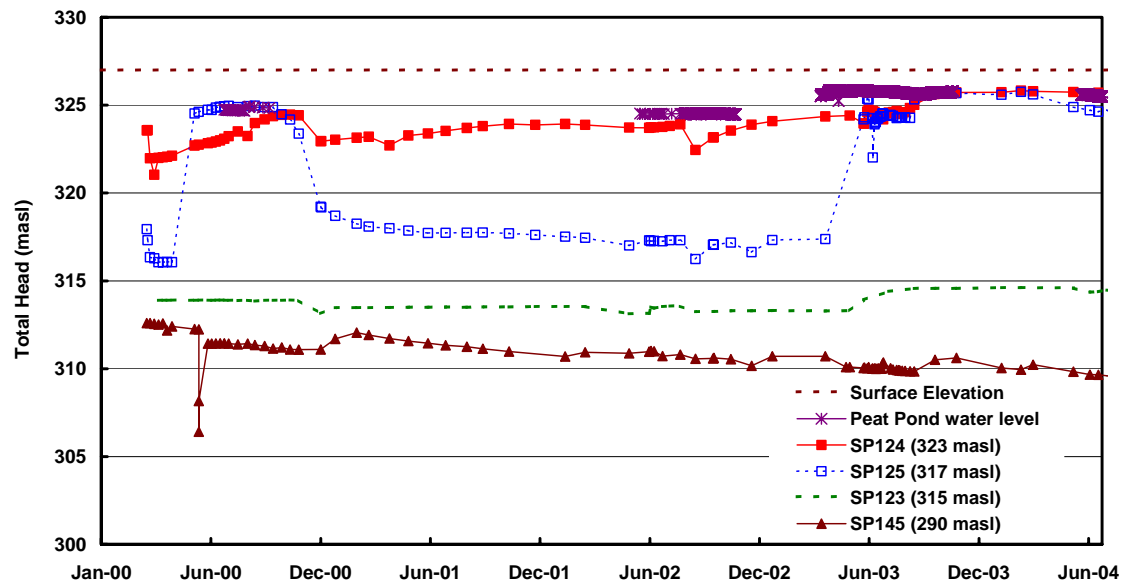


Figure 4.7 Water level readings from piezometers installed at Peat Pond.

4.3.3 S1 Dump – Surface Elevation 340 m (Location C)

Figure 4.8 shows a cross section of the piezometers installed on the S1 dump at a 342 m surface elevation (Location C, Figure 3.1). The S1 dump is constructed mainly of P_0 and P_1 tills in a 2 m lift assembly. Four piezometers in this location are installed in an east-west orientation at depths of 5 m, 10 m, 17 m and 63 m below the surface. Beaver Creek Reservoir, a natural wetland, is on the south side of the S1 dump and is at an elevation of 304 m.

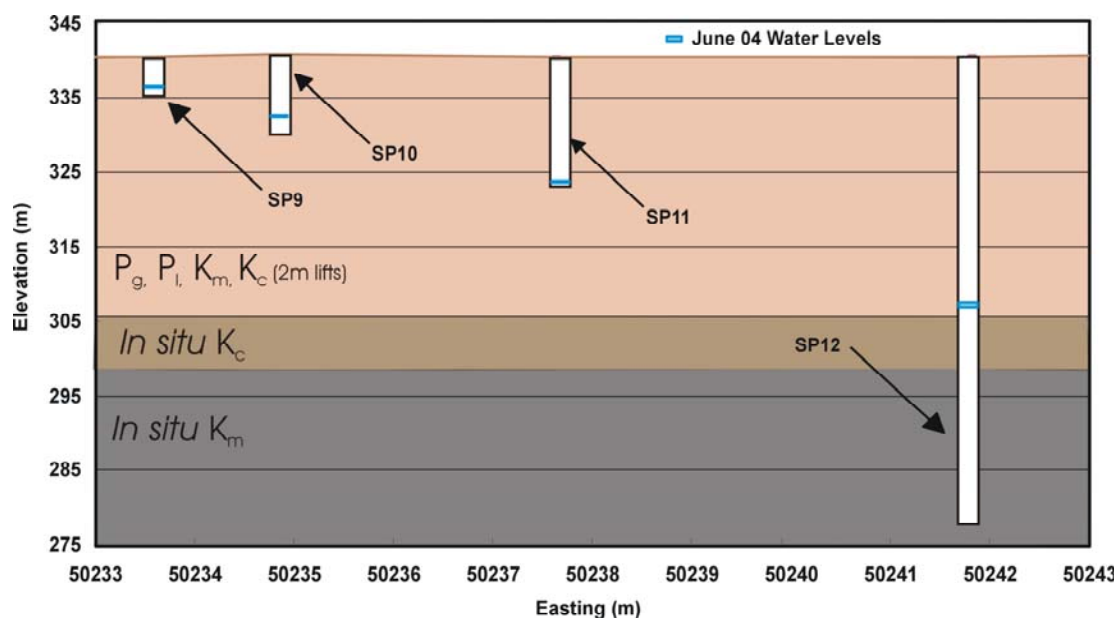


Figure 4.8 Cross section showing water levels measured at piezometer nest on the S1 dump on June 9, 2004.

Figure 4.9 shows the measured water levels for the piezometers at this location since installation. Water levels in the shallow piezometers in this nest (SP11730-09 (SP9), SP11730-10 (SP10), and SP11730-11 (SP11)) appeared to have stabilized rather quickly and have stayed as such. Piezometer SP11 was dry until 2004 where it shows a minimal increase in early 2004. The low-pressure heads indicate that the piezometer tips may be just at the water table or in a perched water table situation. Perched water table conditions are reasonable to assume given the lift construction methods and the clay shale materials, both creating lower hydraulic conductivity layers in the hill. Unconfined (e.g. perched systems) groundwater systems often have stable head readings with slow or gradual changes (Fetter, 1994). The deepest piezometer, SP011730-12 (SP12) whose tip is located in the *in situ* material below the constructed S1 dump shows that the measured water level is slightly above the *in situ* material and has decreased slightly over time, similar to SP145 installed in the *in situ* material at Peat Pond. Placement of the materials above the *in situ* material may have caused pore pressures to initially rise during construction and they may be now gradually dissipating. The water level in this piezometer may also be influenced by the Beaver Creek natural wetland located to the south at an elevation of 304 m.

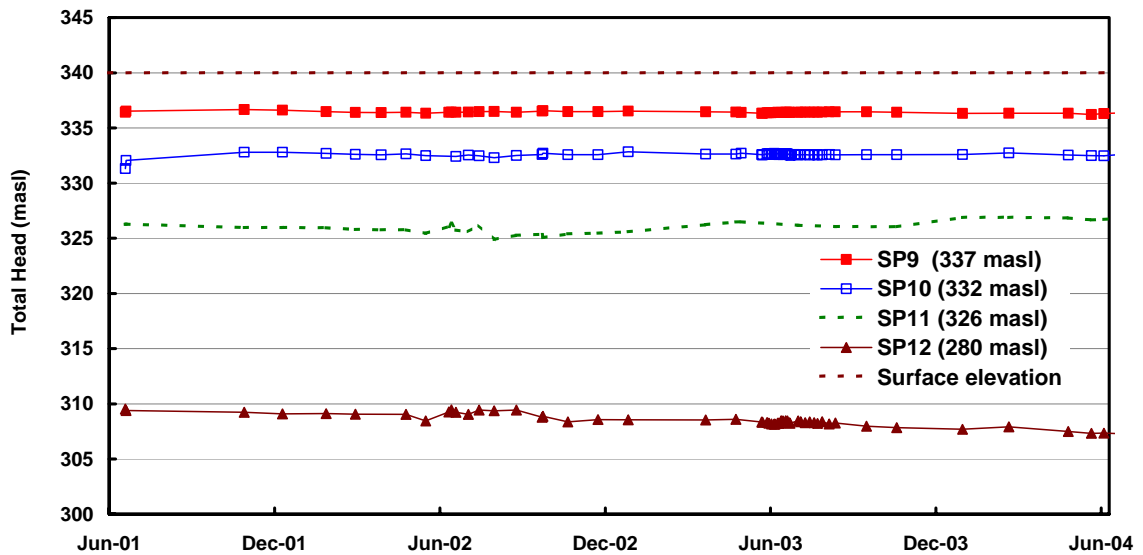


Figure 4.9 Water level readings for piezometers installed on the S1 Dump.

4.3.4 Top South Side of SBH – Surface Elevation 350 m (Location D)

Figure 4.10 shows a cross section and the measured water levels of the piezometer nest on the top, south side, of SBH in Location D (Fig. 3.1) at a surface elevation of 350 m. This nest is oriented in an east-west direction. The shallow piezometers, SP011730-01 (SP1), SP011730-02 (SP2), and SP011730-03 (SP3), are installed in K_c fill in a 5 m lift assembly. According to geological cross-sections, the deepest piezometer SP011730-04 (SP4), installed at a depth of 35 m below the surface is located just below the interface of where SBH overlaps the S1 dump. There is a fifth standpipe located at this nest that is not shown in Figure 4.7. As-built logs for piezometer SP011730-4A (SP 4A) indicate that the tip is located at an elevation of 302 m, however; when readings are taken manually the standpipe is completely blocked at 346 m. There is no record of when the blockage appeared.

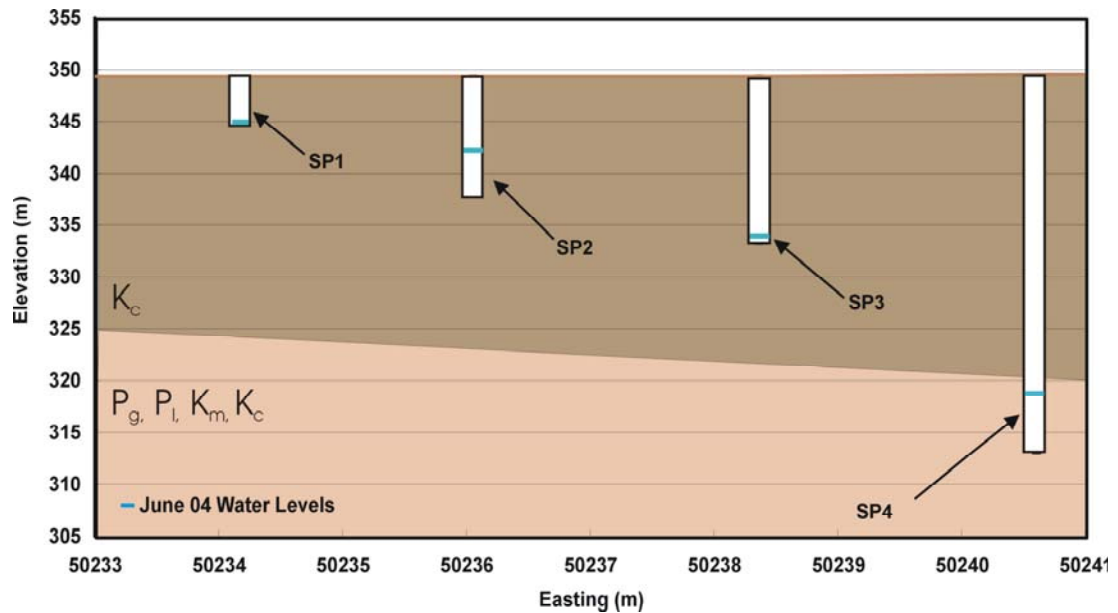


Figure 4.10 Cross-section showing water levels measured at piezometer nest on the located on the top south side of SBH (location D) on June 9, 2004.

Figure 4.11 shows measured water levels since installation. Both SP1 and SP3 have been dry, leaving only two active piezometers at this location, SP2 and SP4. The SP2 tip is located approximately 11 m below the surface. The water level in SP2 shows a gradual increasing trend in water level since installation. A bail test was performed in summer of 2003 and the head increased past the 2002 level by approximately 2 m. This nest is located at the boundary where the 30 dump is placed over the older S1 dump which may locate this tip partially in S1 materials and partially in 30 dump materials. Also because the top portion of SBH was placed in 1998, less than six years ago at the time of this study, there may be some slight settlement occurring affecting the pore pressure in the top portion of SBH. The water level measurements for SP4 stay fairly constant. The higher glacial till content of the S1 dump materials likely have a higher hydraulic conductivity and subsequently the water levels may have stabilized more quickly and remain stable in this material.

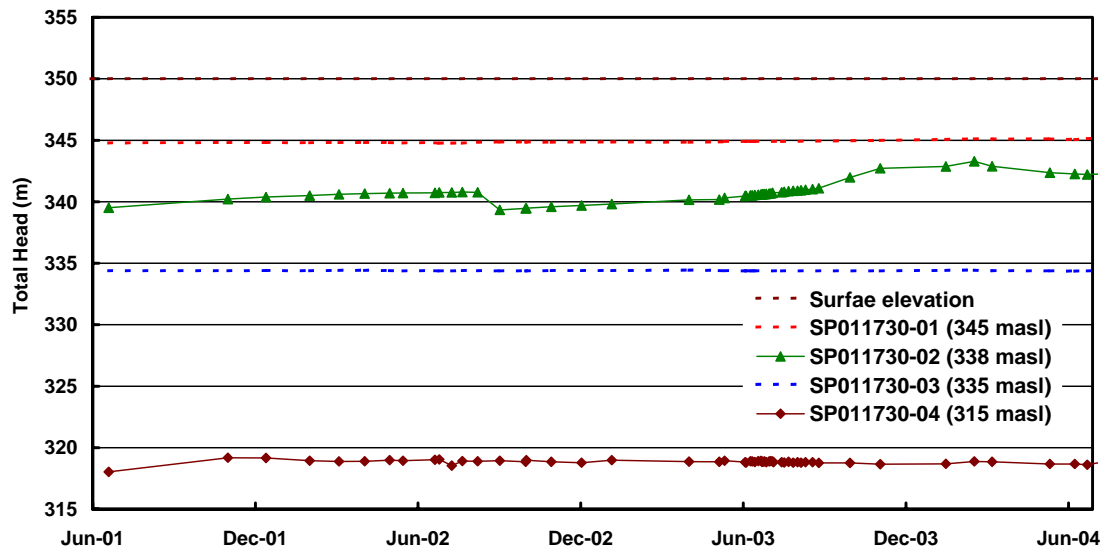


Figure 4.11 Water level readings for piezometer nest installed on south top side of SBH.

4.3.5 Top North Side of SBH – Surface Elevation 350 m (Location E)

Figure 4.12 shows a cross-section of the piezometer nest located at the north central portion of the top of SBH which contains five piezometers at various depths along a north-south orientation (Location E, Fig.3.1). This nest holds particular interest because it contains SP 011730-8A (SP8A), the only piezometer to be installed from the top surface of SBH to the contact between the limestone bedrock and the lower K_c fill, a total depth of approximately 90 m. Four of the piezometers installed at this location are installed in the K_c fill constructed of 5 m lifts. SP011730-05 (SP 5) and SP011730-06 (SP 6) are the shallowest piezometers at a depth of approximately 5 m and 11 m respectively. Both of these piezometers have been dry since the start of measurement. SP011730-07 (SP7), at a depth of 15 m below the surface and SP011730-08 (SP8) at a depth of 25 m below surface have had measurable water levels, however; the water levels have not reached above the screen.

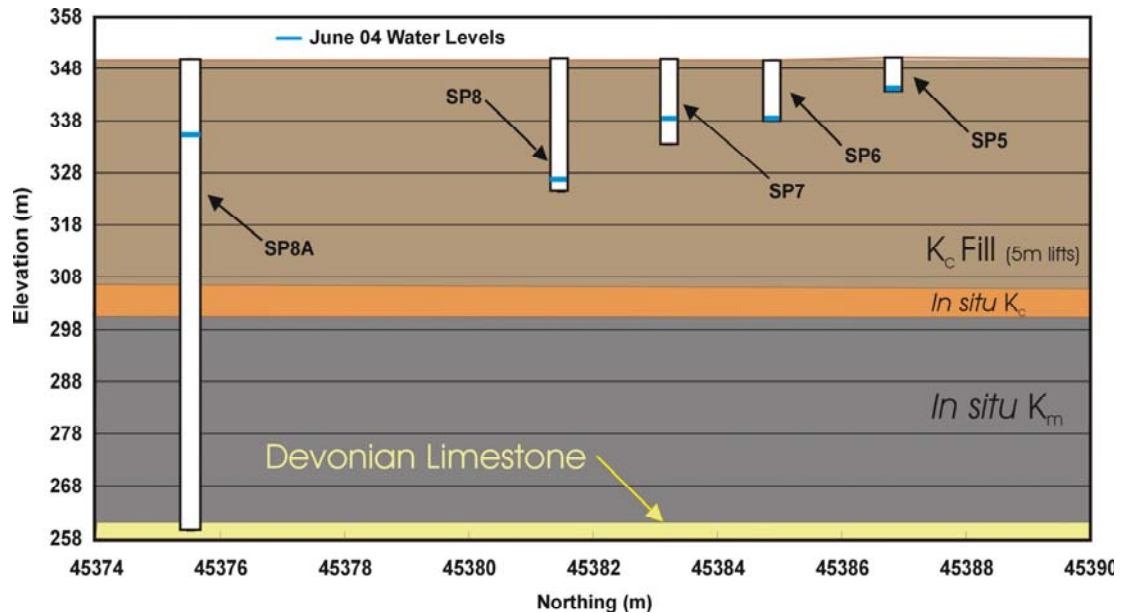


Figure 4.12 Cross-section showing water levels measured at piezometer nest on the located on the top south side of SBH (location E) on June 9, 2004.

Figure 4.13 shows water level measurements at the top north piezometer nest. The wide fluctuations in the water levels in SP8A are most noticeable. There appears to be an overall rise in the average water level within this piezometer. The response of SP8A shows artesian behaviour in that the total head elevation is higher than the surface of the limestone. One of two possibilities exists. First, this piezometer may not be reliable due to the extreme depth of the screen installation. The 2003 drill program has shown that drilling in this material is extremely challenging. A high probability exists for damage to the pipe and couplings to occur and the integrity of the sand pack to be affected. Secondly, the irregular levels may represent what is actually happening in the limestone / fill interface as a result of additional tailings pumped into WIP; however, the source of recharging water which could produce a head close to elevation 338 m is difficult to explain.

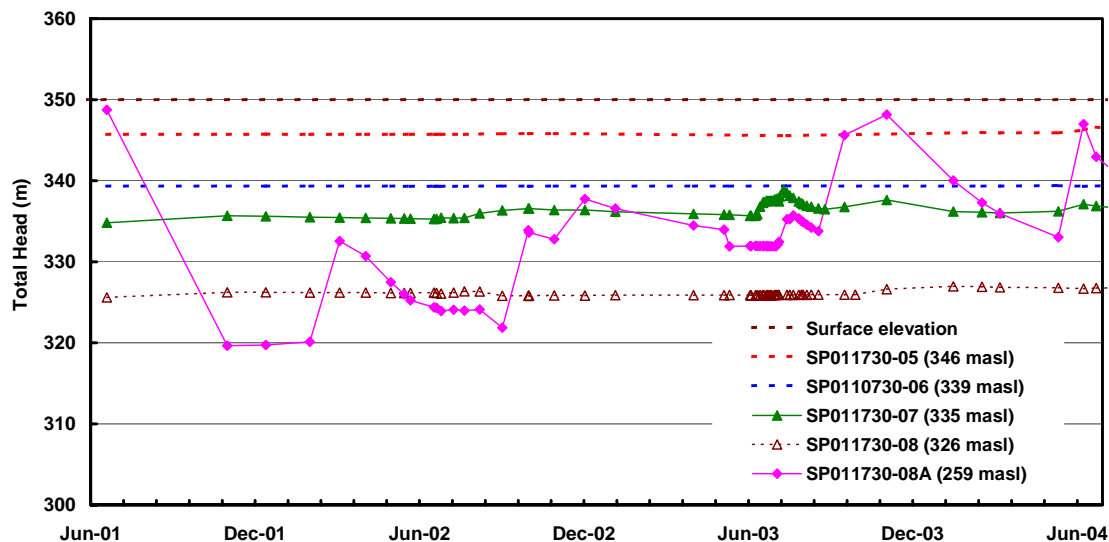


Figure 4.13 Water level readings from Location E nest located at north central portion of SBH.

Piezometer SP7 water levels initially appeared to be relatively stable, until more frequent readings were taken in the summer of 2003 which suggested a seasonal ‘mounding’ of water levels around mid-July. A similar fluctuation can be seen in SP8A with a slight delay in the time for the arrival of the peak water level.

In 2003, according to a climate station set up on the top of SBH, over the month of July approximately 58.6 mm of rain fell, the most received so far in 2003. The more frequent readings may have picked up on the small increases in water levels due to precipitation amounts. However, SP7 does not show any other fluctuations caused by seasonal variances and it is interesting to note that SP6, at a depth of 11 m is not affected at all. If infiltrating water is producing the seasonal rise in water levels in SP7 and SP8A then this evidence would suggest that there may be a preferential flow path transmitting this water to depth possibly along the pipe or within the pipe itself.

A trend is difficult to observe with the fluctuating levels of SP8A. The water levels measured by the shallow piezometers in this location exhibit typically perched water conditions as reflected by consistently stable readings. This is not unexpected given that a 5 m lift construction was used at the top section of SBH.

Figure 4.14 shows the water level elevation of WIP from 1996 to 2003 plotted with SP8A measured water levels. The water levels in WIP and SP8A show similar overall rates of rise with time with the heads in SP8A generally higher than WIP. The piezometers in location D give evidence of separate flow systems occurring within SBH. The four shallow piezometers (SP5,

SP6, SP7, and SP8) show an overall downward flow through top 5 m layered fill with an indication of perched conditions. The upward gradient shown by SP8A indicates that upward recharge is occurring from the base into the pile and not from net percolation into the underlying materials. The change in water level starting from the peak was compared to the time to calculate a rate in m/s. For the three peaks investigated the geometric mean was calculated to be 6.1×10^{-7} m/s which is not an unreasonable hydraulic conductivity for the lower fill materials. The peaks measured in SP8A may be leakage occurring from the surface then dissipating into the pile at a rate close to the K of the material.

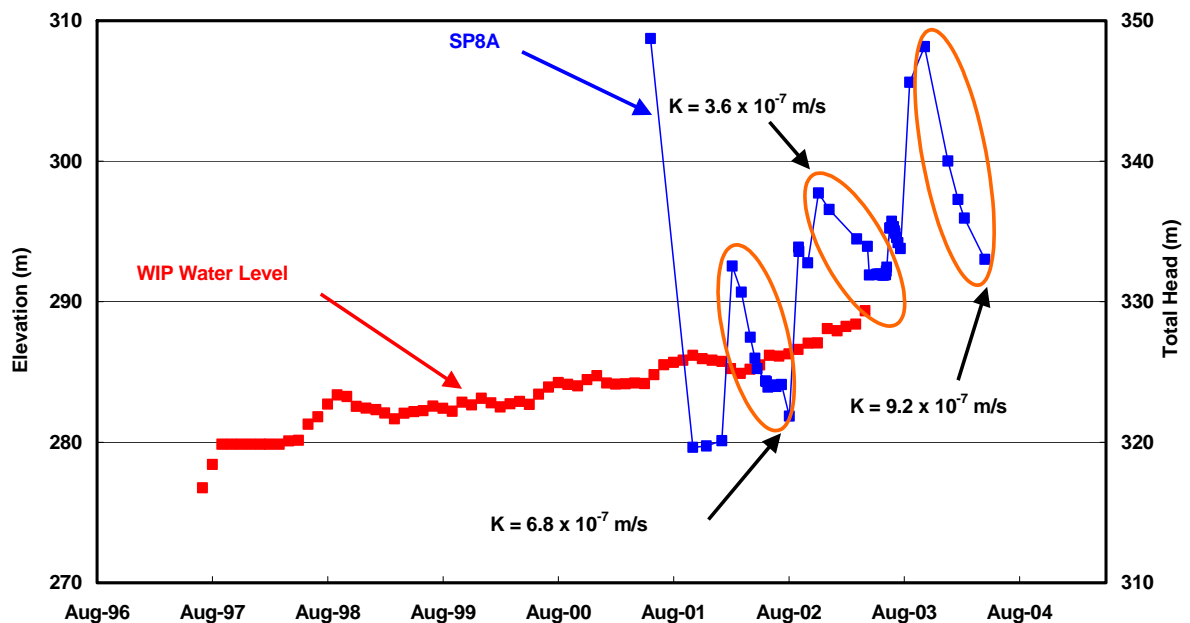


Figure 4.14 WIP water level elevation compared to water level response of SP8A.

4.3.6 Bottom Slope Nest - 330 m Bench (Location F)

Figure 4.15 shows the piezometer nest that is located on the 330 m bench just north of the piezometers on the top of SBH (Location F, Figure 3.1). Piezometer screens at this location are installed in close proximity to the 320 m elevation material break described in Section 4.2. Piezometer SP011730-17 (SP17) is installed above 320 m elevation at a depth of 6 m below surface. Piezometer SP011730-18 (SP18) and Piezometer SP011730-19 (SP 19) are completed in the K_c shale just below the 320 m elevation at depths of 10 m and 15 m below surface respectively. A detailed borehole log was not available for these piezometers, however; as-built summaries suggest that the screens are in the loose K_c fill material. Piezometer SP011730-20 (SP20) is one of the three piezometers that are installed at the bottom of the mined out pit just at the contact with the Devonian limestone base. Drill logs describe the material as K_c fill.

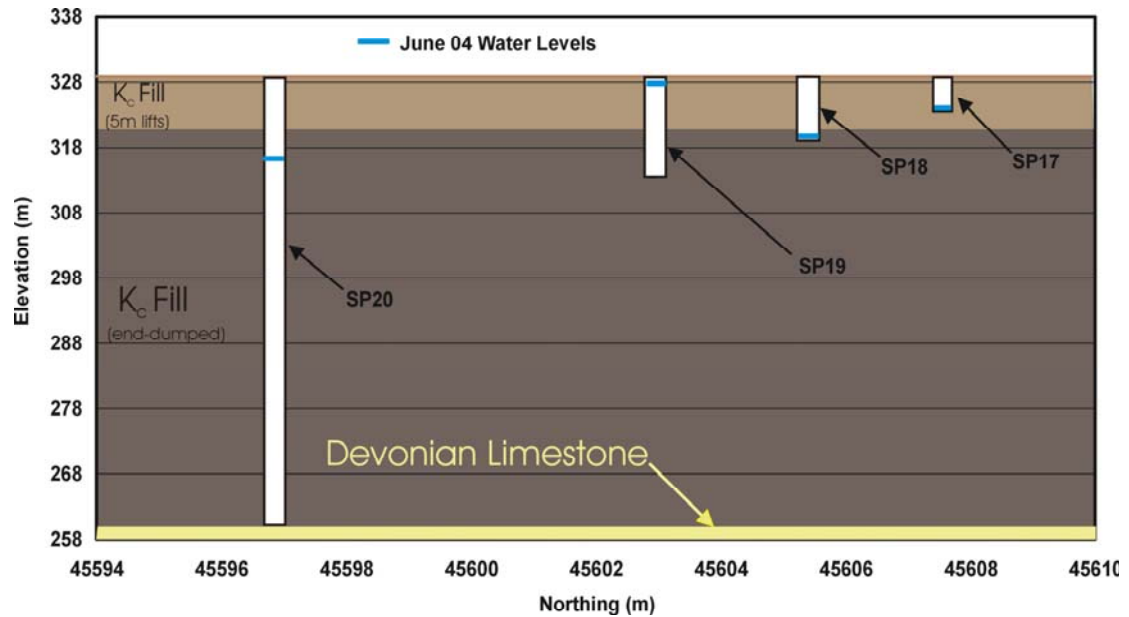


Figure 4.15 Piezometer nest at location F at surface elevation 330 m.

Figure 4.16 shows the water level measurements for the location F piezometers. Piezometers SP17 and SP18 have both contained only a few centimetres of water since installation and were considered to be dry. It is evident that two rising head tests have been completed on SP19, one during the summer of 2002 where approximately 11 m of water was removed and one in the summer of 2003 where approximately 2.5 m of water was removed. Both tests for SP19 have recovered to the same head at 327 m with no noticeable increasing or decreasing in water level through time.

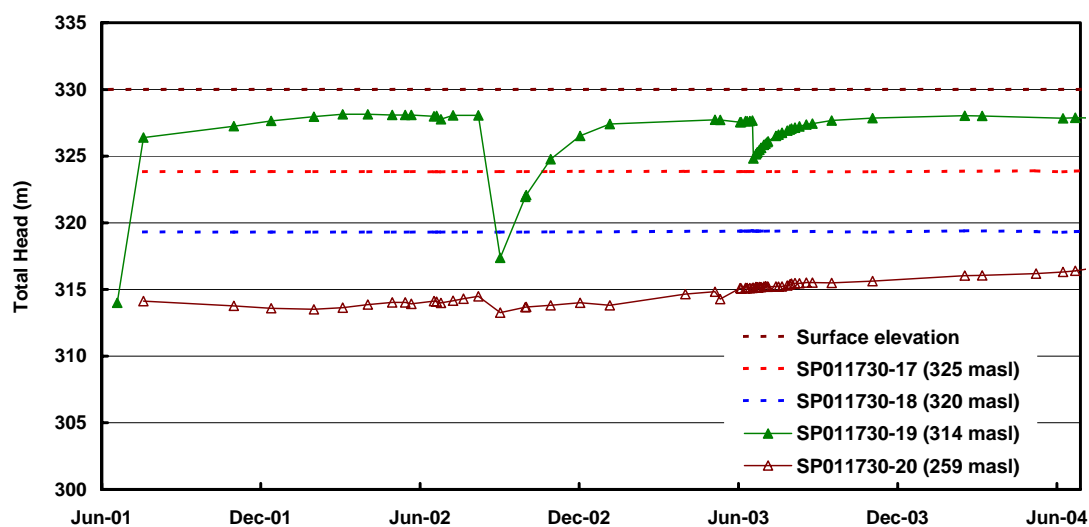


Figure 4.16 Piezometer nest at location F at surface elevation 330 m.

The SP20 piezometer tip, installed near the limestone base has a noticeable high head. The overall water level appears to be rising over the monitoring period which may be connected to the water level rise of WIP as with SP8A (Section 4.3.5). The total head from SP19 is high, but based on geologic cross-sections, this nest is located approximately 290 m north of the lean oil sand pillar. It may also be that the fill materials along the east side of SBH may be contributing to the high head measured in SP19. This material has a lower percentage of K_c and was not compacted in lifts - likely leading to a higher hydraulic conductivity. The head shown in SP19 may be a result of recharge from upland and from the east side of SBH building up behind the pillar causing the head to rise up close to the ground surface.

4.3.7 Northwest Nest – 319.5 m Bench (Location G)

Figure 4.17 shows a cross section at the nest situated at Location F (Fig. 3.1) containing four piezometers installed from a surface elevation of 319.5 m. The shallowest piezometer SP11730-13 (SP13) at a depth of approximately 5 m below the surface has been dry since installation in 2000 and could likely be installed in lift material rather than end-dumped. Piezometer SP011730-14 (SP14) at a depth of 10 m below the surface and SP011730-15 (SP15) at a depth of approximately 15 m below ground surface are installed in end-dumped K_c fill that was not considered to be defined lift construction. Piezometer SP011730-16 (SP16) is located approximately 60 m below ground surface in the underlying Devonian limestone base and is one of the three deepest standpipes in this study.

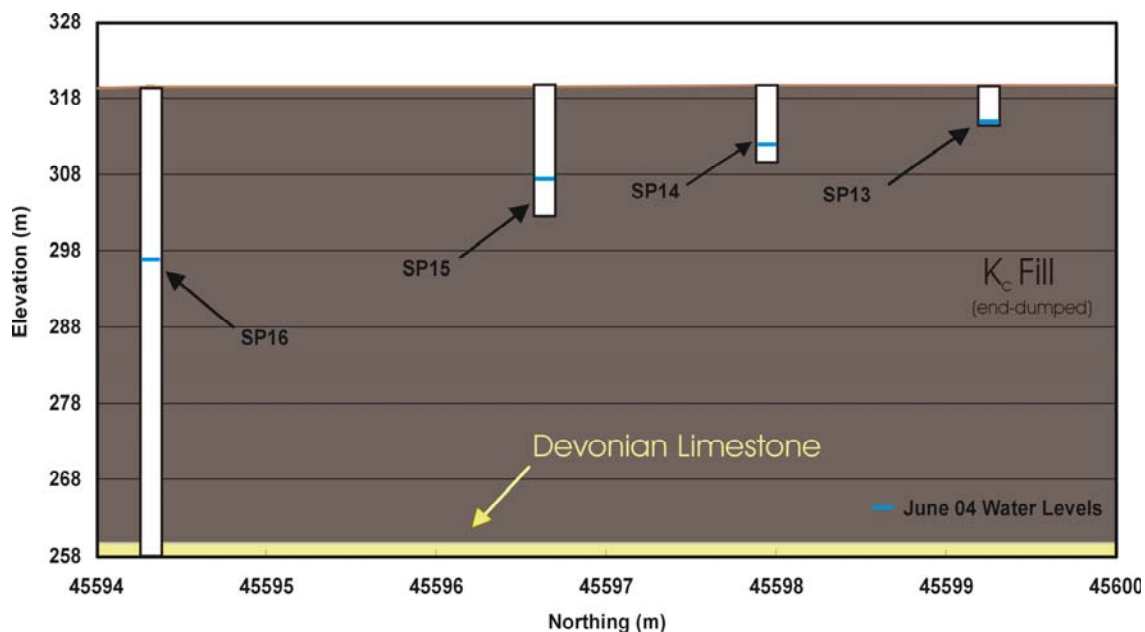


Figure 4.17 Cross-section of piezometer nest at location G at surface elevation on 319.5 m.

The water levels for this piezometer nest are shown in Figure 4.17. SP14 has undergone a gradual increase in head since installation and continued to show a gradual increase following the bail test in 2002. The last readings taken in June 2004, have shown that the head recovered to the previous equilibrium level. Hydraulic conductivity results are discussed in more detail in Section 4.4. Water levels in SP15 have been irregular since installation showing no real trend. The deepest piezometer, SP16 has remained at a constant head throughout the monitoring period with a slight decrease in 2004. SP8A and SP20, also installed at or near the limestone base have shown increasing heads with time. Further monitoring of SP16 is required to confirm if the decrease in head continues.

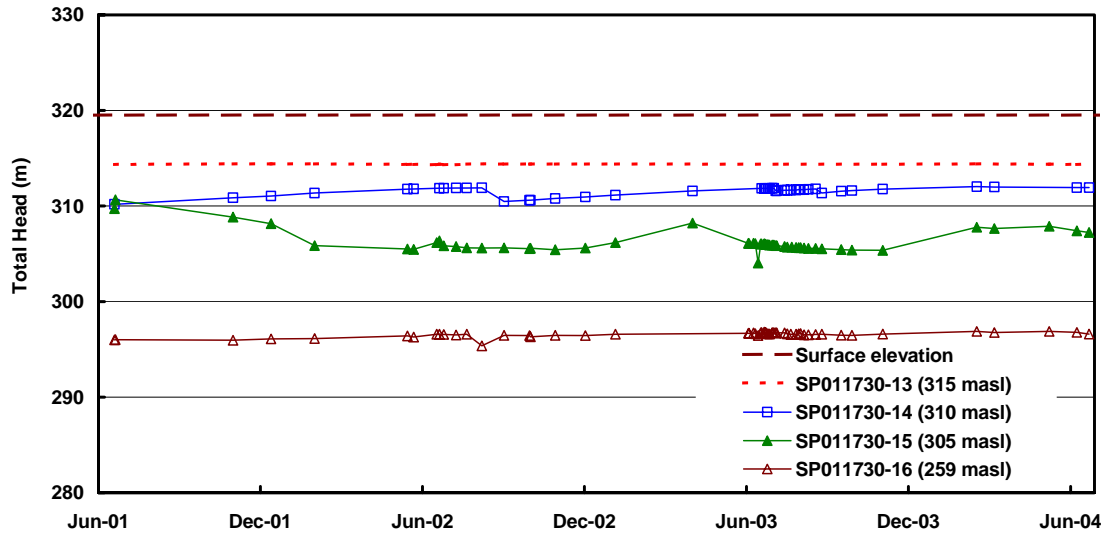


Figure 4.18 Water levels in piezometer nest at location G at surface elevation on 319.5 m.

4.3.8 North Nest – Surface Elevation 316.5 (Location H)

The northern most piezometer nest installed on the SBH is located at an approximate ground surface elevation of 316.5 m, the lowest elevation of all the nests (location H, Figure 3.1). This particular nest contains three piezometers oriented in an east-west direction (Figure 19). SP011730-21 (SP21) is located at a depth of 5 m below ground surface, SP011730-22 (SP22) at a depth of 9 m below surface, and SP011730-23 (SP23) at a depth of 15 m below surface. These piezometers are installed in end-dumped K_c fill similar to Section 4.3.7.

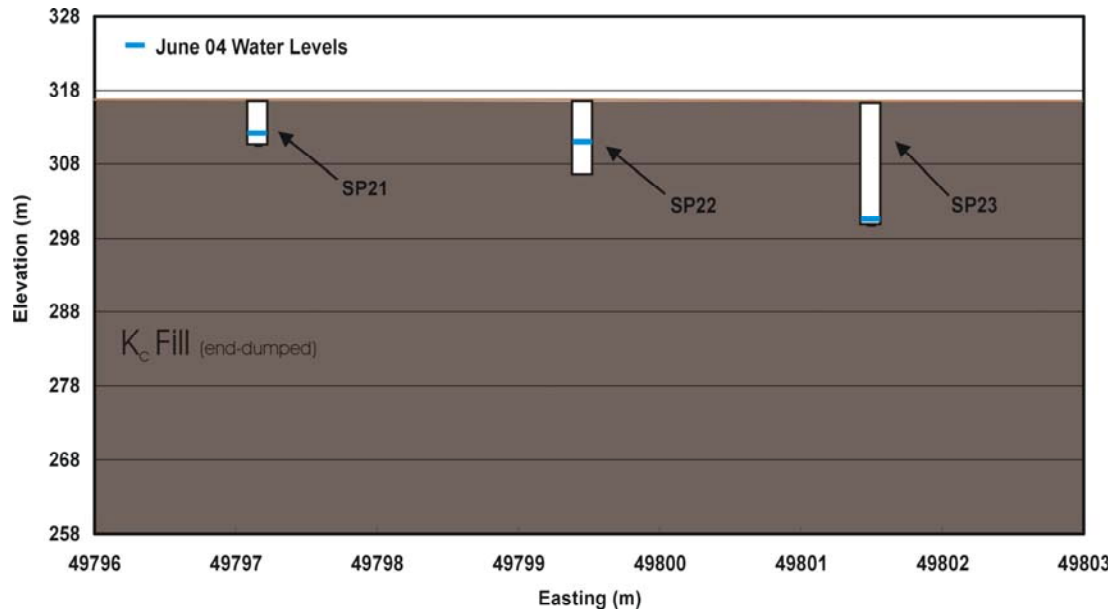


Figure 4.19 Cross-sections of piezometer nest at location H (Figure 3.1) at a surface elevation of 317 m.

All three piezometers in this nest have contained minimal amounts of water with SP 23 containing the most water with a depth of water of approximately 1 m (Figure 4.20). Bail tests were not performed on any of the piezometers at this location. The water levels at this nest have remained constant throughout monitoring 2003. The water level in SP21 rose by approximately 1 m, and the water level in SP 22 rose approximately 5 m, over an 11 month period during the 2003-2004 season. This nest is the most remote nest, and readings are taken less frequently as compared to the other nests, therefore it is not known if the water levels in SP 23 rose suddenly or gradually over this year period.

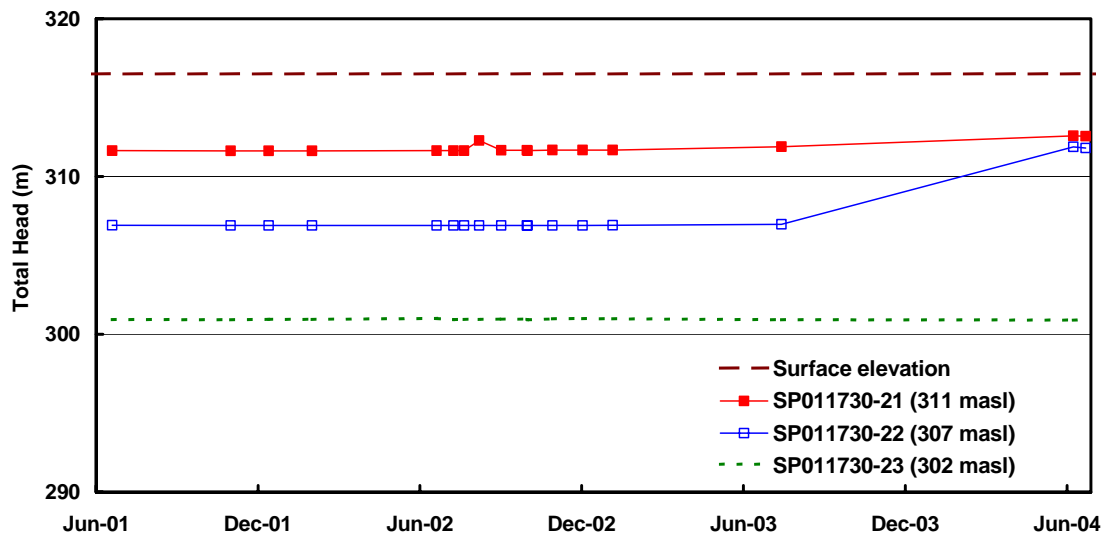


Figure 4.20 Water levels of piezometer nest at location H (Figure 3.1) at a surface elevation of 317 m.

4.3.9 2003 Installation – Surface Elevation 320 m (Location I)

As outlined in Section 3.3.1 additional piezometers were installed to supplement the existing network; however, due to installation difficulties, no additional deep piezometers (i.e. greater than 30 m depth below surface in any location) could be installed and two nests with a 10 m and 30 m pipe were added to the network. It is notable to mention that drilling attempted to reach the base of the pile at two new locations, both to a depth of 260 m, or 60 m below surface. Drilling attempts using a rotary rig, a hammer drill, and a hammer drill with reverse air circulation were unable to advance below 30 m from surface elevations of 350 m and 320 m. Figure 4.21 shows the first nest located on the north central location of SBH at a surface elevation of 320 m (Location I, Figure 3.1). This nest contains two piezometers, SP1-1 at 10 m below the surface and SP 1-2, 30 m below ground surface oriented in an east-west direction. These piezometers are installed in end-dumped K_c fill.

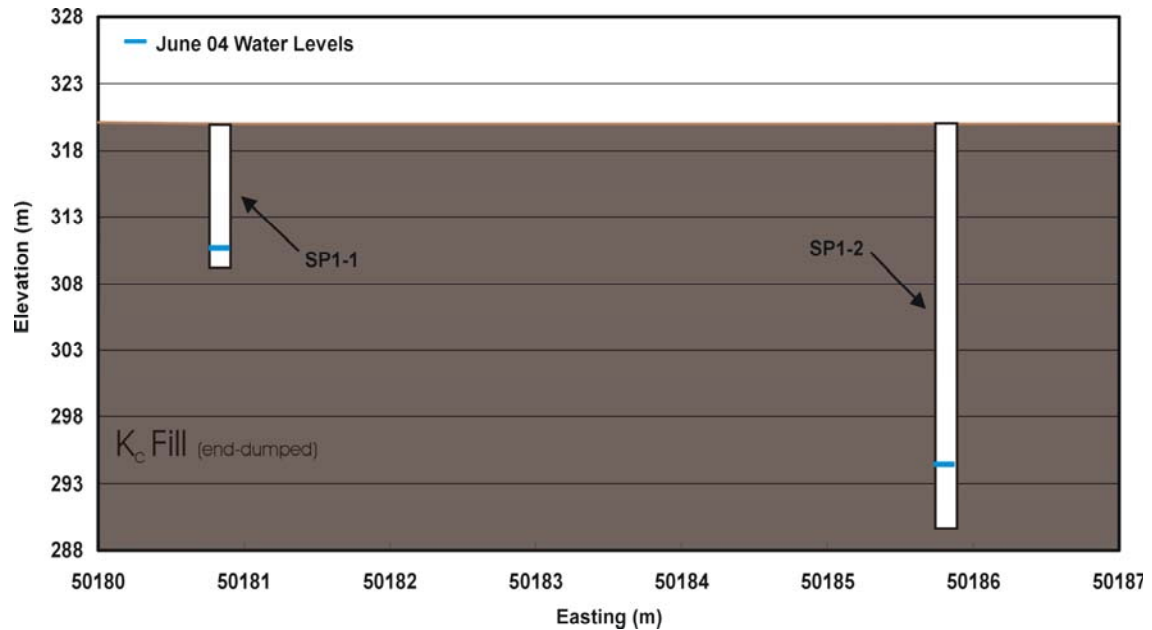


Figure 4.21 Cross-sections of piezometers located at Location I (Figure 3.1) at surface elevation 320 m.

After installation, both piezometers were purged immediately by airlifting the water and bentonite/cement mixture by the grout truck brought to site was used to seal the borehole annulus. Measurements were taken immediately following purging to get an initial idea of water level response for about a month. Each pipe was bailed out again to develop the well and water levels were subsequently recorded. From Figure 4.21, we see that SP 1-1, approximately 10 m below surface has not recovered significantly during the monitoring period. SP 1-2, 30 m below surface, had an initial rise in water levels following first purging but has only recovered 5 m since the second purging. This nest is located approximately 40 m south of the base of the oil sands pillar located on the north side of SBH.

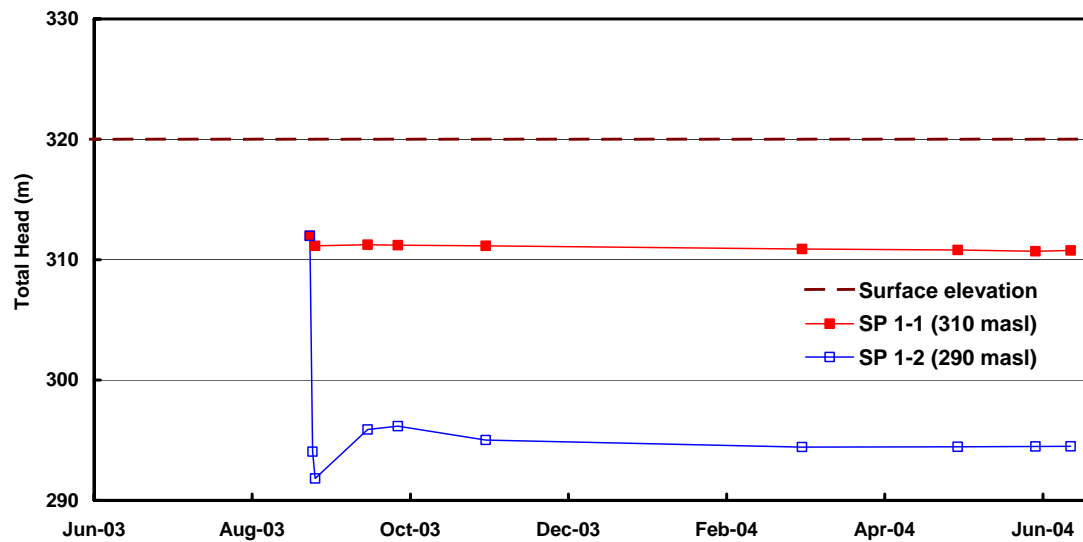


Figure 4.22 Water levels of piezometers located at location I (Figure 3.1) at surface elevation 320 m.

4.3.10 2003 Installation – Surface Elevation 320 m (Location J)

The second set of piezometers installed in 2003 were located approximately 400 m east of the previous Location I, still remaining on the 320 m bench (Location J, Figure 3.1). The nest layout is very similar to the nest located at Location I in that it contains a standpipe (SP 4-1) at a depth of 10 m below surface (320 m) and a second (SP 4-2) 30 m below surface (290 m) as seen in Figure 4.23.

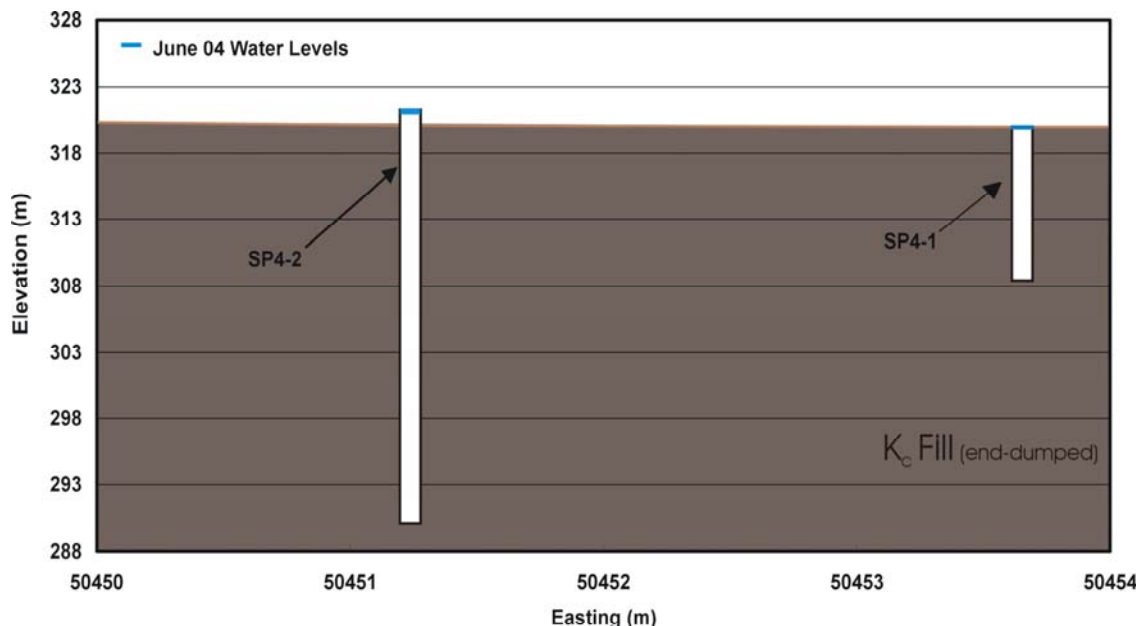


Figure 4.23 Cross-section of piezometers located at location J (Figure 3.1) at surface elevation 320 m.

Figure 4.24 shows the first year of water level measurements at location J. The water levels rose quickly in both piezometers since the first purge and subsequently become flowing artesian. The water level in SP 4-2 rose to the top of the standpipe stickup (321.3 m) and remained that way. In November 2003, when water levels were checked, the water was frozen out the top of the pipe (Figure 4.25) indicating flowing artesian conditions. SP 4-1 almost contained the same level of water, being just at the 320 m elevation. The standpipes in this location will have to be further investigated to determine if this flowing behaviour continues. If flowing conditions exist, then the true heads will have to be determined with a standpipe of sufficient height, or by using a valve and pressure gauge. The heads measured in these standpipes may be a result of their installation location. This piezometer nest is only 60 m south of the base of the oil sands pillar located on the north side of SBH. The low permeability pillar is likely blocking water flowing north towards WIP causing heads to rise above ground surface. In Section 4.3.6, the location F piezometers (located approximately 180 m south of pillar) show a similar head build up. The piezometer nest at location I is located 40 m from the oil sand pillar but does not show the same head response as this nest. The location F and J nests are located further east than Location I and therefore are likely receiving flow from the more permeable materials east of SBH.

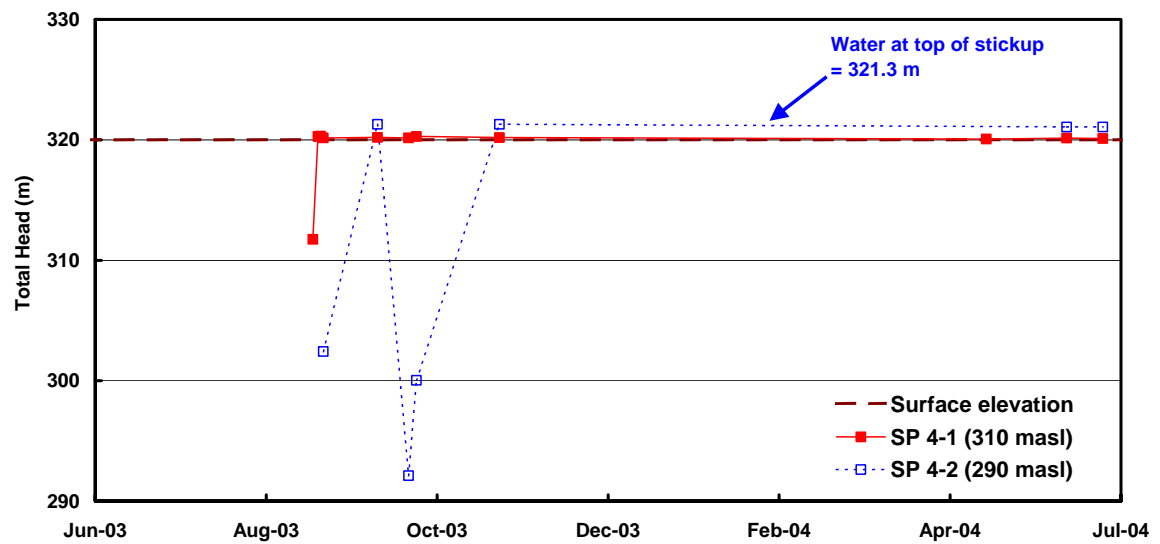


Figure 4.24 Water levels of piezometers located at Location J (Figure 3.1) at surface elevation 320 m.



Figure 4.25 Photograph of SP4-2 showing ice protruding from standpipe November 2003.

4.3.11 Key Trends of SBH Water Levels

4.3.11.1 General head distribution across SBH

Some general observations can be made from the observed water level measurements at the various locations on SBH. In general, the piezometers installed in the sections of SBH constructed with 5 m or 2 m lifts, typically demonstrate downward flow with evidence of perched conditions (hydraulic gradients of approximately one with. dry or low, stable water levels). The systems around Bill's Lake and Peat Pond show downward and outward flow conditions. These conditions indicate that these sections of SBH are in a recharge condition.

4.3.11.2 Total head measured at the base of SBH

Three piezometers in the SBH network are installed at the base of the mined out pit with tip elevations at approximately 260 m. SP8A is located at the highest elevation of 350 m while SP20 is located at an elevation of 330 m and SP16 is at an elevation of 320 m. The location of these piezometers have been projected onto a north-south cross-section through 50200 E (looking west) and are shown in Figure 4.26. The measured water levels for these piezometers and WIP are shown in Figure 4.27. From Figures 4.26 and 4.27, it appears that the ground water deep in the pile is likely flowing north and possibly westward towards WIP, although it is difficult to be sure of this given the limited number of piezometers installed at this elevation. SP20 and SP16 both show a gradual rise in heads, albeit much more gradually, with more subdued fluctuations relative to WIP. This would be consistent with a 'backwater' effect from a rising lake level. SP8A water levels are much higher and more variable, but also appear to rise with the rate of rise measured in WIP (Figure 4.14). SP8A may be affected by the water level in WIP more so than the other two piezometers because of a fracture network that occurs in limestone formations. It is also interesting to note that the regional gradient (excluding SP16) is approximately 50 m/700 m or 0.07. This would produce a total head just south of the lean oil sand pillar of more than 300 m without considering any further build up in heads in order to divert the flow around the pillar itself. Additional piezometers installed to the limestone base south and east of SP8A would be beneficial to further define the flow system.

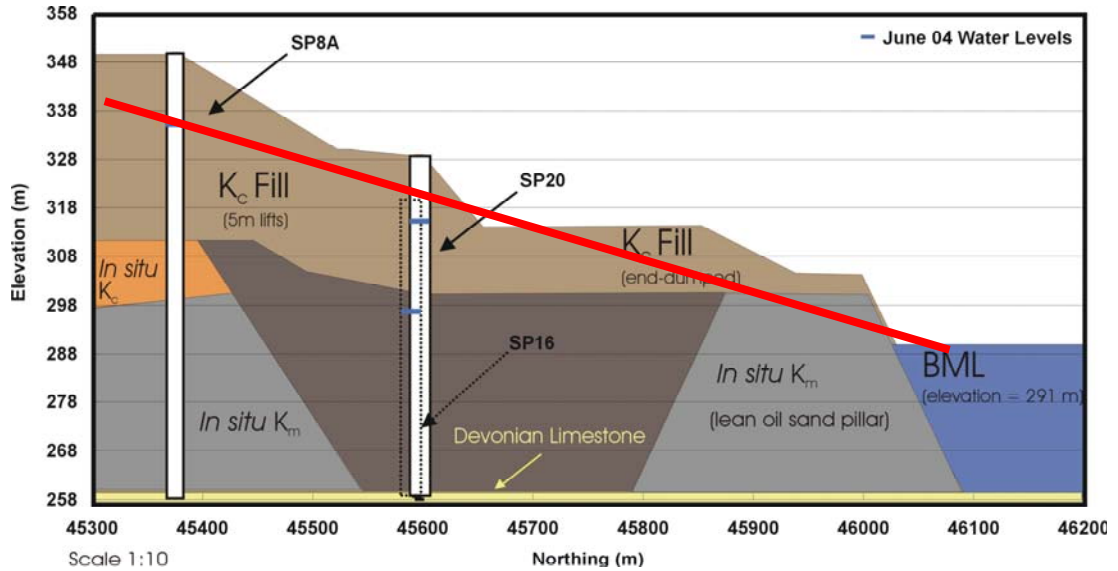


Figure 4.26 Cross-section showing piezometers installed at the contact of Devonian limestone and K_c fill of SBH in relation to water level of WIP.

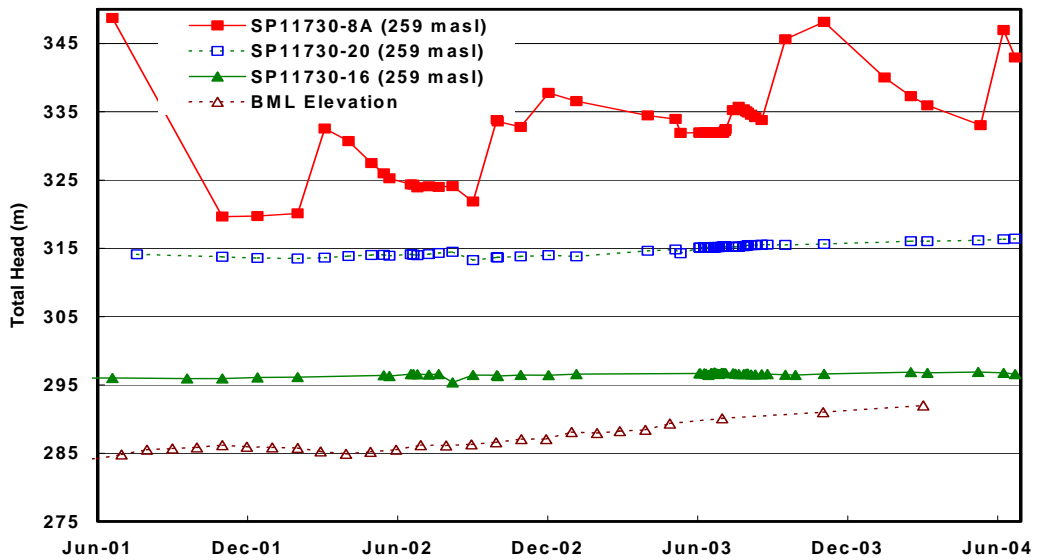


Figure 4.27 Water levels measured in piezometers installed in the Devonian limestone base and WIP water level elevation.

4.3.11.3 Effect of lean oil sand pillar

There are three nests that appear to show the influence of the low permeability lean oil sands pillar. The nests at locations F, I and J are at a distance of 180 m, 40 m, and 20 m away from the bottom of the lean oil sands pillar, respectively. A cross-section of these nests and their

measured water levels starting January 2003 (locations I and J were installed in August 2003) are found in Figures 4.28 and 4.29.

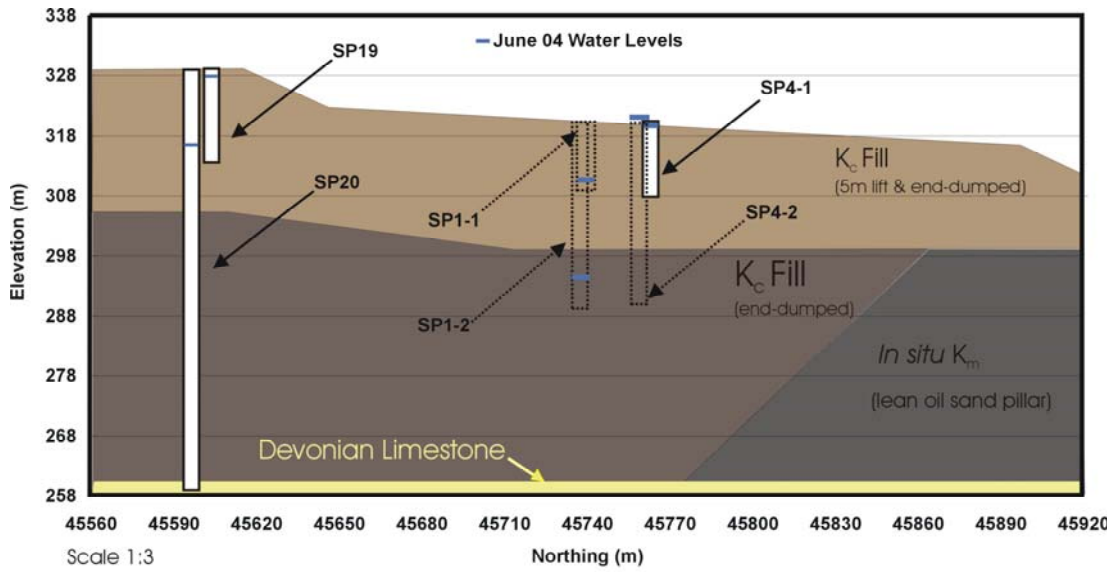


Figure 4.28 Cross-section of piezometers installed closest to lean oil sands pillar located north side of SBH.

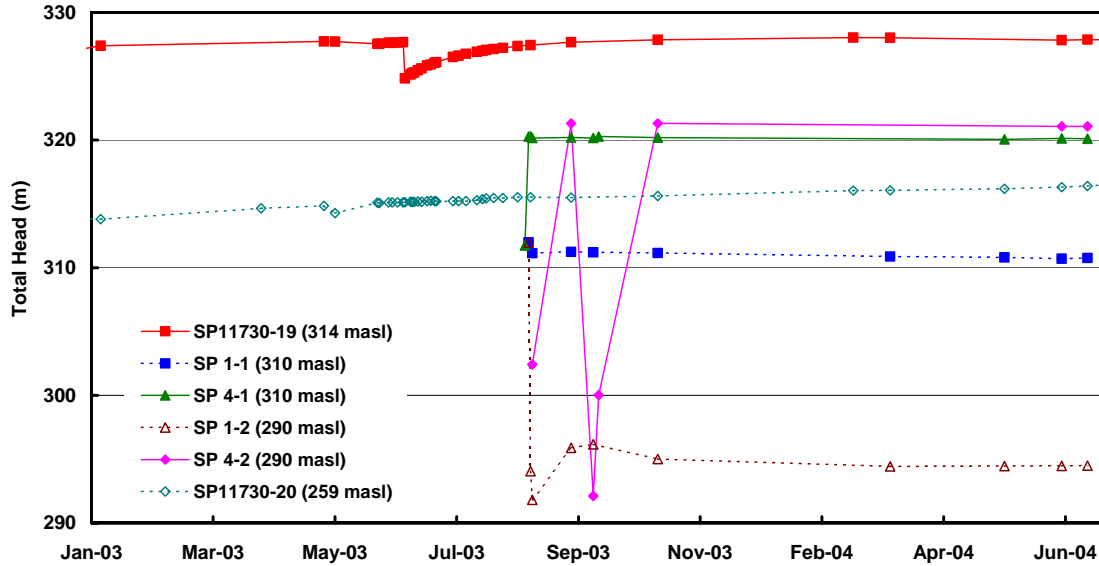


Figure 4.29 Cross-section of piezometers installed closest to lean oil sands pillar located north side of SBH.

Piezometers SP 1-2 and 1-1 show the typical pattern of downward flow across perched water levels. However SP 4-1 and SP 4-2 show upward flow from depth. There may be water flowing

from the upland of SBH north toward WIP and from from the more permeable material located on the east side of SBH. The less permeable lean oil sands pillar is forcing the head to build up as shown in the standpipes located closest to the pillar. As noted in Section 4.3.6, SP20 is installed in at the base of the pile and is likely not affected by the pillar as it does not show the same trend as the other piezometers.

4.4 In Situ Hydraulic Conductivity Tests

The Hvorslev (1951) time-lag analysis method was used to estimate the *in situ* hydraulic conductivity (K) based on measurements of rising head tests performed on the piezometers. The Hvorslev analysis used assumes homogeneous, isotropic, infinite medium in which soil and water are incompressible. The tests were conducted during the summers of both 2002 and 2003 on 20 out of the 32 previously installed standpipes.

For some of the standpipes, the water level in the pipe was located at or below the screened interval. The pipe was purged and sampled for groundwater chemistry. Measurement of hydraulic conductivity is not considered to be valid if the water level falls below the screen due to changes in storage within the screen materials rather than from the actual aquifer materials. Dewatering the screen creates an artificial time lag that affects the determination of the piezometric level and the K value (Chapuis, 2005a and Chapuis, 2005b). Chapuis (2005b) summarizes the findings of several researchers in stating that tests conducted below the screen can be viewed as having two linear portions: first flow into the highly permeable zone around the well followed by the flow from the undisturbed material surrounding the well. The method outlined by Chapuis (2005a and 2005b) was conducted on those standpipes whose water level was at or below the piezometer screen.

The results for the rising head test conducted in 2002 on SP15 are shown in Figure 4.30. The top of the screen for SP15 is at an elevation of 306.4 m and the initial water level was measured at an elevation of 305.5 m. This water level was assumed to be equilibrium piezometric level for this well based on an examination of the historical water levels since 2001. During the test conducted in August 2002, the water level was lowered to an elevation of 304.3 m. In Figure 4.30 the log of head recovery (initial head minus measured head) was plotted versus time. It is apparent that there are two distinct linear portions for this test. The first segment produces a value of hydraulic conductivity of 5.3×10^{-6} cm/s and the second segment a value of 1.3×10^{-9} cm/s. The later is a more reasonable estimate of the hydraulic conductivity of the K_c fill material at this location. This method was used to estimate the K on standpipes where the bail test was conducted within the screened interval. Standpipe SP011730-8A located in nest E (Figure 3.1) is the only standpipe that extends from the top of the pile (surface elevation 350 m) to the

Devonian limestone base. The midpoint of the screen is at elevation 259 m. The water levels in this standpipe have been quite erratic (Figure 4.13) with a general trend which seems to follow the water level changes in WIP and the Hvorslev analysis was not done for this piezometer. Looking at the decay of the three noticed peaks in water level from March 2002 to November 2003, a geometric mean of 6.3×10^{-7} m/s could be estimated (Figure 4.27). Plots for all tests are found in Appendix D.

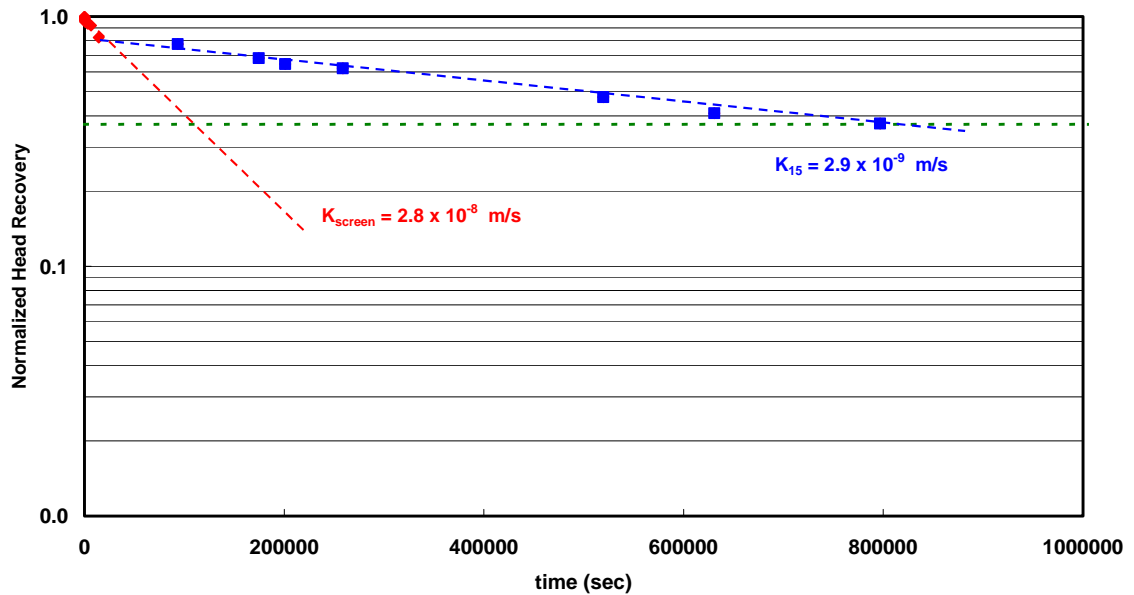


Figure 4.30 Graph of normalized head recovery versus time for SP011730-15 in 2002.

Rutten (2006) also performed a set of bail tests in 2005 on 18 piezometers including those installed in 2003. Results of the calculated *in situ* hydraulic conductivity values from the 2002 and 2003 tests as well as the results from Rutten (2006) are found in Table 4.1. The piezometers have been grouped by screen elevation to help define the relevant geologic materials and fill placement methods.

Table 4.1

In situ K of SBH materials organized by installation in S1 dump, limestone base, screen elevation below 320 m, and screen elevation above 320 m.

	Standpipe ID	Midpoint Screen Elevation (m)	Measured <i>in situ</i> K (m/s)		
			2002	2003	2005 (Rutten, 2006)
S1 Dump	SP10	332	2.0×10^{-8}	2.7×10^{-8}	8.4×10^{-9}
	SP12	280	N/A	3.3×10^{-10}	N/A
Fill 2 (below 320 m)	SP16	259	2.1×10^{-8}	1.7×10^{-8}	1.6×10^{-8}
	SP20	259	1.02×10^{-9}	6.0×10^{-8}	1.5×10^{-9}
	SP145	288	3.5×10^{-8}	3.6×10^{-8}	1.4×10^{-8}
	SP15	304	2.9×10^{-9}	N/A	2.9×10^{-8}
	SP14	310	2.4×10^{-10}	N/A	2.8×10^{-10}
	SP126	312	1.1×10^{-9}	7.4×10^{-10}	1.7×10^{-9}
	SP19	315	9.8×10^{-11}	1.6×10^{-10}	2.0×10^{-10}
	SP04	313	1.3×10^{-8}	4.3×10^{-8}	7.5×10^{-8}
	SP128	317	1.1×10^{-9}	1.9×10^{-9}	3.5×10^{-8}
	SP125	318	8.7×10^{-9}	N/A	2.4×10^{-8}
Fill 4 (above 320 m)	SP127	321	1.4×10^{-9}	1.3×10^{-9}	2.6×10^{-9}
	SP124	323	1.6×10^{-9}	8.2×10^{-9}	3.7×10^{-9}
	SP07	335	3.9×10^{-9}	N/A	N/A
	SP02	339	1.4×10^{-9}	N/A	5.5×10^{-9}

N/A – test was not completed.

An ongoing study by K. De Vito from the University of Alberta to compare the hydrogeologic behaviour of reclaimed wetlands to natural systems (unpublished data, 2004) is examining the shallow flow systems around the Bill's Lake and Peat Pond wetlands on SBH. Several 1" diameter PVC piezometers were installed around both wetlands to investigate the localized flow systems. Bail tests conducted on nine piezometers installed at Bill's Lake and two installed at Peat Pond in October 2004 were analysed using the Hvorslev method and using the AQTESOLV™ software. The piezometer screens elevations were in the range of 322 m to 324 m. The geometric mean of hydraulic conductivity for all eleven tests was found to be 2.4×10^{-9} m/s. The geometric mean for the Peat Pond tests was 3.5×10^{-9} m/s (n=2), which is within the range of hydraulic conductivity calculated for SP124 and SP125. The geometric mean for the Bill's Lake tests was 2.2×10^{-9} m/s (n=9) which is also in the range of hydraulic conductivity values measured for the standpipes located at Bill's Lake (SP126, SP127, and SP128) with a geometric mean of all standpipes of 1.2×10^{-9} m/s.

4.4.1 Summary of Measured and Collected Hydraulic conductivity Data for K_c Materials

Hydraulic conductivity data for the K_c materials, as measured in the SBH piezometers and including tests conducted by Rutten and DeVito is summarized in Table 4.2. The data is separated by construction and apparent material division.

Table 4.2
Summary of K values for SBH materials.

Site	K_{min} (m/s)	K_{max} (m/s)	$K_{geomean}$ (m/s)	No. Sample
SBH S1 Dump	8.4×10^{-9}	2.7×10^{-8}	1.7×10^{-8}	3
SBH Fill above 320 m	1.3×10^{-9}	8.2×10^{-9}	2.8×10^{-9}	16
SBH Fill below 320 m	9.8×10^{-11}	2.1×10^{-7}	5.2×10^{-9}	25
<i>In situ</i> K_m	3.3×10^{-10}	3.6×10^{-8}	2.9×10^{-9}	4

The K values measured at SBH are within a reasonable range as measured by Syncrude in the various materials (Table 2.2, Section 2.4.2). The fill materials below the 320 m elevation are show a large range of measured values and show a skewed distribution (Figure 4.31). The K values measured at the SBH standpipes show that the S1 dump is approximately an order of magnitude more permeable than the fill materials of the remainder of the hill and the fill below 320 m elevation is approximately two times more permeable than the fill materials above the 320 m elevation. The differenced in hydraulic conductivity in the different construction sections are a result of differences in materials and construction methods. Investigating the water chemistry from these standpipes will assist in verifying the hydraulic conductivity results.

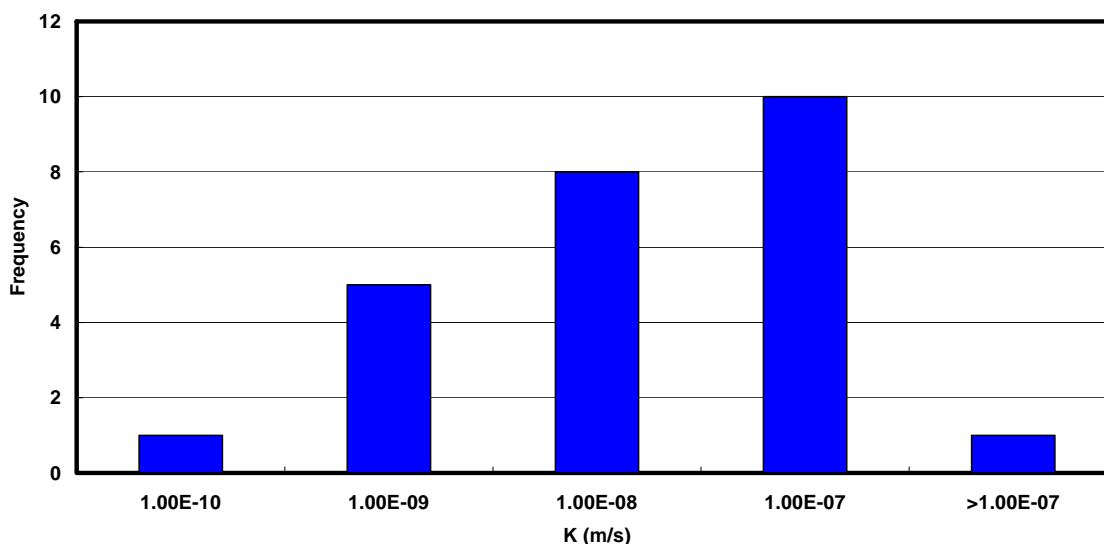


Figure 4.31 Frequency distribution of hydraulic conductivity values for fill materials below 320 m elevation.

4.5 Piezometer Water Chemistry

Water samples for chemical analysis were collected from 18 piezometers late in the summer of 2002 and during the spring of 2003. *In situ* chemistry (Reszat, 2002) and oxidized chemistry from SBH (Wall, 2004) were also examined to assist in determining the geochemical conditions within the pile.

4.5.1 *In Situ* Chemistry of Syncrude Lease Areas

Reszat (2002) investigated possible formations on the Syncrude Mildred Lake mine site suitable for subsurface storage of elemental sulfur produced as a bi-product of the oil upgrading process. He sampled piezometers constructed within the following intact materials (listed in order from deepest to shallowest): the McMurray Formation (K_m), the different 'zones' of the Clearwater Formation (K_{ca}/K_{cb} , K_{cc} , K_{cd}), and the glacial and lacustrine Pleistocene materials (P_g and P_l). Figure 4.32 shows a Piper (trilinear) diagram (Piper 1944) of the main 'zones' of water chemistry from samples collected by Reszat (2002) from *in situ* formations. This data suggests a general trend in which the SO_4 concentrations tend to be slightly higher in layers closer to the surface. This increase in concentration may be due to greater exposure of pyrite rich sediments to oxygenated water from surface. It is also important to note that sodium is the predominant cation in the deepest formation (K_m) while shallower formations have increased levels of calcium and magnesium.

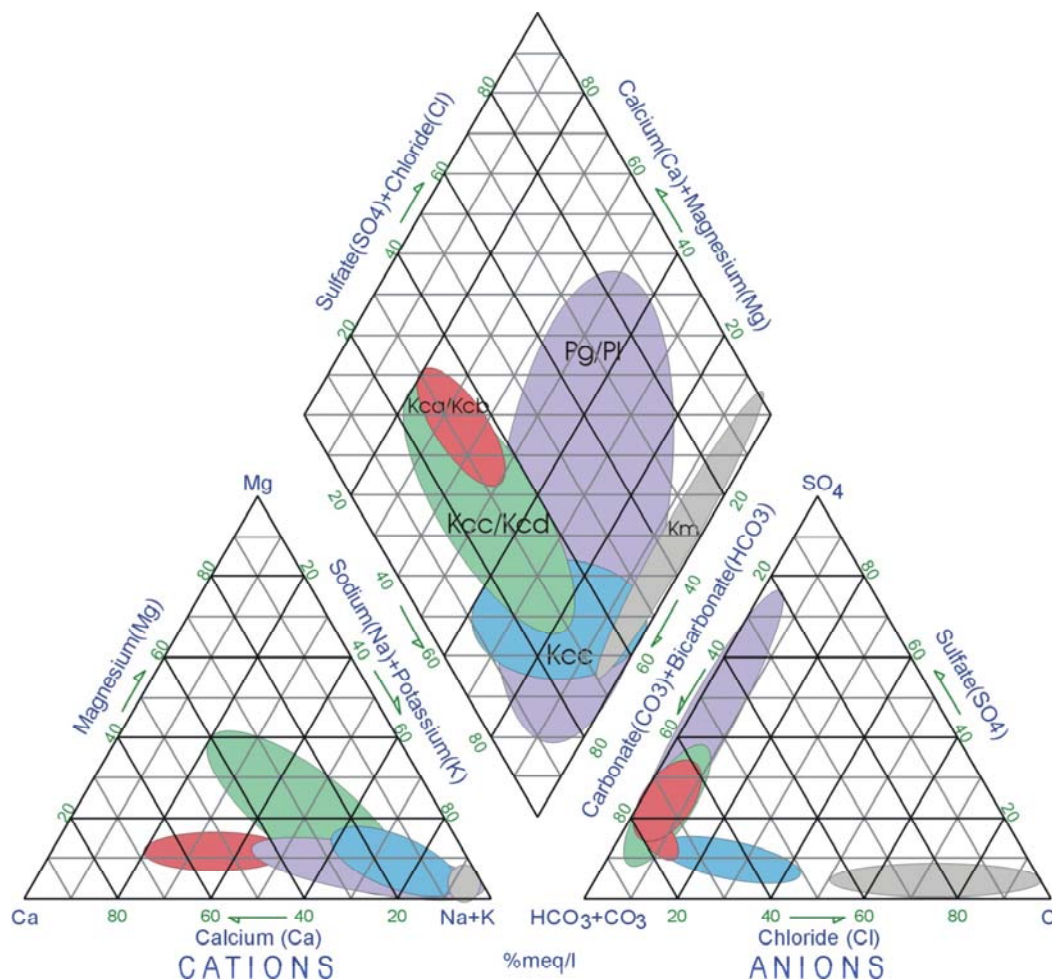


Figure 4.32 Piper plot showing 'zones' of *in situ* formation standpipe chemistry (Reszat, 2002).

4.5.2 SBH Solids Chemistry

Wall (2004) measured the soluble ion concentrations on two profiles of solid soil samples collected from SBH to a depth of approximately 24.6 m below the surface elevation of 350 m. Samples were collected to determine the concentrations of soluble salts in the SBH materials. One sample set, collected in February 2001, was exposed to atmospheric conditions and the second set, collected in August 2002, was processed under anaerobic conditions. Sampling and testing procedures for the samples are described in detail in Wall (2004). Ion chemistry for both sample sets can be found in Appendix C. Wall (2004) found that the dominant soluble cation with depth in the shale for both sample sets was Na followed by Ca. The concentrations of Mg and K were relatively insignificant compared to Na and Ca. Two samples in the profile at depths of 1.4 m and 19.2 m contained elevated levels of Na and Ca relative to the remainder of the profile. These elevated values corresponded to elevated concentrations of SO_4 , suggesting that there may have been an oxidizing environment in the shale at these depths. Samples of the glacial till cover material were also obtained. The results showed that Ca was the only ion with a

higher concentration in the till than in the shale, with the concentration being approximately double in the till. Figure 4.33 shows the Piper plot with the zones of oxidized shale samples, the samples processed under anaerobic conditions, and the till samples. The till samples were analysed under anaerobic conditions, however the samples were collected from depths of 0.61 m, 0.99 m, and 1.37 m and were likely exposed to atmospheric conditions.

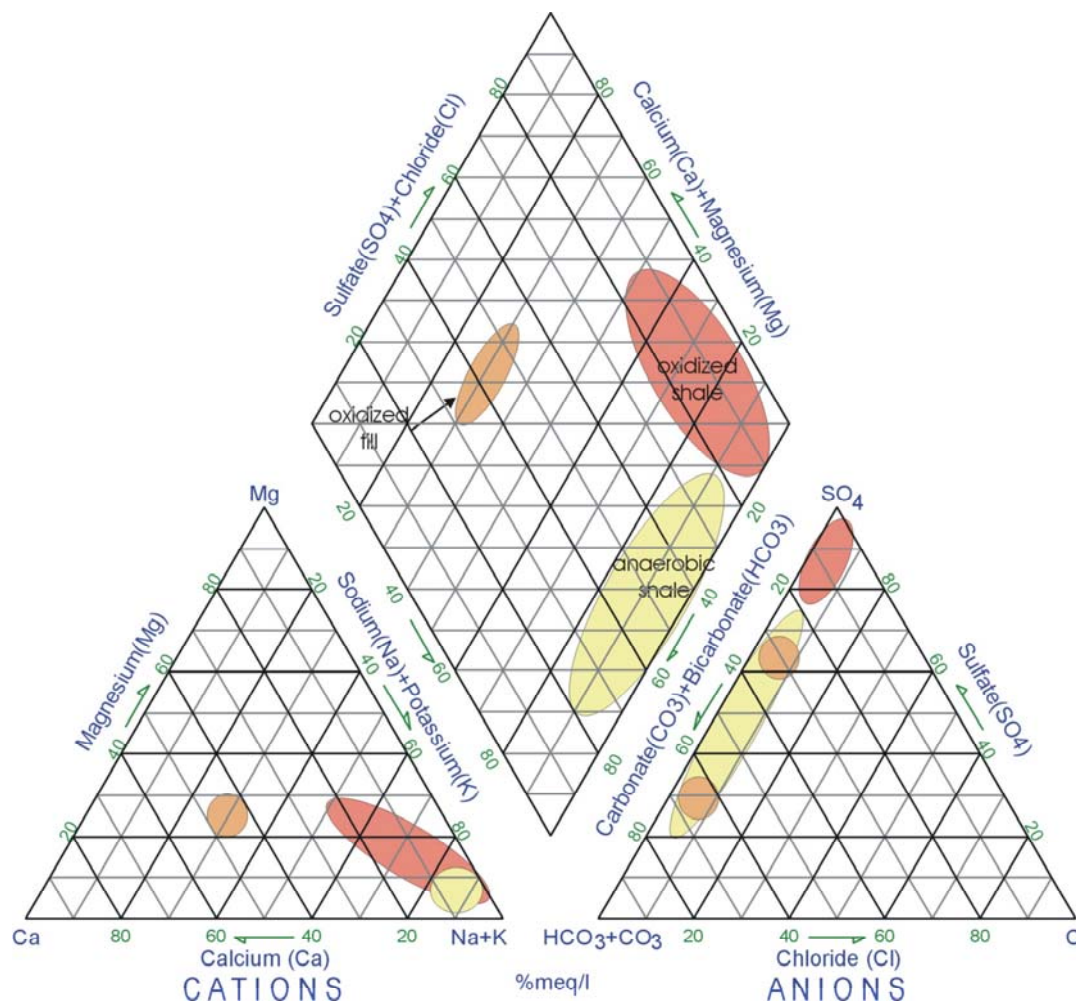


Figure 4.33 Piper plot showing 'zones' of oxidized and anaerobic shale and till samples from Wall (2004).

Comparing Figures 4.32 and 4.33, there is a notable change between the chemical fingerprints of the intact K_c shale units compared to the shale chemistry collected from SBH. There appears to be two possible shifts evident. The first shift occurs from the intact chemistry of the overburden under anaerobic conditions: a shift from Ca-Na-HCO_3 to $\text{Na-HCO}_3\text{-SO}_4$ type chemistry. The second shift occurs from anaerobic conditions ($\text{Na-HCO}_3\text{-SO}_4$) to Na-SO_4 type chemistry found in oxidized shale.

4.5.3 General Observations from SBH Standpipe Chemistry

Tabulated chemical analysis results for the SBH standpipes sampled in 2002 and 2003 are found in Appendix C. Some general geochemical characteristics can be observed. The pH values were similar between 2002 and 2003 ranging from 6.9 to 7.6 with an average pH of 7.2. Based on this range of pH, any alkalinity present is in the bicarbonate form. Electrical conductivity (EC) ranged from 1468 $\mu\text{S}/\text{cm}$ to 13400 $\mu\text{S}/\text{cm}$ which is a typical range for the K_c materials. Standpipe SP12 measured an EC of 136 $\mu\text{S}/\text{cm}$ which is considerably lower than the range of conductivities measured from the remainder of the standpipes. As well, this standpipe is installed in undisturbed K_m material below the S1 dump section according to cross-sections of SBH. SP 12 was only sampled in 2003 due to an obstruction in the pipe encountered in 2002. The obstruction was bypassed in 2003 by using a smaller diameter disposable bailer. The EC value may be indicative of some damage in the pipe which may be causing the unexpected groundwater chemistry in this standpipe.

The standpipe chemistry results were plotted on a Piper plot to illustrate the dominant groundwater chemistry types. Figure 4.34 shows all standpipe chemistry compared to the zones of oxidized and anaerobic chemistry obtained from solid sample analysis by Wall (2004). Figure 4.34 shows that the majority of the standpipe chemistry falls within the 'oxidized' zone ($\text{Na}-\text{SO}_4$ dominated chemistry) with the remainder within the 'anaerobic' zone ($\text{Na}-\text{HCO}_3-\text{SO}_4$) and in a 'transition' zone (slightly higher concentrations of Ca). A summary of the standpipes and their screen elevations is found in Table 4.3.

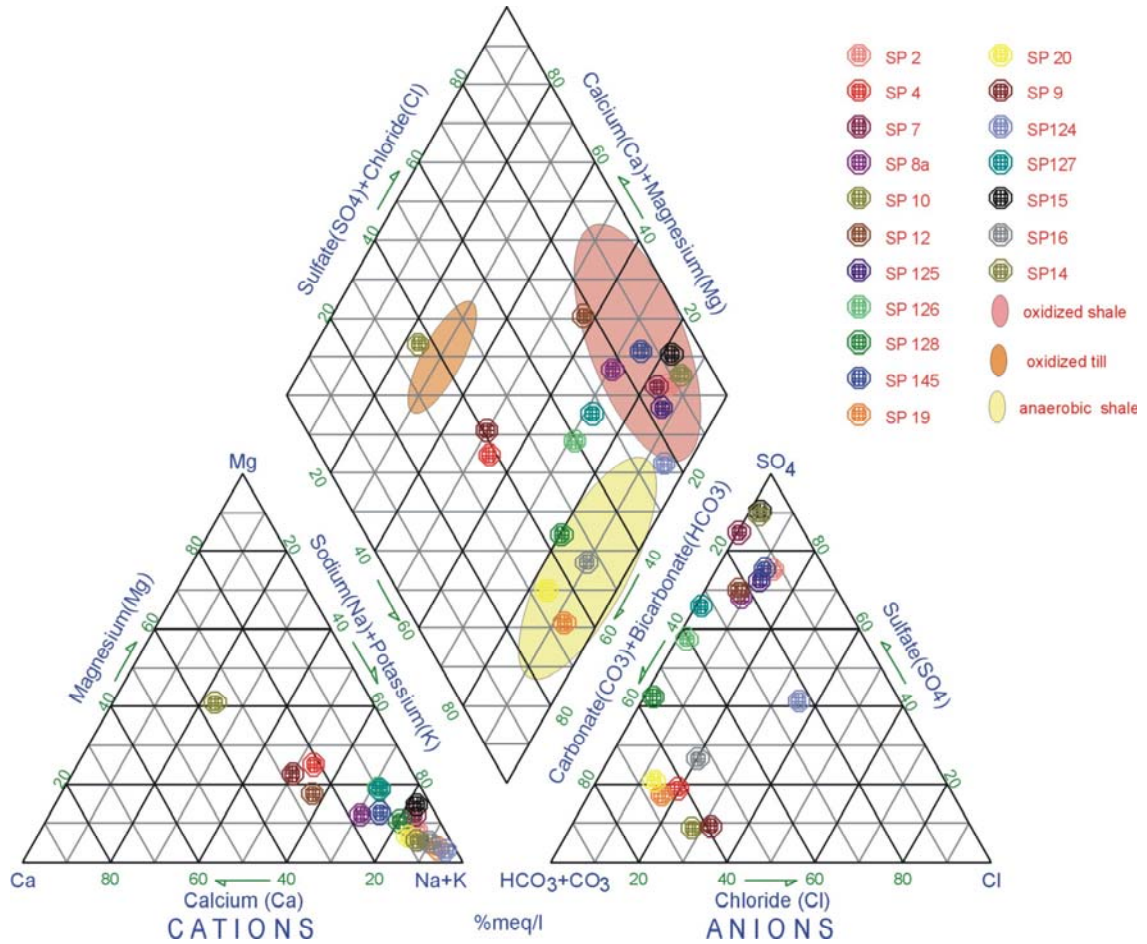


Figure 4.34 SBH standpipe chemistry (shown in symbols) compared to oxidized and anaerobic solid sample analysis (shown by shaded areas).

Table 4.3
Summary of standpipe chemistry

Piper Plot 'Zone'	Standpipe ID	Mid-Point Screen Elevation (m)	Location Notes
Oxidized	SP2	339	Top of SBH; 5 m lift construction
	SP7	335	Top of SBH; 5 m lift construction
	SP12	280	S1 dump installed in <i>in situ</i> K_m material
	SP14	310	End dumped K_c Fill
	SP15	304	End dumped K_c Fill
	SP125	318	6 m south of Peat Pond in end dumped fill
	SP145	288	In situ K_m

Table 4.3 (Cont'd)
Summary of standpipe chemistry

Piper Plot 'Zone'	Standpipe ID	Mid-Point Screen Elevation (m)	Location Notes
Anaerobic	SP16	259	End dumped K _c Fill (contact between Limestone)
	SP19	315	End dumped K _c Fill
	SP20	259	End dumped K _c Fill (contact between Limestone)
	SP128	317	3 m south of Bill's Lake; 5m lift construction
Till	SP10	332	S1 dump; 2 m lift construction
Transition	SP9	337	S1 dump; 2 m lift construction
	SP04	313	Top of SBH; screen in glacial till material of S1 dump
	SP124	323	Peat Pond
	SP126	312	Bill's Lake
	SP127	321	Bill's Lake

4.5.4 Summary - Piezometer Water Chemistry

The chemistry obtained from the SBH standpipes show that there are distinct types of waters. The standpipes located in the top of SBH above 320 m, where higher percentages of K_c materials are present, show chemical signatures of oxidized shale materials. The standpipes installed deep into the lower fill are Na-SO₄ dominated and have higher concentrations of HCO₃ compared to the rest of the hill. The chemistry from the standpipes located on the S1 dump are Na to Ca type waters dominated by HCO₃ corresponding to the higher amount of glacial materials. Those standpipes that fall outside the three distinct zones are found near the Bill's Lake and Peat Pond wetlands and may represent mixing between the localized flow system and deeper groundwater.

4.6 Investigation of Potential Flow Systems on SBH

Geological information, piezometer head data, hydraulic conductivity data, and chemistry data was used to identify the various hydrogeological units consisting of the potential groundwater flow system within SBH. From the investigation of water level measurements, it is evident that the piezometer water levels installed in the 2 m and 5 m construction lift areas, not installed near a wetland, show downward flow with evidence of perched conditions. In addition, shallow piezometers installed in the northwest region of the hill where the K_c fill materials are reported to

be greater than 25 percent of the material volume also show perched water table characteristics. Hydraulic conductivity values for these areas are consistent within similar material types (i.e. S1 dump glacial materials with a $K_{\text{geomean}} = 1.7 \times 10^{-8}$ m/s; K_c fill materials demonstrating perched conditions and a $K_{\text{geomean}} = 2.8 \times 10^{-9}$ m/s). The chemistry results are also fairly consistent in the different sections of SBH based on material type, with the northwest piezometers showing the highest EC values. A summary of the characteristics of the piezometers showing a 'perched' water table are found in Table 4.4.

Table 4.4
Summary of piezometer characteristics showing perched water table conditions.

Piezometer ID	K (m/s)	Species	EC (mS/cm)
SP10 (S1 Dump; 2 m lift)	1.6×10^{-8}	Ca-Mg-Na-HCO ₃	1770
SP9 (S1 Dump; 2m lift)	N/A	Na-Ca-HCO ₃	3060
SP4 (5m lift)	3.5×10^{-8}	Na-Ca-HCO ₃	2220
SP2 (5m lift)	2.8×10^{-9}	Na-SO ₄	7380
SP7 (5m lift)	3.9×10^{-9}	Na-SO ₄	13400
SP8 (5m lift)	2.8×10^{-9}	Na-SO ₄	8730
SP14 (Northwest)	2.6×10^{-10}	Na-SO ₄	15100
SP15 (Northwest)	9.2×10^{-9}	Na-SO ₄	12240
SP21 (Northwest)	N/A	N/A	N/A
SP22 (Northwest)	1.8×10^{-9}	N/A	N/A

Value from Rutten (2006)

Piezometers SP 21 and SP 22 did not have hydraulic conductivity tests or chemistry samples taken during 2002 and 2003 and showed low, constant water depths until 2004 when one hydraulic conductivity test was completed on SP 22 by Rutten (2006). These standpipes are considered to be in 'perched' conditions, however; they should be investigated further in future to determine if the water levels continue to rise and whether samples of the water can be collected for chemical analysis.

A second grouping can be distinguished in the shallow piezometers around the Peat Pond and Bill's Lake wetlands. For both Peat Pond and Bill's Lake, there is evidence of the development of a localized flow system that responds to the water level in the pond. For the majority of the year, both wetlands act as recharge areas with water flowing away from the ponds. Chemistry results from these piezometers show that there may be some mixing between the groundwater and the pond water. The pond water chemistry is influenced by runoff and interflow through the cover system of glacial soil while the groundwater is determined by the saline-sodic overburden. Table 4.5 shows the characteristics of the piezometers around the ponds.

Table 4.5

Summary of piezometer characteristics installed around Peat Pond and Bill's Lake shallow wetlands.

Piezometer ID	Location Description	Hydraulic Conductivity (m/s)	Species	EC (mS/cm)
SP124	Peat Pond	3.6×10^{-9}	Na-SO ₄ -Cl-HCO ₃	11440
SP125	Peat Pond	1.4×10^{-8}	Na-SO ₄ -HCO ₃	6210
SP126	Bill's Lake	1.1×10^{-9}	Na-SO ₄ -HCO ₃	5280
SP127	Bill's Lake	1.7×10^{-9}	Na-SO ₄ -HCO ₃	4150
SP128	Bill's Lake	4.2×10^{-9}	Na- HCO ₃ -SO ₄	5100

The third main group consists of those piezometers that are installed to the base of the pile at the interface of the limestone and the K_c fill. The characteristics of the three piezometers are found in Table 4.6. The water level in all three show artesian behaviour with heads increasing slightly over time, possibly in response to the increase in WIP water levels. Chemically, these standpipes are fairly similar with approximately 65 percent HCO₃ indicating that the water has exposed to less oxidizing conditions than the surface K_c fill materials.

Table 4.6

Summary of piezometer characteristics located at contact limestone base of SBH.

Piezometer ID	Hydraulic Conductivity (m/s)	Species	EC (mS/cm)
SP 8a	N/A	Na-HCO ₃ -SO ₄	1468
SP 16	1.8×10^{-8}	Na-HCO ₃ -SO ₄ -Cl	2430
SP 20	4.5×10^{-9}	Na-HCO ₃ -SO ₄ -Cl	2582

Table 4.7 shows the two piezometers that are installed in undisturbed K_m. The chemistry and hydraulic conductivity values in these standpipes vary slightly. Water samples collected by Reszat (2002) installed in undisturbed K_m materials were found to be predominantly Na-Cl to Na-Cl-SO₄. SP145 shows Na/Ca as a percentage of total cations as 75%/25% and SO₄/Cl as a percentage of total anions as 75%/25%. The difference in chemistry may be attributed to slightly different material types in these areas. The Ca level found in SP12 is consistent with the chemistry found in the shallower standpipes in the same nest installed in the glacial S1 materials. As noted in Section 4.3.3, this standpipe may have experienced some damage which is causing leakage. Both values of hydraulic conductivity are within the given range of 1.0×10^{-10} m/s to 1.0×10^{-5} m/s for *in situ* K_m at the Mildred Lake site as provided by Syncrude (2005). The water levels are decreasing over time in both standpipes, which may indicate that pore pressures may be dissipating after the overburden load placement or that this formation is draining.

Table 4.7
Summary of piezometer characteristics in *in situ* K_m material.

Piezometer ID	Hydraulic Conductivity (m/s)	Species	EC (mS/cm)
SP 12	3.3×10^{-10}	Na-Ca-SO ₄ -HCO ₃	136
SP 145	$3.6 \times 10^{-8*}$	Na-SO ₄	8660

Standpipes (SP 1-1, SP1-2, SP 4-1, and SP 4-2) installed late in 2003 (Table 4.8) were not included in the 2003 hydraulic conductivity testing or did not have samples collected for chemical analysis. Hydraulic conductivity tests were performed on SP 4-1 by Rutten (2006). Looking at the first year of water level data, SP1-1 and SP 1-2 are displaying perched behaviour over the first year of installation reaching steady-state levels quickly and remaining there, while standpipes SP 4-1 and SP 4-2 show artesian conditions. The artesian conditions may be a result of build up of pore pressure behind the lean oil sands pillar located to the north.

Table 4.8
Summary of piezometer characteristics of piezometers showing artesian conditions in K_c fill.

Piezometer ID	Hydraulic Conductivity (m/s)	Species	EC (mS/cm)
SP 19	3.3×10^{-10}	Na-Ca-SO ₄ -HCO ₃	136
SP 4-1	N/A	N/A	N/A
SP 4-2	$2.1 \times 10^{-7*}$	N/A	N/A

Value from Rutten (2006)

Standpipe SP 19 is located in the same nest as SP 20, but the tip is installed at an elevation of 315 m in fill placed in 5 m lifts. This standpipe has been included in this group because it also shows similar artesian behaviour and is located 200 m south of the nest containing SP 4-1 and SP 4-2. The hydraulic conductivity is consistent with that of K_c material, however the chemistry is similar to the piezometers installed to the base of the pile. These standpipes may be receiving flow from east where the materials used to construct this area are estimated to be less than 15 percent K_c compared to greater than 25 percent K_c on the west side of SBH. Additional piezometers installed on the east side of the hill would be beneficial to define flow patterns from the east side.

4.7 *In situ* Moisture and Density using Neutron Probe

A neutron access tube consisting of carbon steel was installed in August 2002 to investigate *in situ* volumetric water content using a neutron moisture gauge. Details of the access tube installation can be found in Wall (2004). Neutron counts were converted to volumetric water

content using a calibration curve for the carbon steel access tube. One density profile was measured in 2005. Figure 4.35 shows the neutron probe readings from October 2002 to August 2005. The density profile measured in October 2005 is shown in Figure 4.36. It should be noted the location of the neutron access tube is on the top surface of SBH to a depth of 330 m and is likely not reflective of all areas of SBH.

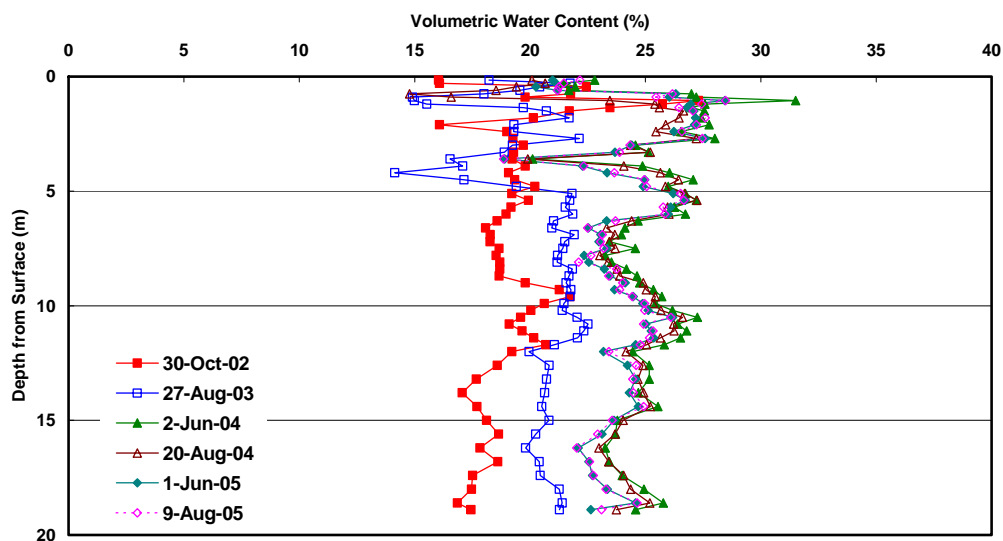


Figure 4.35 Volumetric water content measured with the neutron probe for October 2002 to August 2005.

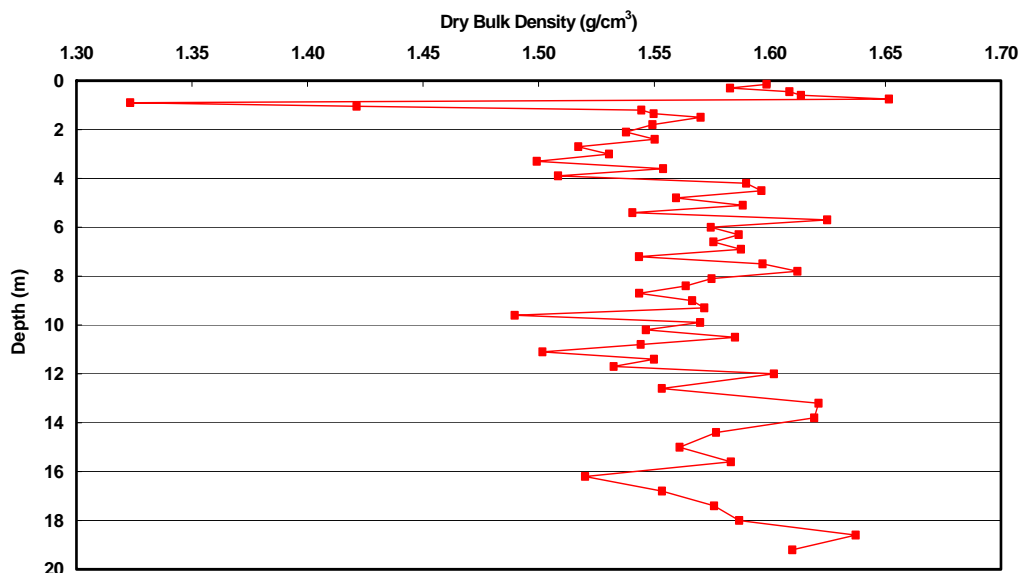


Figure 4.36 Dry bulk density profile measured with the neutron probe for October 2005.

From the moisture profile shown in Figure 4.35, there appears to be a large increase in the moisture content over the three years; however, it is likely that the readings from 2002 and 2003

are not reflective of true conditions due to the installation technique. The tube was installed using a hammer drill which pounded a 5 inch diameter casing to 20 m and then 71 mm rods were pushed down inside the casing and the casing was removed. This type of installation relies on the shale collapsing and sealing the contact between the casing and the access tube thus any loose material or open sections around the access tube would register low water contents. The readings from 2004 and 2005 are likely more accurate and give consistent readings within the profile between the two years. From Figure 4.34, it appears that the moisture content in the profile has decreased slightly from 2004 to 2005 with an average volumetric water content of approximately 0.25. Figure 4.35 shows slightly different density zones. The density values are summarized in Table 4.9 with median density values varying between 1.55 and 1.59 g/cm³. Looking at the correlation between moisture content and density, there appears to be a peak in moisture content just at the top of each zone that measures a higher density. The different zones may be a reflection of the 5 m lift construction at the top of the hill.

Table 4.9

Summary of different 'zones' as measured by density probe in deep access tube

Depth (m)	Dry Density (g/cm ³)		
	Minimum Value	Maximum Value	Median Value
0 – 1.2	1.32	1.65	1.59
1.2 – 3.9	1.50	1.57	1.54
3.9 – 8.4	1.54	1.62	1.59
8.4 – 12.6	1.49	1.60	1.55
12.6 – 19.2	1.52	1.64	1.58

An analysis was done to investigate the possible change in *in situ* properties of the overburden, such as volumetric water content and degree of saturation, due to excavation and placement. Table 4.10 shows values of density and porosity of *in situ* and rehandled K_c material according to Lord and Isaac (1989). Volume-mass relationships were used to estimate the density and volumetric water content of the SBH placed K_c material using the original density and gravimetric water contents of *in situ* K_c, and assuming an average placement density.

Table 4.10

Measured and calculated values for K_c properties (Lord and Isaac, 1989).

Material Property	Bulk Density (kg/m ³)			Dry Density (kg/m ³)			Porosity		
	Max	Min	Average	Max	Min	Average	Max	Min	Average
<i>In situ</i> K _c	2100	2070	2085	1780	1760	1770	0.35	0.34	0.34
Rehandled K _c	2000	1700	1850	1634	1375	1510	0.49	0.39	0.44

It is assumed that the *in situ* material was saturated (degree of saturation, $S = 1$) prior to excavation with a pre-excavation dry density of 1770 kg/m^3 (Table 4.10). This corresponds to an *in situ* porosity of 34% and a gravimetric water content of 0.19. The average placement dry density of rehandled K_c was assumed to be 1510 kg/m^3 for (Table 4.10) with a specific gravity of 2.7 (Boese, 2003) and a constant gravimetric water content of 0.19, which is a reasonable assumption based on findings from Lord and Isaac (1989). The resulting porosity of the K_c fill at time of placement is then calculated as 44%, with a volumetric water content of 0.29 which corresponds to a degree of saturation of 0.67. Based on these initial conditions, a range of dry densities and volumetric water contents were plotted to compare conditions measured at SBH. Figure 4.37 shows that the volumetric water contents are within the expected range at the lower densities, however as the density increases, the measured water contents at SBH are lower than expected, indicating that drainage may be occurring within the pile.

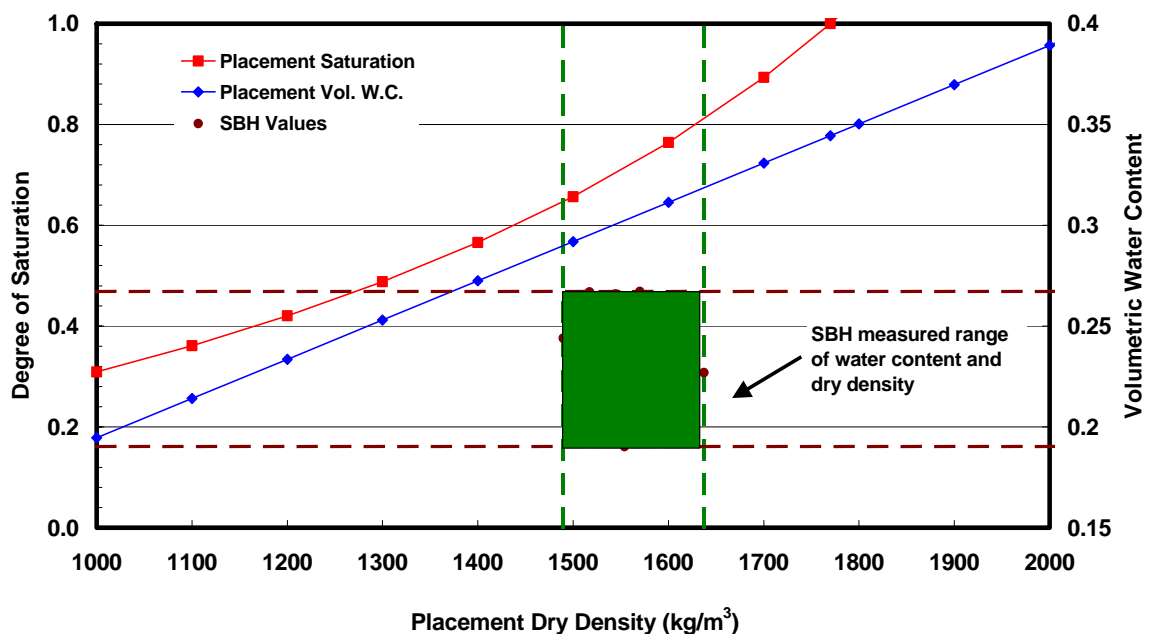


Figure 4.37 Range of placement saturation and volumetric water content compared to conditions measured at SBH in 2005.

A simple analysis was also undertaken to determine to what of degree subsidence might have occurred since placement based on the above assumptions and using a placement dry density of 1510 kg/m^3 . It is assumed that volume of water within the fill has remained constant and that subsidence has decreased the total volume (and volume of voids). Figure 4.38 shows the changes in water content and saturation that would have occurred for various levels of subsidence in the pile. It is apparent that the volumetric water content is relatively insensitive to subsidence, while the degree of saturation is much more sensitive. For example, over a range of subsidence values from 0 to 6% the volumetric water content increases from 29% to 30%

while the degree of saturation increases from 0.67 to 0.77. The value of 30% for volumetric water content is approximately the water content measured in 2005. A subsidence of the pile of approximately 6% since placement in 1996 is equivalent to 1.2 m of subsidence over the 20 m profile of the neutron access tube. As noted in Section 4.2, long-term subsidence up to several meters was expected due to variability in materials, construction methods, and exposure to meteoric water (McKenna, 2002).

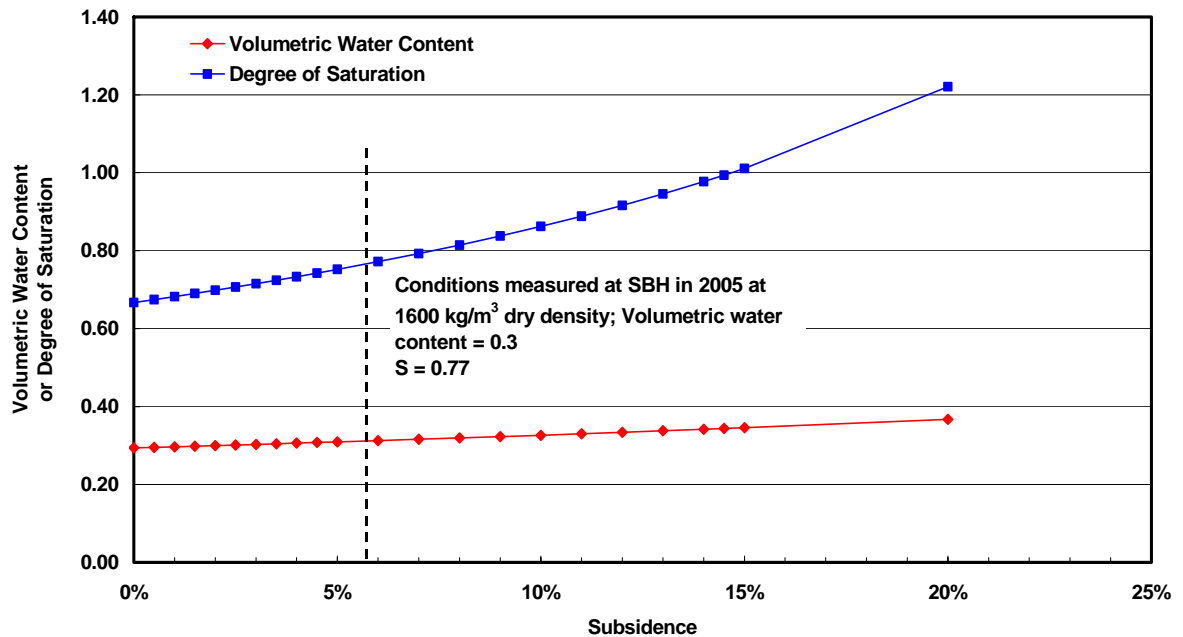


Figure 4.38 Subsidence with changes in volumetric water content and saturation at SBH.

4.8 Seepage Indicators and Measured Seepage Rates

Ground surveys of the base of both the north and south faces of SBH were undertaken in order to observe any indication of groundwater seepage on any of the slope faces as outlined in Section 3.8. The north side of the hill faces the WIP and south side of the hill is adjacent to the Beaver Creek wetland, at an elevation of 304 m. The two faces were extremely different in terms of vegetation establishment and construction as shown in Figures 4.39 and 4.40 due to differences in cover placement and age (cover and revegetation on south side versus no reclamation efforts on north side). There was no visible evidence of any groundwater discharge on the north face of SBH.



Figure 4.39. North side of SBH showing vegetation.



Figure 4.40 South side of SBH showing lush varying vegetation

The south side S1 was walked in during the summers of 2002 and a small ditch of water at an elevation of 310 m was observed at the base. A small stream of bright orange water was observed which contributed to the 'main' ditch approximately half way across the base of the hill

(Fig. 4.41). Observations made by Dr. Brett Purdy, University of Alberta (personal communication, August 2002) during a site visit to investigate vegetation seepage indicators, concluded that the vegetation that was establishing on this site is typical of disturbed conditions, and could not provide direct evidence of groundwater seepage locations.



Figure 4.41 Seepage stream observed on South side of SBH.

4.8.1 Seepage Stream Flow Rates

Groundwater discharge rates were estimated by taking manual measurements from the drainage ditch along the south side of the hill as described in Section 3.2. Measurements started in July of 2002 and continued on a bi-weekly basis through to October, resuming again in May 2003. A simple analysis was done in attempt to investigate the discharge rate to the south side of SBH. Equation 4.1 describes the inputs and outputs for the ditch located on the south side. All values are in m^3/s .

$$Q_{SBH} + Q_P - Q_{PE} - Q_{BC} = Q_o - Q_{in} \quad [4.1]$$

Where Q_{SBH} is the seepage into the ditch from SBH, Q_P is the precipitation (P) and Q_{PE} is the potential evaporation (PE) from the free water surface of the ditch. Both P and PE values are obtained from a Syncrude automated meteorological station located at the top central surface of SBH at an elevation of 350 m. Flow rates for P and PE are calculated as the value measured (mm) taken over the area of the ditch (m^2) during the time period between inlet and outlet measurement (seconds). Q_{BC} is the loss to Beaver Creek on the south side due to the elevation

difference (ditch elevation 310 m and Beaver Creek 304 m) and $Q_o - Q_{in}$ is the difference between flow rates measured at the outlet and inlet pipes of the ditch. The loss to Beaver Creek is considered to be negligible due to the low permeability of the *in situ* K_c materials below the ditch to Beaver Creek.

Equation 4.1 can be rearranged to calculate the flow rate of seepage discharge into the ditch from the south side of SBH [Eq. 4.2].

$$Q_{SBH} = Q_o - Q_{in} + Q_{PE} - Q_P \quad [4.2]$$

Figure 4.41 shows a plot of Q_{out-in} and Q_{PPT-PE} compared to Q_{SBH} over the period of measurement.

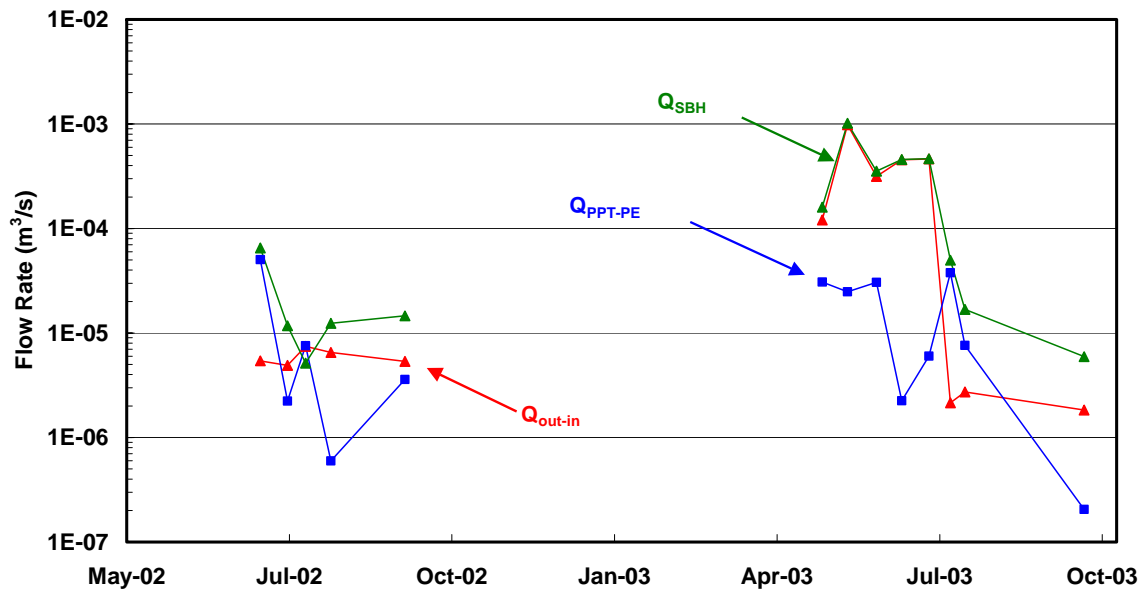


Figure 4.41 Flow rates measured from inlet and outlet pipes on south side of SBH in 2002 and 2003.

From Figure 4.41, it appears as though contributions to the ditch are seasonally based. In May and June, there appears to be a large contribution to the stream and using Equation 4.2, this indicates that the contribution is from groundwater seepage from SBH. It is important to note that 'discharge' from SBH would also include components of runoff due to snowmelt or rainfall as well. It is more likely that the elevated rates in May and June are the result of spring melt / runoff since groundwater seepage is not largely affected by seasonal changes. From July to October, the input to the ditch appears to be dominated by the seepage from SBH. From Figure 4.41, the groundwater seepage from SBH can be estimated to be in the range of $6.0 \times 10^{-6} \text{ m}^3/\text{s}$ to $2.0 \times 10^{-5} \text{ m}^3/\text{s}$.

The S1 dump is an order of magnitude more permeable than the remainder of SBH mainly due to the difference in construction material (P_g and P_l tills used at the S1 dump versus mainly K_c clays for the remainder of SBH). A preliminary analysis was done using the measured flow on the south side of the S1 dump to estimate the flow system out the south side of SBH. Dupuit (Fetter, 1994) developed a method to account for the changing hydraulic gradient in an unconfined aquifer. The theory was based on the following assumptions:

- 1) The hydraulic gradient is equal to the slope of the water table; and
- 2) The streamlines are horizontal and equipotential lines are vertical for small water table gradients.

These assumptions are limited in that they do not account for a seepage face above the outflow side, the vertical component of flow is ignored, and the calculation of flow, Q is simplified to one-dimension (Fetter 1994). Developed from Darcy's Law, the Dupuit equation used in the following analysis is as follows:

$$h = \sqrt{h_1^2 + \frac{w}{K}(L-x)x} \quad [4.3]$$

where h_1 is the saturated thickness of the aquifer at the origin (m), w is the recharge rate (m/s), K is the hydraulic conductivity (m/s), and L is the flow length (m), and x is the horizontal distance along the aquifer (Fetter, 1994).

To use the Dupuit analysis in this case, the flow system is assumed to start at the seepage face on the south side at an estimated saturated thickness of 1 m. Assuming that $h_1 = h_2$ (the analysis of half of a symmetrical system) and the distance from the south edge of S1 to the start of K_c dump is $L/2 = 325$ m, the h_{\max} of the flow system can be found at the interface of the S1 dump and the K_c portion of SBH.

The recharge value, w , was estimated over a range measured from the seepage stream. The measured range fell between 6×10^{-6} to 2×10^{-5} m^3/s which when taken over the area of the base of S1, considered to be the area of the unconfined aquifer (325 m (north to south) \times 1000 m (east to west)) ranged between 0.1 mm/year and 0.3 mm/year of recharge. The K values were all varied to investigate the parameters which would result in a reasonable flow system for the S1 portion of SBH. The results using the Dupuit analysis is found in Figure 4.42

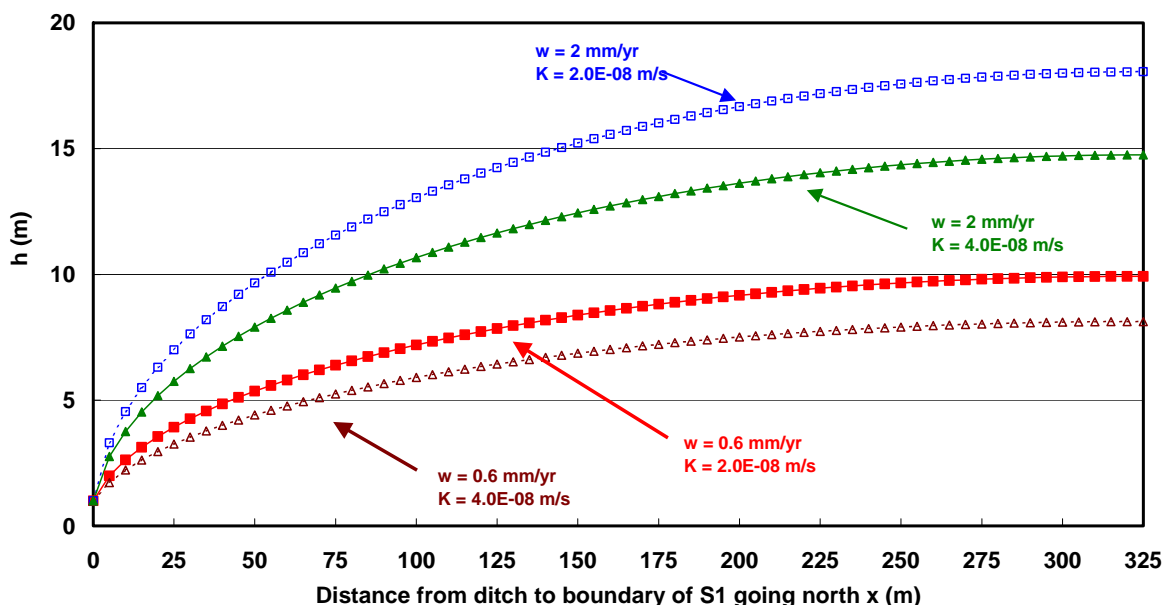


Figure 4.42 S1 heads versus location (N-S) for various recharge rates using Dupuit analysis.

Figure 4.42 shows that an increase of only 1.4 mm recharge results in a notable change in the maximum height of the aquifer, which is more significant with a lower permeability value. It is difficult to directly compare the heads produced by the Dupuit analysis to field conditions since the piezometers installed in the S1 dump show perched conditions (Section 4.3.3). Piezometer SP4 is the deepest piezometer located on the top, south side with a tip elevation of approximately 315 m in S1 dump materials just below the interface of the till and the K_c materials of the rest of SBH (Figure 4.9, Section 4.3.4). The head measured in this standpipe has remained relatively constant since installation at approximately 318 m. If the head value measured at SP4 was considered to be at the location of maximum head, a K of 4×10^{-8} m/s and a recharge rate of 0.6 mm/year give a reasonable estimation of the flow out the south of SBH based on the head measurement at SP4 on the north side of the S1 dump. These results can be used to verify conceptual numerical model in Chapter 5.

4.9 Summary

South Bison Hill is a newly constructed overburden pile constructed mainly of K_c clays that are saline-sodic in nature. Characterization of this evolving hydrogeological system requires that a number of features of this system be evaluated including the topography and geology, hydraulic properties such as hydraulic conductivity, water content and saturation, chemistry and the distribution of total head.

The construction and geologic make up of the pile was put together through investigation of mine records and interviews with site personnel. These searches revealed that this pile was constructed over a 16-year period in four main sections. Each section had different types of construction materials and methods that provide distinct characteristics for each section.

Some general observations can be taken from the historic water level measurements from the SBH piezometer network. The piezometers installed in sections constructed of 2 m or 5 m lifts show downward flow with evidence of perched conditions. The piezometers installed around the Bill's Lake and Peat Pond wetlands show downward and outward flow conditions indicating that the wetlands are in a recharge condition. Three piezometers installed to the base of the pit provide some indication that the groundwater flow deep within the pile is likely north to south and possibly from the west. All three piezometers show a rise in water level over time, with one showing more irregular behaviour. The rise in the water levels in these three piezometers may be a reflection of the WIP tailings pond on the north side of SBH. Water levels located on the north side of SBH show some evidence of being influenced by the lean oil sands pillar located on the north side of SBH. The piezometers that are located distances of 20 to 180 m away from the pillar show higher than expected water levels.

Hydraulic conductivity and water chemistry was investigated from a network of standpipe piezometers installed in the study area. Information collected from the piezometers is fairly consistent with construction materials and methods. The section of the hill known as the S1 dump contained higher amounts of glacial till and was constructed in 2 m lifts. The geometric mean K value measured 1.7×10^{-8} m/s. This section is approximately one order of magnitude more permeable than other sections of SBH and the geochemistry shows to contain higher amounts of Ca and HCO_3 as compared to remainder of SBH composed of higher amounts of K_c clays. The section of SBH from 320 m to 350 m elevation was constructed in 5 m lifts and consists of the highest percentage of K_c clays. The geometric mean K value was calculated to be 2.8×10^{-9} m/s. Groundwater collected from piezometers installed in this section of SBH is mainly Na- SO_4 dominant waters, characteristic of oxidized shale.

The section of SBH from an elevation of 320 m to the limestone base of 260 m consists of less amounts of K_c compared to the top portion, with some K_{cw} and glacial till material. This section of SBH is approximately half an order of magnitude more permeable than upper section with a geometric mean K value of 5.2×10^{-9} and contains higher amounts of HCO_3 compared to the top of SBH indicating that it has experienced less oxidation than the top section of the pile. The three piezometers installed at the base of the pile provided limited data. Geochemistry from these standpipes is mainly Na- HCO_3 - SO_4 . Limited hydraulic conductivity data shows that the piezometers installed at this depth are more permeable than fill at higher elevations. Two

piezometers were installed in *in situ* K_m material. Values of measured hydraulic conductivity were within the range measured for this formation in the region with a mean value of 2.9×10^{-9} m/s, however geochemistry results from these two piezometers were quite different. The differences in the two may be due to damage in one of the standpipes resulting in leakage.

Volumetric moisture content and density data was collected from a deep neutron access tube located on the top of the hill. A preliminary analysis was undertaken to compare these measured values of volumetric water content within SBH to the *in situ* conditions, and placement conditions. The measured volumetric water contents measured are within the expected range at lower densities, but as the density increases the measured volumetric water contents are lower than expected indicating that drainage may be occurring in the pile. Based on measured conditions compared to placement conditions, it is estimated that the pile has subsided approximately 6% equivalent to 1.2 m over the 20 m profile of the access tube. This is not surprising since long-term subsidence of the pile up to several meters was anticipated and incorporated into the design of the surface of SBH.

A seepage stream was observed at the base of SBH of which a base flow was measured in 2002 and 2003 of a discharge rate per linear meter of stream of 6.0×10^{-9} m³/s/m and 1.0×10^{-9} m³/s/m respectively. The recharge values were used in a preliminary analysis to characterize the flow system of an unconfined aquifer using the analysis developed by Dupuit. This analysis was applied to the south side known as the S1 dump which is estimated to be one order of magnitude more permeable than the rest of SBH due to the till construction materials. The analysis showed that the head within the S1 dump was sensitive to recharge rates and an increase in recharge rate of only 1.6 mm/year resulted in an increase in the maximum head of 3 m. A reasonable flow system through S1 using the Dupuit analysis resulted using a recharge rate of 0.6 mm/year and a K of 4×10^{-8} m/s. All data acquired by the analysis conducted in Chapter 4 will be used in the development of a conceptual steady-state model of SBH described in Chapter 5.

CHAPTER 5

CONCEPTUAL FLOW MODEL

5.1 Introduction

The field and research data were compiled to create a simple conceptual two-dimensional numerical model of the hydrogeologic system within the South Bison Hill (SBH). The apparent 'geology' of SBH can be divided into five distinct sections as determined by mine construction records and verified by hydraulic conductivity and groundwater chemistry patterns obtained from previously and newly installed standpipe piezometers. The steady-state model will be used to investigate the sensitivity of the water table location with changes in head boundaries, infiltration rates, and hydraulic conductivity.

5.2 Purpose and Approach

SBH construction was completed in 1996. The West In Pit (WIP) and Beaver Creek Reservoir border the north and south sides of the hill. WIP is a composite tailings reservoir that is continuously receiving additional tailings. The head of WIP is expected to rise to a level of 310 m and reclaimed by capping with an additional 5 m of fresh water by 2012. The purpose of the modelling exercise is to determine whether the conditions measured in the field provide a reasonable representation of the hydrogeologic system of SBH. A two-dimensional (2-D) steady-state numerical seepage model was carried out using SEEP/W (Krahn, 2004), a finite element analysis package.

The modelling programme developed for this project was divided into four parts:

- Development of a model mesh based on the conceptual geological model, measured K-values, and head boundary conditions;
- Prediction of steady-state seepage conditions for SBH including a sensitivity analysis of key input parameters for the model; and
- Prediction of seepage conditions for SBH following rise in north head boundary WIP.

5.3 Development of the Model Area

The numerical model of SBH is focused on north to south flow based on Beaver Creek Reservoir on the south and WIP on the north. A cross-section running north/south (Section 50200 E looking west) was selected to incorporate the major sections of SBH. The composition of SBH in the model was based on the geologic model developed in Section 4.2 and consists of the S1 dump, the lower K_c fill from 260 m to 320 m elevation, upper K_c fill material from 320 to 350 m elevation, and *in situ* K_c and *in situ* K_m which includes the pillar remaining at the north end of the hill. *In situ* hydraulic conductivity (K) values used in the model were measured during the 2002 and 2003 field program, as well as values obtained from the literature, which are summarised in Table 5.1.

The flow system is likely to be three dimensional in nature given that some of the flow 'backed up' by the oil sands pillar will flow to the east and west around the pillar as well as over the pillar. The two dimensional model will force all of the flow to go over the oil sands pillar and consequently will tend to overestimate the head levels behind the pillar. Further investigation of the three dimensional nature of this flow system is recommended in future work.

Table 5.1
In situ K values used in the SBH numerical model.

Material	Saturated Hydraulic Conductivity (K) (m/s)
S1	1.7×10^{-8}
Fill 1 (above 320 m)	2.8×10^{-9}
Fill 2 (below 320 m)	5.0×10^{-9}
<i>In situ</i> K_m	$7.0 \times 10^{-9*}$
<i>In situ</i> K_c	$3.2 \times 10^{-12*}$

(Syncrude, 2005)

The 2-D model of SBH is focused on steady-state, saturated or perched flow. A simplification of K-functions was assumed. The hydraulic conductivity functions used for the different materials of SBH are assumed that $K = K_{sat}$ at a pressure of -1 kPa and dropping to $K = K_{sat}/1000$ at -100 kPa. Figure 5.1 shows the model mesh used for the steady-state analysis.

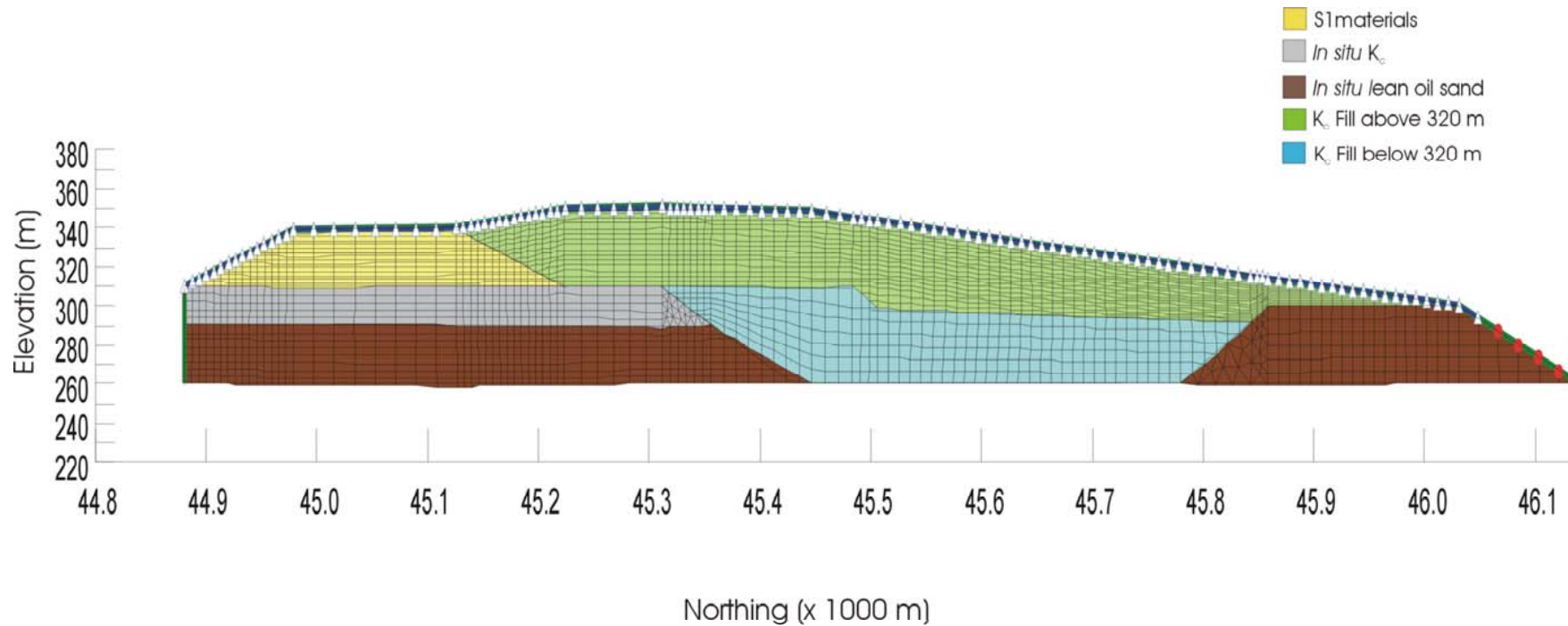


Figure 5.1 Model mesh through Section 50200 E used for the SBH steady-state seepage analysis.

5.4 Boundary Conditions and Simulation Scenarios

5.4.1 Model Inputs and Assumptions

The key inputs used in the steady-state SEEP/W analysis include field measured K, described in Section 5.3, and boundary conditions including the net recharge across the surface of the pile, and head boundary conditions to the north and south. A zero flux or no-flow boundary was set at the limestone base based on studies conducted by Syncrude (G. Kampala, personal communication) where water is prevented from entering or escaping. A no flow boundary was set on the south side due to the distance to Beaver Creek Reservoir although a free surface (seepage face) is allowed to form along the downstream of S1. A head boundary of 290 m of the WIP was set on the north side according to 2004 survey results conducted by Syncrude. The surface flux into the pile is assumed to be equally distributed across the pile although a free surface is allowed to form if required.

5.4.2 Steady State Analysis

An initial analysis was performed to develop a reasonable steady-state interpretation of the flow system using the specified input parameters. To provide a reasonable estimation of the flow system of SBH, a range of surface flux values were simulated was chosen between 0.1% and 5% of total precipitation (approximately 450 mm annually). This range of flux values is reasonable based on work by Boese (2003). A field program conducted by Boese (2003) used automated moisture content and matric suction sensors installed with depth through three different layered cover designs over the K_c shale on the north-facing slope of SBH to investigate cover field performance. These sensors showed that the moisture content in the deeper shale sediments (approximately 30 cm below the shale/cover interface of the three different covers) only fluctuated by approximately 2% indicating that there is little percolation into the underlying shale beyond the interface of the shale and cover material. For illustration purposes, the steady state results for values of surface flux (% of precipitation) of 0.6 mm/yr (from Dupuit analysis, Section 4.8.1, 0.13%), 4 mm/yr (0.9%), 8 mm/yr (1.8%) and 20 mm/yr (4.4%) flux values are presented in figures 5.2, 5.3, 5.4, and 5.5 respectively. The field measured piezometer water levels found in the modelled cross-section are represented by the vertical lines and the modelled water table is shown in each figure

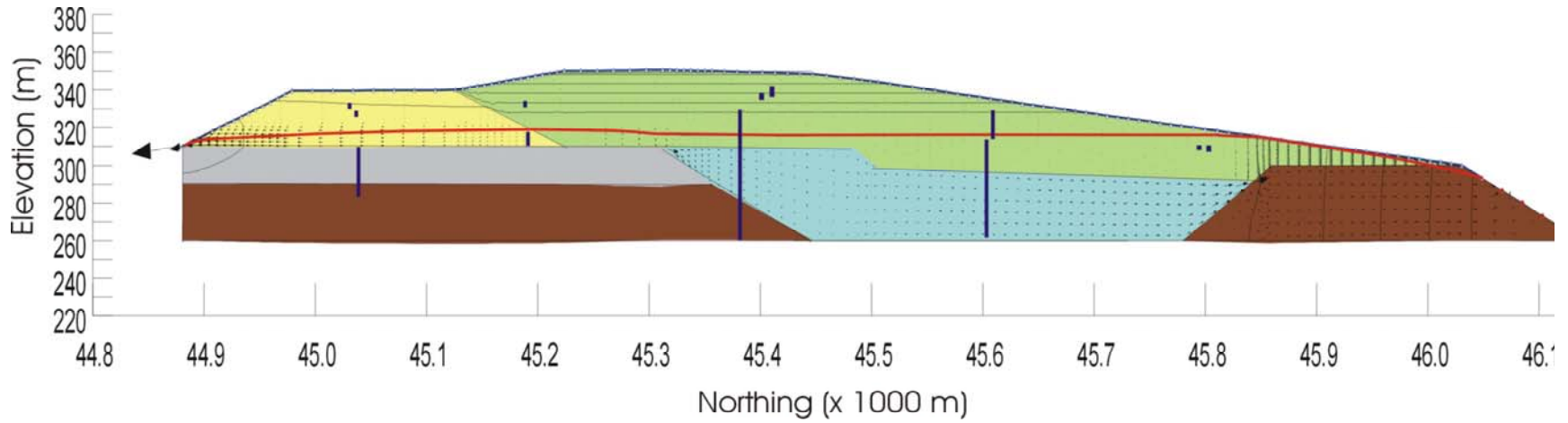


Figure 5.2 SBH steady-state seepage analysis for 0.4 mm/yr flux value.

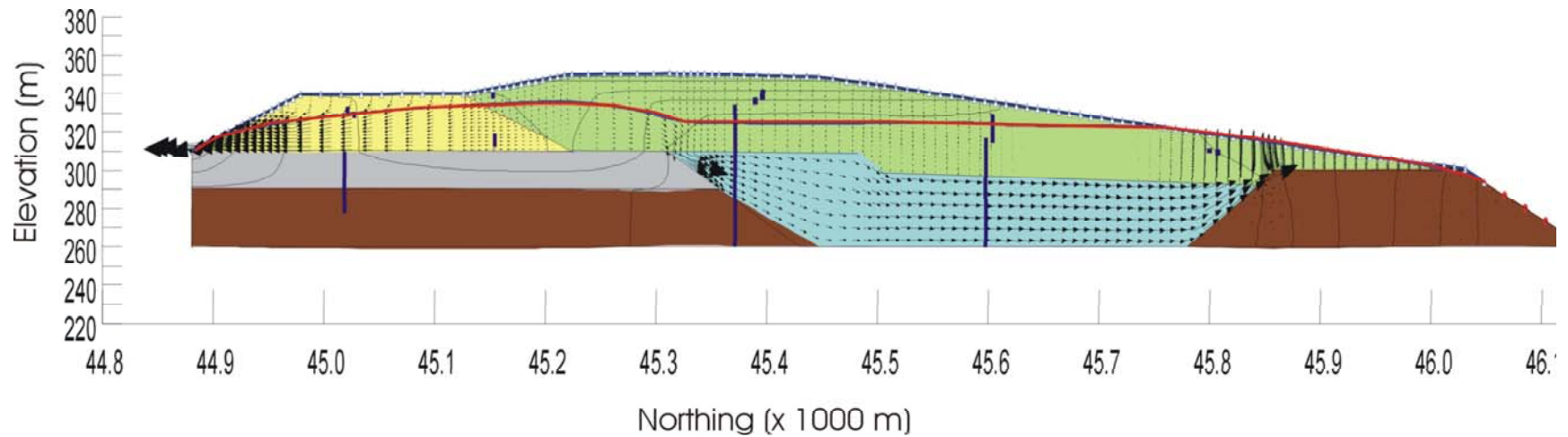


Figure 5.3 SBH steady-state seepage analysis for 4 mm/yr flux value.

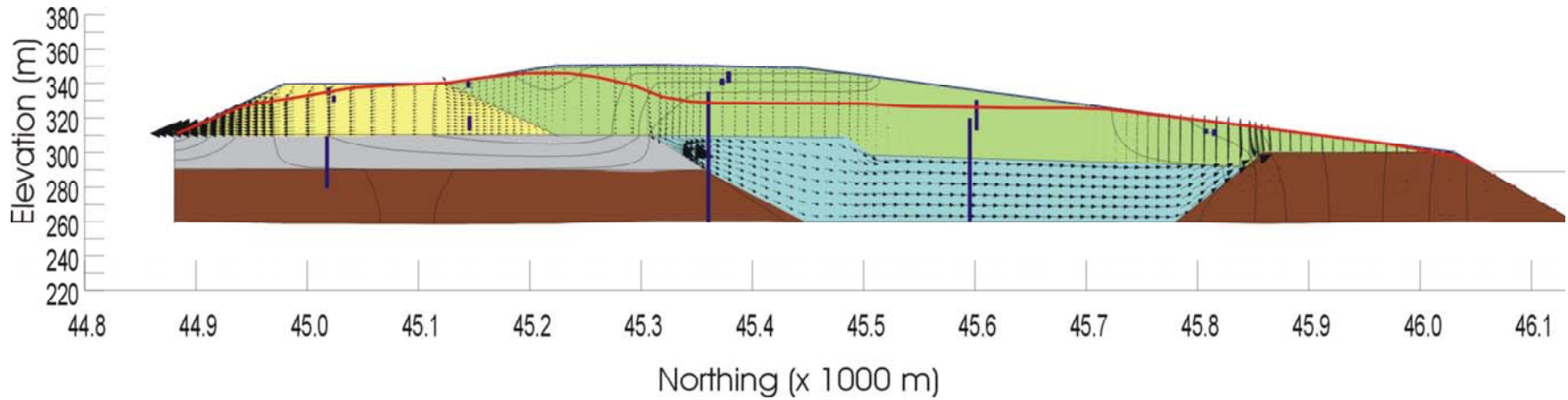


Figure 5.4 SBH steady-state seepage analysis for 8 mm/yr flux value.

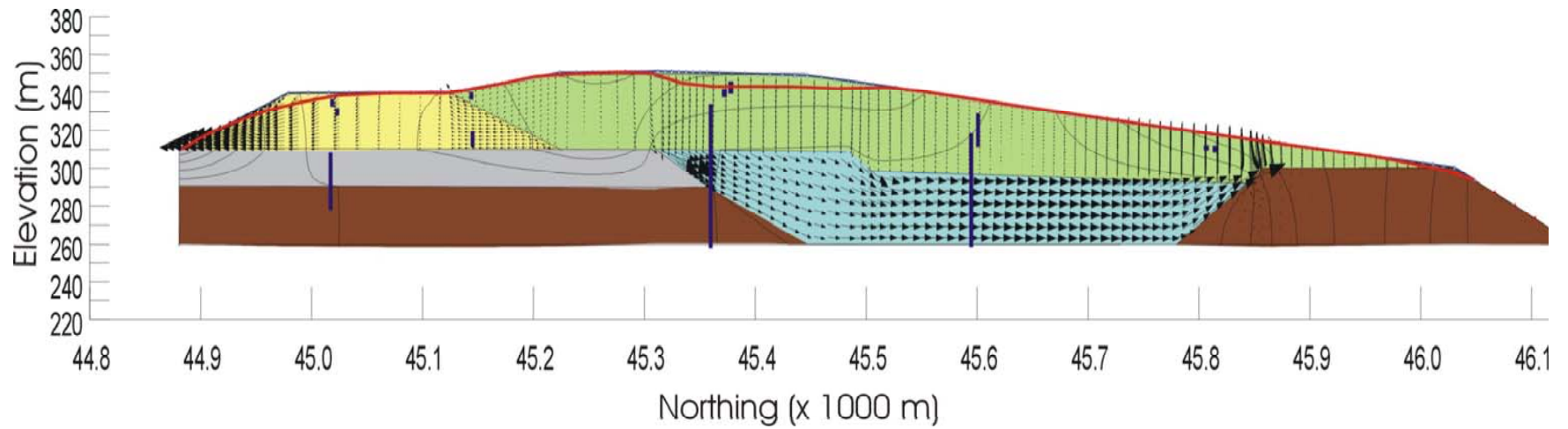


Figure 5.5 SBH steady-state seepage analysis for 20 mm/yr flux value.

In general for the different flux scenarios, the shape of the water table is similar. Starting at 45200 m (northing), water drains toward the south through the more permeable S1 dump materials. Moving toward the north from 45200 m, mounding occur in the upper fill materials above the *in situ* K_c material, then a drops over the location of the filled in pit where the unstructured K_c fill has a higher permeability. The flow to the north occurs in the lower fill materials. The water table mounds slightly as it approaches the lean oil sand pillar with a K slightly less permeable than the lower fill materials. The modelled results of the S1 water table and the mounded water table on the north side of the hill in all flux conditions is higher than expected compared to water levels measured in the field.

With increasing fluxes, the water table increases with increasing flux as expected and the groundwater divide shifts northward. The water table appears to be controlled by the height of the WIP head boundary on the north side for the 0.4 mm/yr (1.4×10^{-11} m/s) flux value. This flux value is two orders of magnitude lower than the hydraulic conductivity of the Fill 1 materials (2.8×10^{-9} m/s) and therefore, any flux that is reaching the pile moves through the upper materials and is drained through the S1 to the south and through the lower fill materials to the north. For the 4 mm/yr, 8 mm/yr, and 20 mm/yr the height of the water table is determined by the ratio of q to K of the upper fill materials. Of the flux scenarios simulated, the 8 mm/yr flux value shows the most reasonable match to field conditions through the Fill 1 section of the hill but is higher on the south through the S1 dump. A sensitivity analysis will address this further in Section 5.4.3. On the north side, the simulated heads are higher as well. Looking at the field water level measurements on the north side of the hill, it was hypothesized that the lean oil sand pillar on the north side was causing head build up to a distance of 180 m south of the pillar. The simulated results are in agreement, but only show the affect of the pillar within a range of 50 to 100 m south of the pillar. The head build up further south of the pillar is a result of the higher head in the lower Fill 2 material as a result of draining the upper fill causing slight head build up north in the cross-section.

5.4.2.1 Sensitivity Analysis

A sensitivity analysis, was conducted using the flux condition of 8 mm/yr (2.8×10^{-10} m/s) as it provided the most reasonable match of a simulated water table to field measured conditions through the Fill 1 materials. This value is 1.8% of annual precipitation of 450 mm and is one order of magnitude lower than the K value of the upper fill materials. Conditions that are examined in the sensitivity analysis are the hydraulic conductivity of the S1 dump, the flux into the S1 dump, the hydraulic conductivity of the sections of the hill constructed in lifts (S1 and Fill 1), and the rise of the north head boundary of the WIP.

5.4.2.2 S1 Dump

The S1 water table in all simulations is higher than the levels measured by the piezometers in the field. The simulated water table may not match that of field conditions due to limited instrumentation to adequately measure field K value or a difference in flux rate through this section of SBH. Only one nest of four piezometers exists on S1 at depths of 5 m, 10 m, 16 m, and 62 m (see Section 4.3.3). To get a reasonable match of the water levels measured by the piezometers, the hydraulic conductivity of this section was increased by two orders of magnitude from 1.7×10^{-8} m/s to 1.7×10^{-7} m/s and the results are shown in Figure 5.6. This is at the high end of the range of K values for a glacial till (Freeze and Cherry, 1979). This K value may not be unreasonable in that *in situ* materials were removed from one area of the mine, transported and placed on the surface and constructed into a pile altering material properties.

A second reason of a simulated higher water table in the S1 dump may be attributed to the flux value. The S1 section of the hill was the first section of SBH to be reclaimed, over a decade before the top of SBH, and supports mature established vegetation. By using the Dupuit analysis in Section 4.8.1, a flux value of only 0.6 mm/yr was required to achieve the maximum head measured in the field of the SP4 piezometer located on the north-most side of the S1 section. It is reasonable to assume that flux into the S1 section would be lower than that of the rest of SBH. The flux was decreased by an order of magnitude from 8 mm/yr (2.8×10^{-10} m/s) to 0.8 mm/yr (2.8×10^{-11} m/s). The results are shown in Figure 5.7.

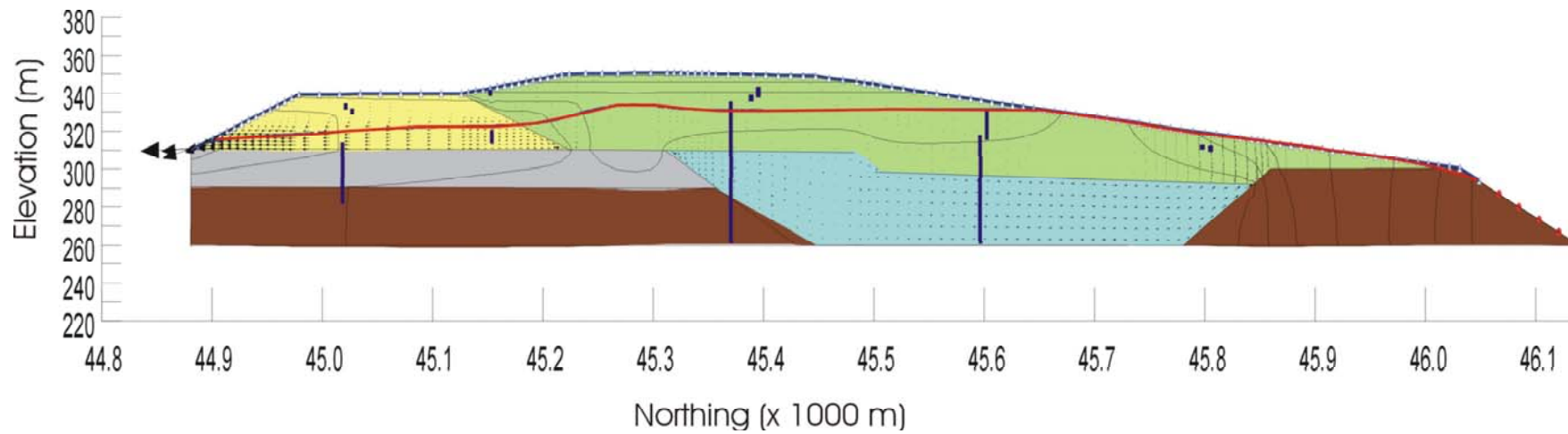


Figure 5.6 SBH steady-state seepage analysis for 8 mm/yr flux value and increasing S1 K value to 1.7×10^{-7} m/s.

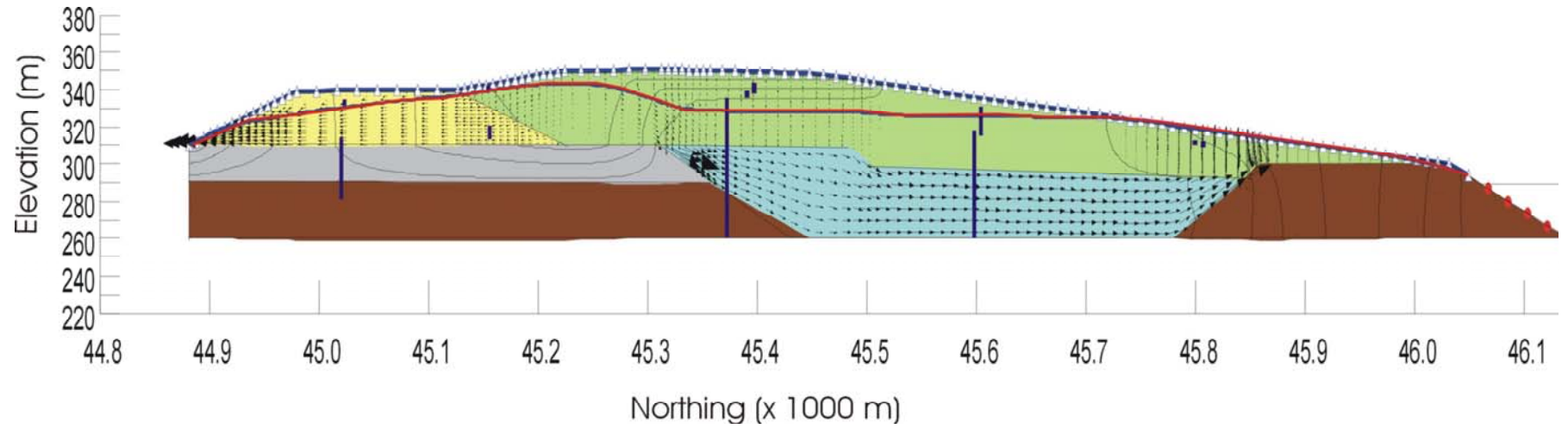


Figure 5.7 SBH steady-state seepage analysis for 8 mm/yr flux value and decreasing flux value to 0.8 mm/yr (2.8×10^{-11} m/s) over S1 dump surface.

The lower flux on the S1 section of SBH did not lower the water table over the entire S1 section. The lower flux only resulted in lowering the water table on the south side of S1 compared to the scenarios where the flux was equivalent. The water table adjacent to the fill materials remains the same. This simulation shows how the water table in the S1 is affected what is occurring in the fill materials. When the S1 is receiving a very small amount of flux into the pile, a water table develops by draining the upper fill. The sensitivity analyses conducted on the S1 portion of SBH shows that the flow in the S1 section of SBH is influenced more by the K value of the material rather than the flux into the pile. The actual K is likely higher than what was measured in the field. This section of SBH is important in that it acts as a drain controlling the water table and thus influences what is occurring in the remainder of the overburden hill. Additional instrumentation would be beneficial to verify the K value used the modelled results.

5.4.3 Lift Construction

To investigate the effect of the lift construction, a scenario was run using a 'bulk' K value lift method construction. In the 5 m lift system, the top 2 m of the lift is estimated to be two-orders of magnitude less than the bottom 3 m. It is likely that the piezometers that are reporting water levels in the upper sections of SBH are installed in the in the less permeable layers of the construction lift resulting in a overestimated K results from the standpipe bail tests. For the Fill 1 the bottom three metres of the lift is assumed to have a K of 2.8×10^{-9} m/s and the top two metres to have a K of 2.8×10^{-11} m/s with a bulk K of 1.7×10^{-9} m/s. Section S1 is also constructed in 2 m so the top 1 m of the lift was considered to be an order of magnitude less permeable in the 2 m lift system. However, the S1 section permeability remained at 1.7×10^{-8} m/s since from the analysis in Section 5.4.4.2 showed that the water table in the S1 section is higher than expected, likely as a result of an underestimated K value. The results of the simulation are shown in Figure 5.8. The decreased K in the upper Fill 1 materials as a result of a lift construction system showed an increase in water table elevation as a result of the flux not being able to reach the drain of the lower fill materials.

5.4.3.1 Rise of West-In-Pit (WIP)

One of the most important changes in the case of SBH is the certain rise of the WIP head boundary on the north side as a result of closure activities. The head of WIP was increased from 290 m in 2004 to an elevation of 315 m in 2012 according to final closure plans for the area. An 8 mm/yr flux was used and a K value of 1.7×10^{-7} for S1. The numerical model results are shown in Figure 5.9.

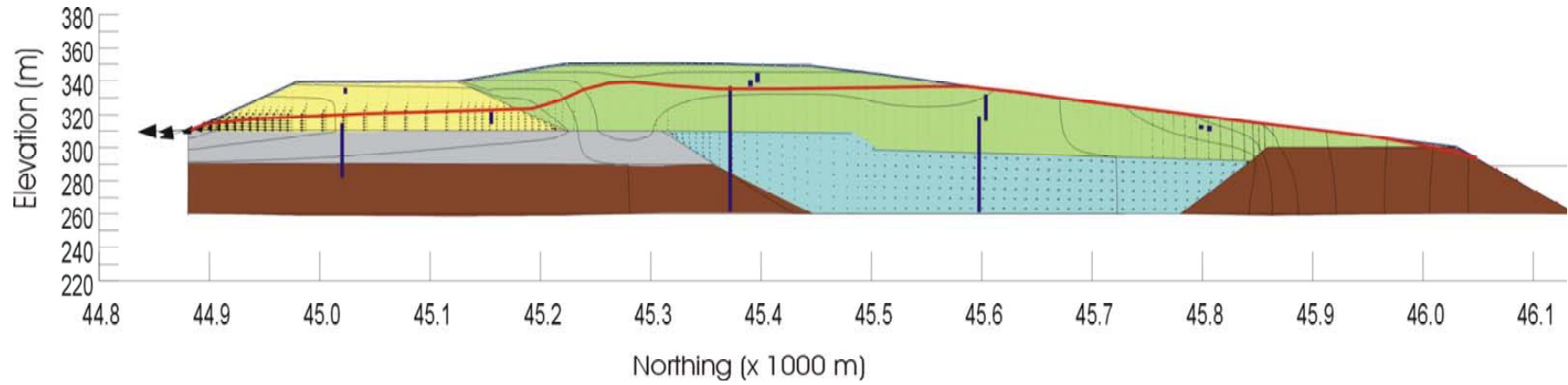


Figure 5.8 Steady state SEEP/W results increasing K value of upper Fill 1 materials to 1.7×10^{-9} m/s.

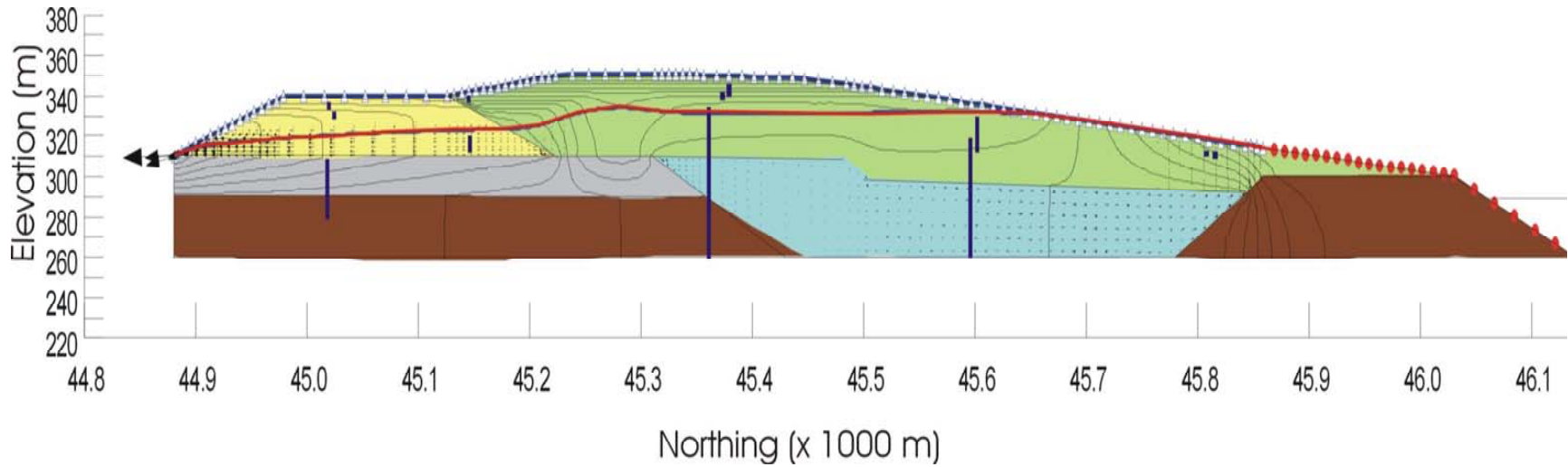


Figure 5.9 Steady state SEEP/W results for increase in WIP to 315 m.

From Figure 5.9, the water table now appears to be controlled by the increase in the head of WIP rather than the drainage of the lower fill materials. Drainage is still occurring through the S1 section on the south side.

5.4.4 Model Limitations

The seepage model presented in this section is a mathematical representation of the water flow through SBH. The model was constructed to develop an understanding of developing hydrogeologic system and seepage conditions in SBH. Using available resources, results from the field program, as well as general inferences, the composition of SBH was simplified into a conceptual model that could be represented in a mathematical model. It was assumed that the hydraulic conductivity in the four different sections was constant throughout the section. The numerical model is thus limited by the accuracy and detail of the conceptual model, the assumptions made, and the data available for use as model inputs.

The following limitations should be noted when interpreting the results of the model predictions for SBH flow:

- Water movement in the SBH was simulated using a simplified two-dimensional representation of the hill along a selected cross-section of the area. This cross-section was assumed to be representative of the general north to south flow within SBH; other cross-sections were not evaluated.
- The presence of the lean oil sands pillar and the different texture of the material below 320 m elevation would likely promote a 3-D flow system.
- The limestone base was assumed to be a no flow boundary. Limestone can range in K values from 1×10^{-10} m/s to 1×10^{-2} m/s in a fractured medium. The influence of the limestone base is recommended in future modelling programs.
- The flux is assumed to be equally distributed across the pile.
- The conceptual model assumes that materials with homogeneous material properties are representative of the different geological sections. The potential influence of local heterogeneity within a given material type was not investigated.

5.5 Three Dimensional Modelling Program

Rutten (2006) used the finite element method code FEMWATER, to conceptualize a three-dimensional (3D) groundwater flow system for SBH. The focus of this research was to evaluate the principal factors controlling spatial and temporal distribution of hydraulic heads. Rutten found that the steady-state 3D model followed the site topography and that hydraulic heads were affected by the hydraulic conductivity and thickness fill materials. Transient simulations were carried out to predict changes in fluctuating surface water levels.

The 2D and 3D models were both used to help Syncrude to gain an understanding for the flow systems that may develop in a reclaimed saline-sodic overburden structure such as SBH. It is important to realize the relationship between the two different modelling programs. The focus of the 2D modelling program was utilized to highlight features of the conceptual model developed to 'reconstruct' SBH while the 3D model used this conceptual model to generate one numerical representation of the dataset.

5.6 Summary

A steady-state two-dimensional model was developed of SBH using the conceptual geological model and data collected from the 2002-03 field program. The numerical model illustrated the importance of the higher permeability of the lower S1 and Fill 2 materials which act as drains preventing the water table from significantly building up in SBH. A reasonable match to field conditions in the Fill 1 materials was achieved using a flux rate of 8 mm/yr, however; heads in the S1 section and on the north of SBH were higher than expected. The lean oil sands pillar located on the north side appears to be causing a build up of heads noticeably approximately 50 m south of the pillar.

Sensitivity analysis was performed on the K and the flux of the S1 section, the K of the Fill 1 materials, and the change in head boundary of WIP. The K value of the S1 materials was increased by an order of magnitude to better match field conditions and the flux was decreased an order of magnitude. The increase in the K value showed the most significant affect to the water table causing a faster drain lowering the water table. The decrease in the K of the upper fill materials resulted in increasing the elevation of the water table. The low permeability materials prevented the flux from reaching the more permeable lower Fill 2 materials causing a rise in the water table elevation. By increasing the head of WIP from 290 m to 315 m, the water table position was dictated by the head boundary and the lower fill materials no longer provided significant drainage.

The steady-state numerical model was used to verify the conceptual geological model and to determine whether measured piezometric water levels and measured seepage rate, and flux rates are reasonable. The model provided a reasonable match using a flux of 8 mm/yr and field measured K values, with the S1 K value increased by an order of magnitude. The seepage model developed for SBH should be used as a qualitative decision making tool in providing an understanding for the long-term impact as opposed to focussing on the absolute values predicted by the model.

CHAPTER 6

SUMMARY AND RECOMMENDATIONS FOR FUTURE RESEARCH

6.1 Conclusions

The hydrogeology of a newly constructed overburden hill, South Bison Hill (SBH) at the Syncrude Canada Ltd. Mildred Lake operation located in the Athabasca oil sands region of northeastern Alberta was investigated. Saline-sodic overburden structures will compose approximately one-third of the final landscape. SBH provides an opportunity to investigate the evolution of the groundwater flow system in a newly reclaimed overburden pile. One of the most important components of the research included creating a conceptual geological model of the hill using resources from literature, Syncrude company records, and personal communications with site operators. Hydrogeological properties of the hill were investigated through an existing piezometer network including total head measurement and groundwater quality sampling. Supplementary piezometer nests were installed to gain additional information at key locations on the pile in 2003. Qualitative observations were made to identify any indicators of groundwater seepage along the faces of the pile. The collected data was used to develop a conceptual two-dimensional steady state model of SBH. The model can be used as a tool to determine the fate of SBH flow system with changing conditions.

A groundwater flow system was found to have developed in SBH, a newly reclaimed saline-sodic overburden hill located at the Syncrude Canada Mildred Lake operation. The system of SBH is largely influenced by the contrast in the hydraulic conductivity caused by the different construction methods and materials. The results of the 2D modelling program illustrate that the higher permeability of the S1 dump on the south side of SBH and the in-pit fill materials appears to be controlling the height of the water table which is beneficial for both geotechnical stability and salt release into reclaimed soils and wetlands. Future construction of saline-sodic

overburden hills may want to consider having such contrasts in permeability, whether by construction methods or by materials used, to help to prevent groundwater build up in the structures protecting reclamation efforts.

6.1.1 General Flow Patterns

Some general flow patterns could be identified on SBH based on construction methods and materials. The flow patterns could be distinguished in areas of perched water table conditions (from 320 to 350 m elevation), *in situ* K_m , and conditions below 320 m.

6.1.1.1 Fill Materials

The piezometer network installed on SBH provided water level data, hydraulic conductivity, and geochemistry data to investigate distinguishable flow paths on SBH. Piezometer water levels have been measured since 2001. Some key findings from analysis of the piezometer water levels show that the piezometers installed in the sections of the hill constructed of 2 m or 5 m lift assembly typically show evidence of downward flow with evidence of perched conditions showing low, stable, water levels. The Peat Pond and Bill's Lake wetlands show downward and outward flow conditions for the majority of the year. These conditions present evidence that areas of the overburden hill are in a recharge condition. Hydraulic conductivity values in the upper portion of the hill constructed in 5 m lifts and of a majority K_c clays range from 1.3×10^{-9} to 8.2×10^{-9} m/s. The S1 section constructed of mostly glacial tills in a 2 m lift assembly was found to be more permeable than other sections of the hill with a measured hydraulic conductivity range of 8.4×10^{-9} to 2.7×10^{-8} m/s ($K_{\text{geommean}} = 2.8 \times 10^{-9}$ m/s). Geochemistry supports the difference found hydraulic conductivity data between the till and the K_c clay. Geochemistry data obtained from the till shows higher amounts of Ca and HCO_3 , typical of glacial material while the data obtained in the K_c clay is dominantly Na SO_4 type, indicative of oxidized shale. The exception to this is the geochemistry obtained from the piezometers installed near the two wetlands. The geochemistry shows that there is likely a mixing between the groundwater and the pond water, consistent with the historic water level data showing that the ponds are in a recharge condition and most likely have a separate localized flow system.

The section of SBH from 260 m to 320 m elevation consists of K_c fill materials considered to be more sandy than fills used from 320 m to 350 m and without the effects of lift type placement, being end-dumped into the open pit rather than constructed in a defined lift assembly. As a result, the geometric mean of those piezometers installed in the lower fill material is more permeable than the fill above 320 m with a range of 9.8×10^{-11} to 2.1×10^{-7} m/s ($K_{\text{geommean}} = 4.5 \times 10^{-9}$ m/s). The chemistry in these piezometers are Na SO_4 dominated which is expecting since

these fill materials have been exposed to oxidizing conditions and meteoric waters during construction and placement.

6.1.1.2 Deep Flow Conditions

There are three piezometers installed to contact of the fill and the limestone base of SBH. While this is a limited number, a few general trends can be seen. These piezometers exhibit artesian behaviour and measured water levels show a general increase with time which may be influenced by the rising level of WIP to the north of the hill. The water levels measured in the limestone base show that the water level is flowing toward the north and possibly to the west toward WIP. Hydraulic conductivity values from the piezometers at this depth range from 1.0×10^{-9} to 6.0×10^{-8} m/s. Geochemistry data obtained from these pipes are Na-HCO₃-SO₄ type waters which with the higher concentration of HCO₃ that groundwater from this portion of the overburden hill has been exposed to less oxidizing conditions. Additional data from this depth would be beneficial to confirm trends exhibited by the three existing piezometers and to confirm if the rising level in WIP is affecting heads in the limestone formation.

6.1.1.3 In situ K_m Material

As with the limestone base material, there is limited data from piezometers installed in this material given that only two exist. It is important however to gain some understanding of materials of this nature have on the development on the hydrogeologic system of SBH. Of particular interest is the lean oil sands 'pillar' left to on the north side of the hill. The water levels measured in both piezometers show to be slightly decreasing over time which may indicate that this formation is draining or that the pore pressures that built up with the load placement of materials are slowly dissipating. The hydraulic conductivity between the two piezometers vary by two orders of magnitude from 3.3×10^{-10} to 2.6×10^{-8} m/s; however still fall within the range of conductivities for regional K_m measured by Syncrude (2005) of 1.0×10^{-10} to 1.0×10^{-5} m/s. Geochemistry data is also found to be different varying between Na-Ca-SO₄-HCO₃ for the less permeable piezometer and Na-SO₄ and for the more permeable piezometer. The differences between these two piezometers may be attributed to material differences between the different locations. There appears to be a head build up in those piezometers installed in line with the lean oil sands pillar on the north side of the hill.

6.1.2 Conceptual Model Results

A two dimensional steady-state numerical model was developed to verify conditions measured in the field. The model was performed on one cross-section to incorporate the different geologic sections of the hill. A conceptual model was developed using field measured hydraulic

conductivities where available as well as historic data. A reasonable flow system to match field conditions was developed using a flux value of 8 mm/yr and increasing the K value of the S1 section by an order of magnitude.

The main findings of the numerical model was the importance of the lower permeability sections which included the S1 section and the lower fill materials. These two sections act as drains in the overburden hill which aid in keeping the water table at a lower elevation. The model also showed that the lean oil sand pillar is causing head build up to the south of the pillar, however; further south in the pile head build up is caused by overwhelming the lower fill materials as it is draining flow accumulated over the *in situ* materials. The numerical model of SBH is a simplified representation of the flow system through SBH and should be considered a starting point for further more involved analysis of the flow system.

6.2 Recommendations for Future Research

In order to gain an understanding of the developing hydrogeologic system of the newly placed SBH over burden hill, a number of tasks had to be carried out. One of the most important aspects of this study was developing a geologic model. The geologic model was developed to using mine records supplemented with personal interviews. It is important to note that while the best effort at obtaining accurate information was attempted, it is likely that there are some sections of the hill that require further examination. A hydrogeological study requires a thorough understanding of the hill materials and material properties. Additional instrumentation (i.e. standpipe piezometers, pneumatic piezometers) would be beneficial to obtain more information and verify measurements made by existing piezometers, particularly in the S1 section and around the lean oil sands pillar at the north end of SBH.

Additional groundwater chemistry analysis using environmental isotopes such as oxygen-18 and deuterium is recommended to gain a better understanding of recharge into the deep groundwater system. This data would determine if the system is obtaining recharge from recent precipitation or from some other source.

Future monitoring of the piezometer water levels and the overall stability of SBH is recommended, as this data would provide useful information of the behaviour of overburden materials and how the groundwater flow system evolves as the WIP reaches its final elevation of 315 m. The SBH has provided a unique opportunity to see a groundwater system develop in a K_c overburden hill from time zero through a rapidly changing system (i.e the rise of the WIP).

The two-dimensional conceptual model developed for this study was used to verify the geological model and the conditions measured in the field. This model should be considered to

be as starting point for future modelling endeavours. A continuation of this study was conducted by Rutten (2006) and provides details of a three-dimensional flow model of the SBH.

REFERENCES

- Alberta Environment (AE). 1999. Surface water quality guidelines for use in Alberta. Report ISBN: 0-7785-0897-8. November 1999.
- American Society for Testing Materials (ASTM). 1996a. Standard Test Method (Field Procedure) for Instantaneous Change in Head (Slug) Tests for Determining Hydraulic Properties of Aquifers. In 1996 Annual Book of ASTM Standards, Volume 4.08. ASTM, Philadelphia, Pa., pp. 453 - 455.
- American Society for Testing Materials (ASTM). 1996b. Standard Guide for Sampling Groundwater Monitoring Wells (D 4448 – 85a). In 1996 Annual Book of ASTM Standards, Volume 4.08. ASTM, Philadelphia, Pa., pp. 430 - 443.
- American Society for Testing Materials (ASTM). 1996c. Standard Guide for Planning and Preparing for a Groundwater Sampling Event (D 5903-96). In 1996 Annual Book of ASTM Standards, Volume 4.08. ASTM, Philadelphia, Pa., pp. 426 - 429.
- Barth, R.C. and Martin, B.K. 1984. Soil depth requirements for revegetation of surface-mined areas in Wyoming, Montana, and North Dakota. J. Environ. Qual.13: 399-404.
- Bell, J.P. 1987. Neutron probe practise. Institute of Hydrology, Wallingford, Report 19. September.
- Boese, C. D. 2003. The design and installation of field instrumentation program for the evaluation of soil-atmosphere water fluxes in a vegetated cover over saline/sodic shale overburden. M.Sc. Thesis, Department of Civil Engineering, University of Saskatchewan, Saskatoon, Saskatchewan.
- Bouwer, H. and Rice, R.C. 1976. A slug test for determining hydraulic conductivity of unconfined aquifers with completely or partially penetrating wells. Water Resources Research, 12 (4): 423-428.

- Chapuis, R.P. and Sabourin, L. 1989. Effects of installation of piezometers and wells on groundwater characteristics and measurements. *Can. Geotech. J.*, 26: 604-613.
- Chapuis, R.P. 2005a. Using the Velocity Graph Method to Interpret Rising-Head Permeability Tests After Dewatering the Screen. *Geotechnical Testing Journal*, 28(3), p. 305-312.
- Chapuis, R.P. 2005b. Numerical Modelling of Rising-Head Permeability Tests in Monitoring Wells After Lowering the Water Level Down to the Screen. *Canadian Geotechnical Journal*, 42(3):. 705-715.
- Conly, F.M., Crosely, R.W., and Headley, J.V. 2002. Characterizing sediment sources and natural hydrocarbon inputs in the lower Athabasca River, Canada. *J. Environ. Eng. Sci.*, 1: 187-199.
- Cooper, H.H., Bredehoeft, J.D., and Papadopoulos, I.S. 1967. Response to a finite diameter well to an instantaneous charge of water. *Water Res. Res.*, 3: 263-269.
- Domenico, P.A. & Schwartz, W., 1998. *Physical and Chemical Hydrogeology* Second Edition, Wiley.
- Flach, P.D. 1984. Oil sands geology: Athabasca deposits north. Geological Survey Department, Alberta Research Council, Edmonton, Alta., Canada. 31 p.
- Fetter, C.W. 1994. *Applied Hydrogeology* (Third Ed.), Prentice-Hall Inc. Englewood Cliffs, New Jersey.
- Freeze, R.A. and Cherry, J.A. 1979. *Groundwater*, Prentice-Hall Inc. Englewood Cliffs, New Jersey.
- Gingras, M. and Rokosh, D. 2004. A brief overview of the geology of heavy oil, bitumen and oil sand deposits. In *Proceedings 2004 CSEG National Convention*. Calgary, AB, May 11-13.
- Hein, F.J. and Cotterill, D.K. 2006. The Athabasca oil sands – a regional geological perspective, Fort McMurray area, Alberta, Canada. *Natural Resources Research*, 15(2): 85-102.
- Hendry, M.J. 1982. Hydraulic conductivity of a glacial till in Alberta. *Ground Water* 20(2): 162-169.

- Herzog, B.L. and Morse, W.J. 1984. Hydraulic Conductivity at a Hazardous Waste Disposal Site: Comparison of laboratory and field-determined values. *Waste Management & Research* 4: 177-187.
- Hvorslev, M.J. 1951. Time-lag and soil permeability in groundwater observations, Bull. 36, U.S. Army Corps of Eng. Waterways Exp. Stn., Vicksburg, Miss.
- InfoMine. 2006. Mining Company & Property Database.
http://www.infomine.com/index/companies/SYNCRUDE_CANADA_LTD..html.
- Isaac, B.A., Dusseault, M.B., Lobb, G.D., and Root, J.D. 1982. Characterization of the lower cretaceous overburden for oil sands surface mining within Syncrude Canada Ltd. leases northeast Alberta, Canada. In *Proceedings of the IV International Association of Engineering Geology*. Volume II, New Delhi.
- Jiao, J.J. 2000. Modification of regional groundwater regimes by land reclamation. *Hong Kong Geologist* 6: 29-36.
- Jiao, J.J., Nandy, S., and Li, H. 2001. Analytical Studies on the Impact of Land Reclamation on Ground Water Flow. *Ground Water* 39(6); 912-920.
- Kampala, Grey, Feb 18, 2004. Personal Communication.
- Klijin, F. and Witte, J.P. 1999. Eco-hydrology: groundwater flow and site factors in plant ecology. *Hydrogeology Journal*. 7: 65-77.
- Krahn, J. 2004. Seepage modelling with SEEP/W: An engineering methodology. Geo-Slope International Ltd.
- Lord E.R.F and Isaac, B.A.A. 1989. Geotechnical investigations of dredged overburden at Syncrude oil sand mine in northern Alberta, Canada. *Can. Geotech.* 26: 132-153.
- Lussier, L., S. Griffiths, C. Tucker and W. Mirmura. 2000. Seepage test pits dug into pads constructed using 0.75m, 1.0 m, and 1.5 m lifts of Kc-clays. Geotechnical Division Report. Ft. McMurray, AB: Syncrude Canada Ltd.
- McKenna, G., Geotechnical Engineer, R. Cameron, Geotechnical Engineer and G. Kampala, Hydrogeologist, Suncrude, personal communication, August 2002.

- McKenna, G.T. 2002. Sustainable mine reclamation and landscape engineering. Ph. D. Thesis, Department of Civil and Environmental Engineering, University of Alberta, Edmonton, Alberta, Canada.
- Merrill, S.D., Smith, S.J., and Power, J.F. 1985. Effect of disturbed soil thickness on soil water use and movement under perennial grass. *Soil Sc. Soc. Am. J.* 49: 196-202.
- Mossop, G.D. 1980. Geology of the Athabasca oil sands. *Science* 207 (4427): 145-152.
- Nguyen, V. and Pinder, G. 1984. Direct calculation of aquifer parameters in slug test analysis. In *Groundwater Hydraulics*, J. Rosenhein and G.D. Bennett, eds. American Geophysical Union Water Resources Monograph 9. pp 222-239.
- Oddie, T. A, and Bailey, A.W. 1988. Subsoil thickness effects on yield and soil water when reclaiming sodic minespoil. *J. Environ. Qual.* 17(4): 623-627.
- Piper, A.M. 1944. A graphic procedure in the geochemical interpretation of water analyses: *American Geophysical Union Transactions*, v. 25, p. 914-923.
- Reszat, T. 2002. Stability of elemental sulphur in groundwater environments at Syncrude Canada, Ltd. Undergraduate study, Department of Geological Sciences, University of Saskatchewan, Saskatoon, Saskatchewan, Canada.
- Rockware Inc. Hydrochem Revision 97.2.28 Cation/Anion Diagram Plotting. Copyright 1983-97 by Licenced to the University of Saskatchewan.
- Rutten K. 2006. Long-term Controls in a Groundwater Flow System. M.Eng. Thesis, Department of Civil Engineering, University of Saskatchewan, Saskatoon, Saskatchewan, Canada.
- Sawatsky, L., G. McKenna, M. Keys, D. Long. 2000. Towards Minimizing the Long-term Liability of Reclaimed Mine Sites. *Land Construction and Monangement*. Vol 1. pp 21-36.
- Seelig, B.D. 2000. Salinity and sodicity in North Dakota soils. North Dakota State University (NSDU) Extension Service Report EB 57. May.
- Shaw, R. J. and M. J. Hendry. 1998. Hydrogeology of a thick clay till and Cretaceous clay sequence, Saskatchewan, Canada. *Can. Geotech. J.* 35: 1041-1052.

- Strueby, B. 1996. Field falling head tests on 5 m lifts of Kc-clay fills. Geotechnical Division Report. Ft. McMurray, AB: Syncrude Canada Ltd.
- Syncrude Canada Ltd. (Syncrude). 1999. Geotechnical Properties of the Pre-Reclamation Surface Materials at Syncrude's Landform Grading Demonstration Area. Syncrude Report TC-R171. Ft McMurray, AB: Bitumen Production Development , Syncrude Canada Ltd.
- Syncrude Canada Ltd (Syncrude). 2007. Syncrude Company Profile. http://www.Syncrude.com/who_we_are/index.html (2007/01/25).
- Swanson, G.A., Adomaitis, V.A., Lee, F.B., Serie, J.R. Shoessmith, J.A. 1984. Limnological conditions influencing duckling use of saline lakes in south-central North Dakota. *Journal of Wildlife Management*. 48: 340-349.
- van der Kamp, G. 2000. Methods for determining the in situ hydraulic conductivity of shallow aquitards – an overview. *Hydrogeology Journal* 9: 5–16.
- Wall, S. 2004. Characterizing geochemical reactions in an overburden waste pile Syncrude Mine Site, Fort McMurray, Alberta, Canada. M.Sc. Thesis, Department of Geology, University of Saskatchewan, Saskatoon, Saskatchewan.
- Washington Department of Ecology, 2006 <http://www.ecy.wa.gov/programs/sea/pubs/95-107/sldrain01.html#groundwater>.
- Wedage, A.M.P, N.R. Morgenstern, and D.H. Chan. 1988. Simulation of Time-Dependent Movements in Syncrude Tailings Dyke Foundation. *Can. Geotech. J.* 35: 284-298.
- Wightman, D.M., Attalla, M.N., Wynne, D.A., Strobl, R.S., Berhane, H., Cotterill, D.K. and Berezniuk, T. 1995. Resource characterization of the McMurray/Wabiskaw Deposit in the Athabasca Oil Sands Area: a synthesis. AOSTRA Technical Publication Series No. 10, 220p.
- Wilson, E.A. 1971. Vegetation indicators of terrain conditions in southern Saskatchewan. M.Sc. Thesis, Department of Civil Engineering, University of Saskatchewan, Saskatoon, Saskatchewan, Canada.
- Wisconsin Department of Natural Resources (WDNR). 1993. Guidance for design, installation, and operation of groundwater extraction and product recovery systems. Madison, WI. PUBL-SW183-93, August.

APPENDIX A

**South Bison Hill Piezometer
Completion Details**

Table A1
Completion Details for South Bison Hill Piezometers

Piezometer ID	Mine Northing (m)	Mine Easting (m)	Surface Elevation (m)	Top of Sandpack (m)	Bottom of Sandpack (m)	Borehole Diameter (m)	Piezometer Diameter (m)
SP99990123	45278.4	49892.1	327.6	316.0	314.2	0.13	0.05
SP99990124	45284.2	49890.1	326.9	324.5	322.6	0.13	0.05
SP99990125	45281.4	49890.8	327.2	319.0	316.2	0.13	0.05
SP99990145	45269.7	49893.4	328.4	290.6	286.3	0.13	0.05
SP99990126	45649.6	50756.2	325.8	313.0	310.9	0.13	0.05
SP99990127	45654.6	50756.1	324.9	322.2	320.0	0.13	0.05
SP99990128	45652.1	50756.7	325.5	318.1	315.7	0.13	0.05
SP011730-01	45153.4	50234.2	349.3	346.9	344.7	0.13	0.05
SP011730-02	45153.5	50236.0	349.4	340.9	337.7	0.13	0.05
SP011730-03	45153.7	50238.4	349.4	336.3	333.3	0.13	0.05
SP011730-04	45154.1	50240.6	348.6	316.6	313.0	0.13	0.05
SP011730-05	45386.8	50217.5	350.2	347.8	344.7	0.13	0.05
SP011730-06	45384.9	50218.2	349.6	341.1	338.0	0.13	0.05
SP011730-07	45383.2	50218.8	349.7	336.6	333.6	0.13	0.05
SP011730-08	45381.5	50219.7	349.9	327.6	324.4	0.13	0.05
SP011730-08A	45375.5	50222.7	349.8	261.0	259.5	0.13	0.05
SP011730-09	45035.4	50233.5	340.5	337.8	335.5	0.13	0.05
SP011730-10	45035.6	50234.8	340.7	333.1	330.2	0.13	0.05
SP011730-11	45035.4	50237.6	341.8	327.4	323.9	0.13	0.05
SP011730-12	45035.4	50241.8	341.9	281.8	277.9	0.13	0.05
SP011730-13	45599.2	49873.5	319.5	317.1	314.7	0.13	0.05
SP011730-14	45597.9	49875.8	319.5	311.9	309.8	0.13	0.05
SP011730-15	45596.6	49878.3	319.5	306.4	302.6	0.13	0.05
SP011730-16	45594.3	49881.5	319.5	260.6	258.1	0.13	0.05
SP011730-17	45607.5	50194.6	328.9	326.2	324.0	0.13	0.05
SP011730-18	45605.4	50195.3	328.9	320.6	319.1	0.13	0.05
SP011730-19	45603.0	50195.9	328.8	315.7	313.6	0.13	0.05
SP011730-20	45596.8	50199.8	328.8	260.8	258.7	0.13	0.05
SP011730-21	45792.4	49797.2	316.6	312.6	310.5	0.13	0.05
SP011730-22	45794.1	49799.4	316.6	309.0	306.8	0.13	0.05
SP011730-23	45795.7	49801.5	316.5	303.4	299.7	0.13	0.05
SP1-1	45737.4	50180.8	320.0	311.7	309.3	0.16	0.05
SP1-2	45737.0	50185.8	320.0	292.9	289.7	0.16	0.05
SP4-1	45760.3	50453.7	320.0	310.7	308.4	0.13	0.05
SP4-2	45758.8	50451.2	320.0	292.3	290.1	0.15	0.05

APPENDIX B

South Bison Hill Cross-Sections

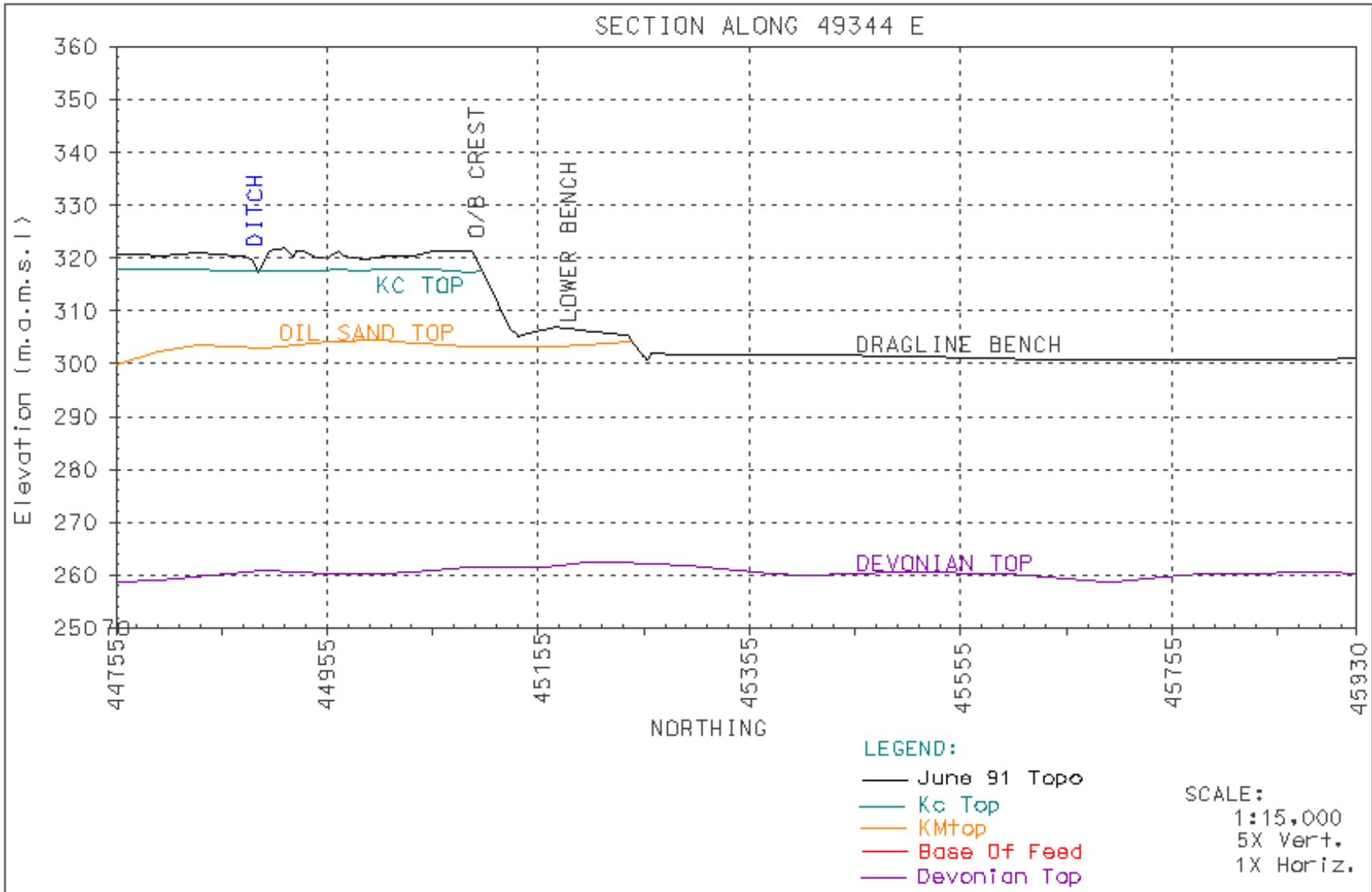


Figure B2 Section along 49344 E looking west.

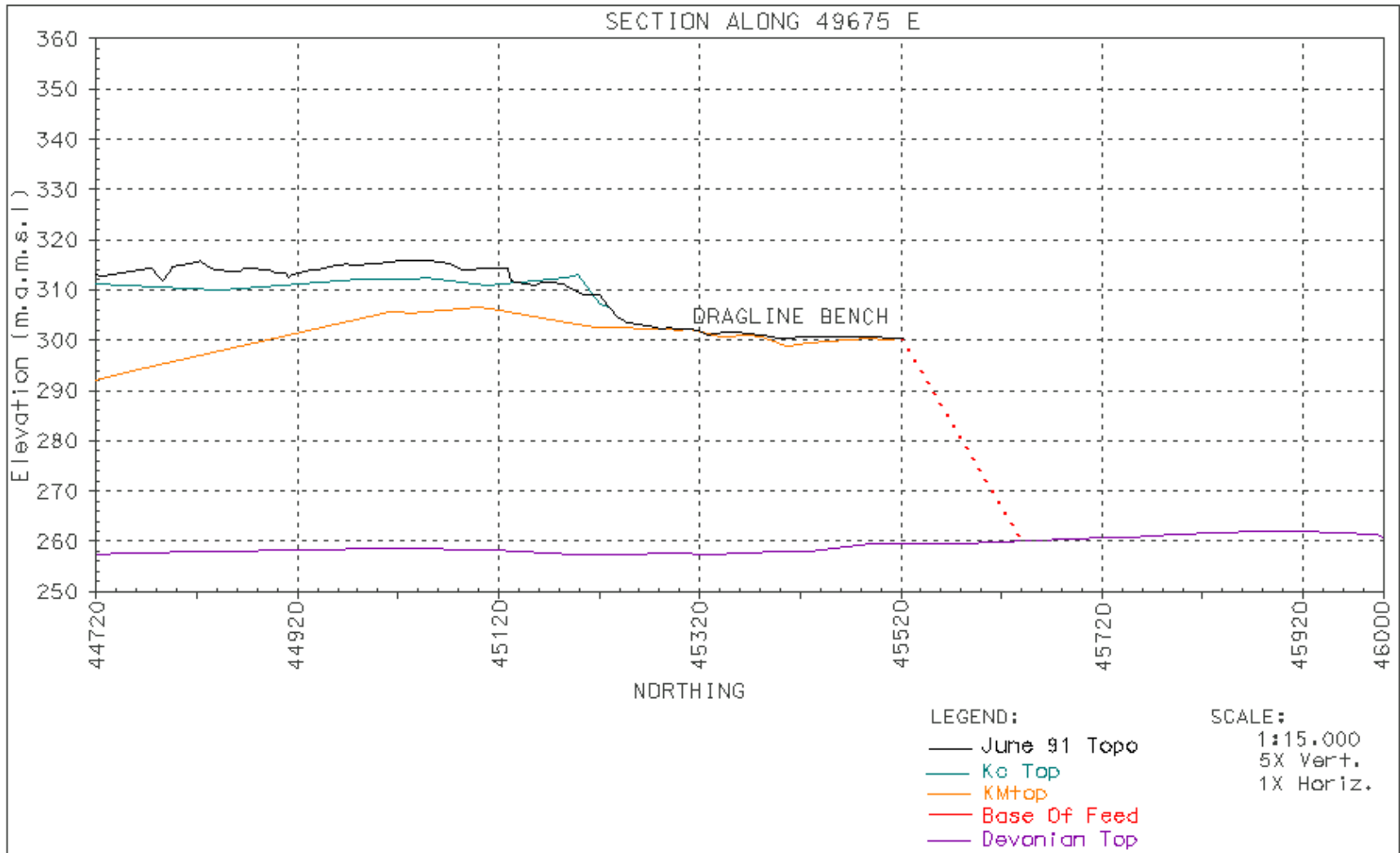


Figure B3 June 1991 topographic map showing section 49657E looking west.

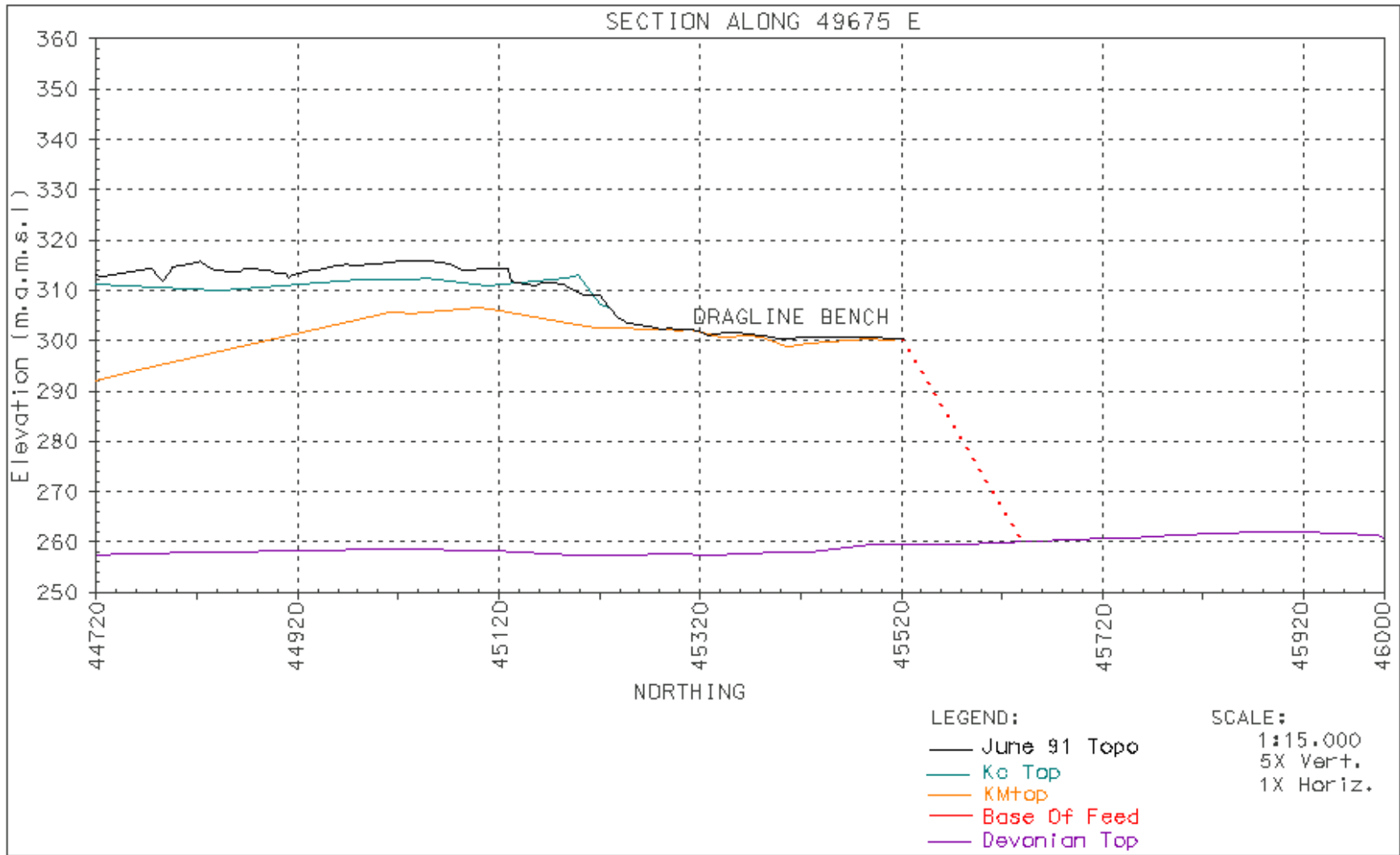


Figure B4 June 1991 topographic map showing section 49675 E looking west.

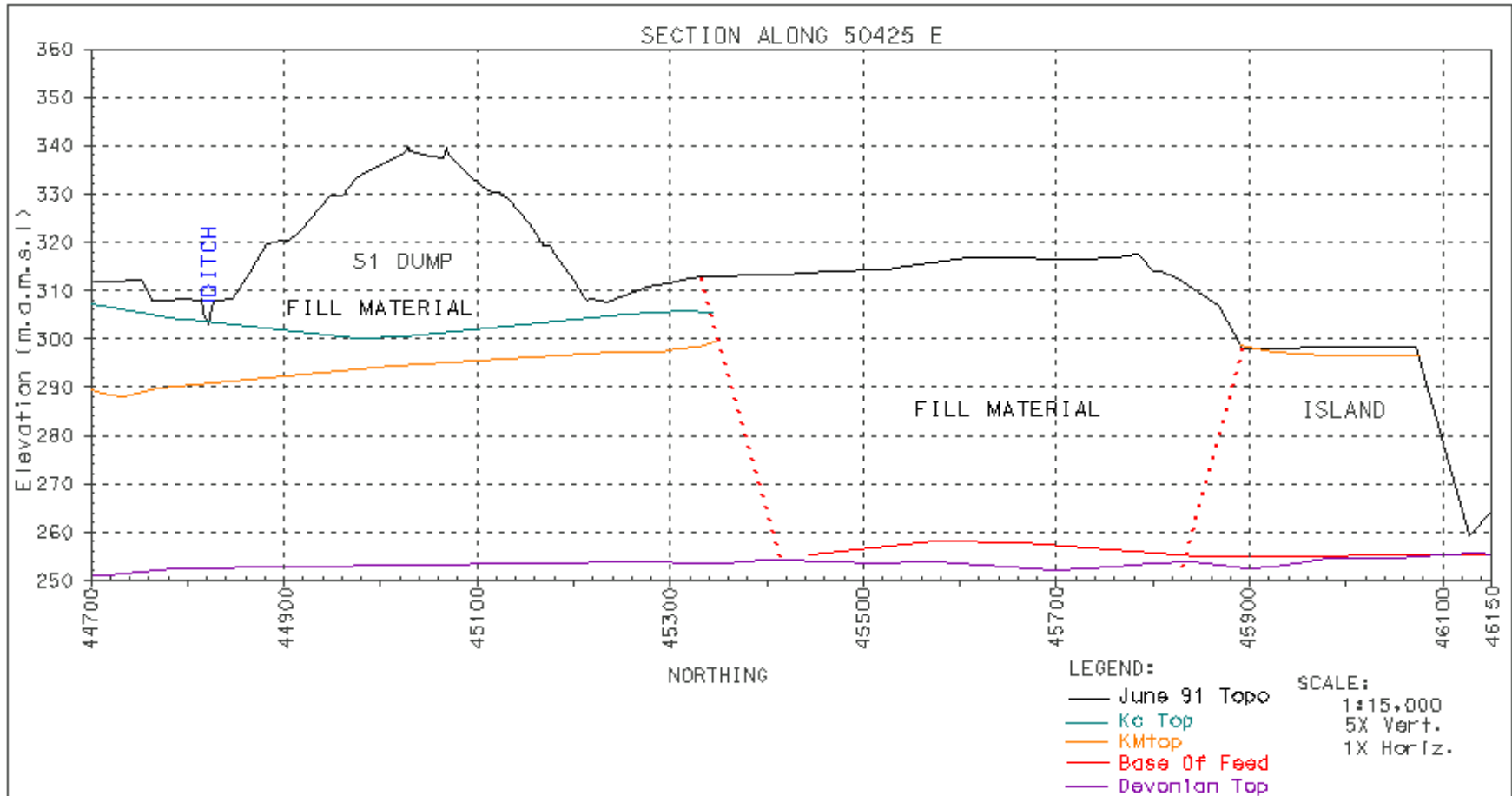


Figure B5 June 1991 topographic map showing section 50425 E looking west.

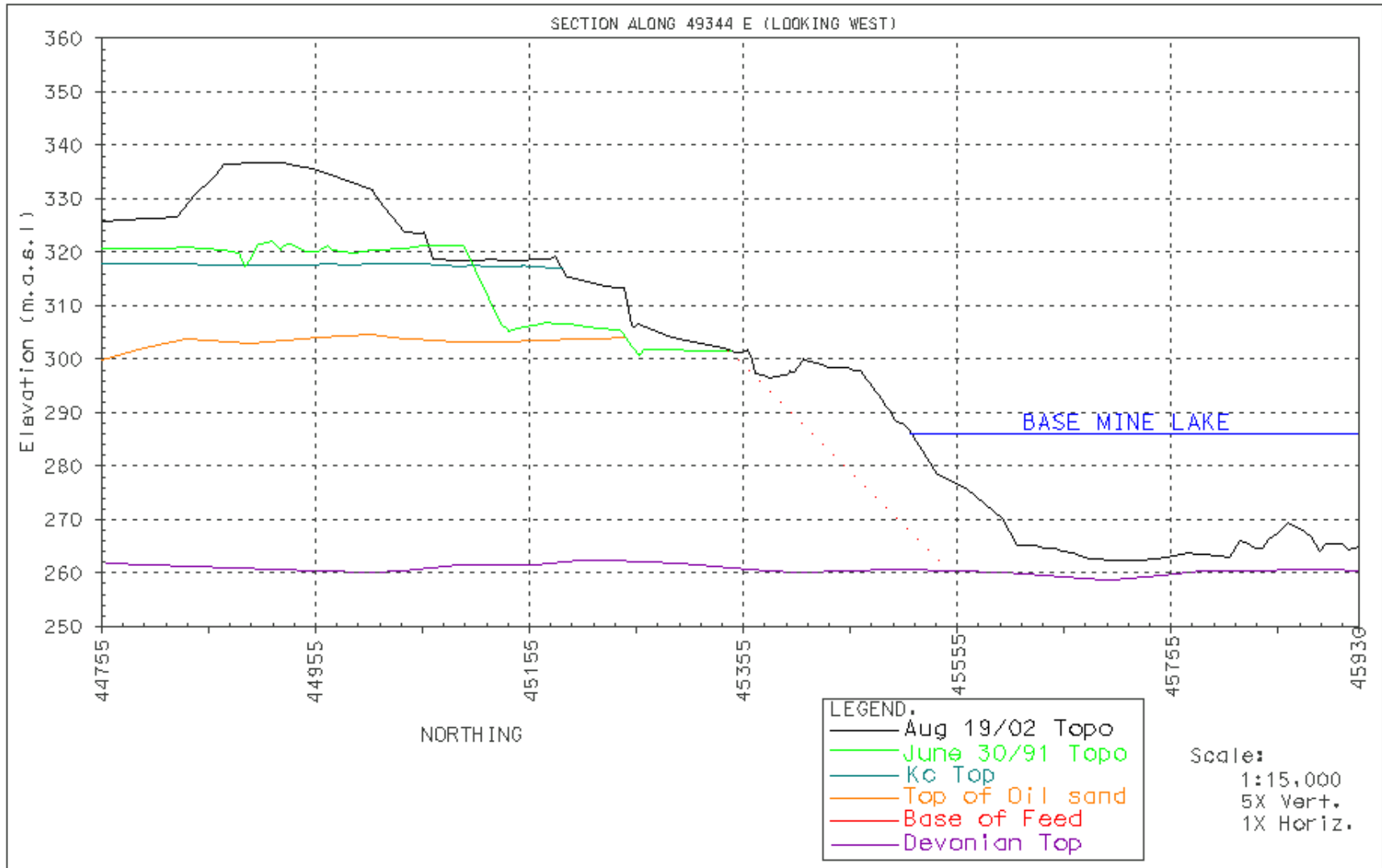


Figure B6 August 2002 topographic map showing section 49344 E looking west.

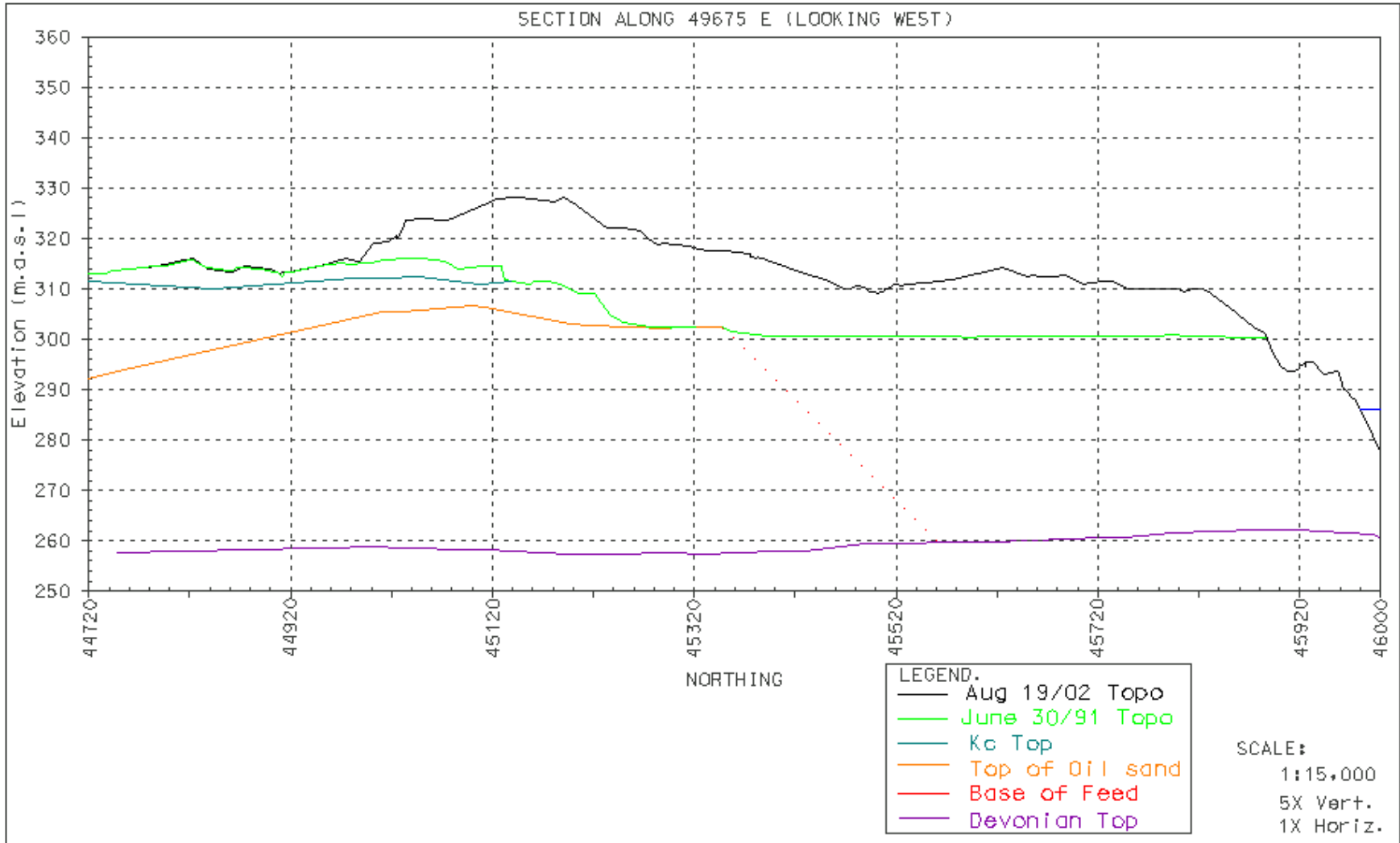


Figure B7 August 2002 topographic map showing section 49675 E looking west.

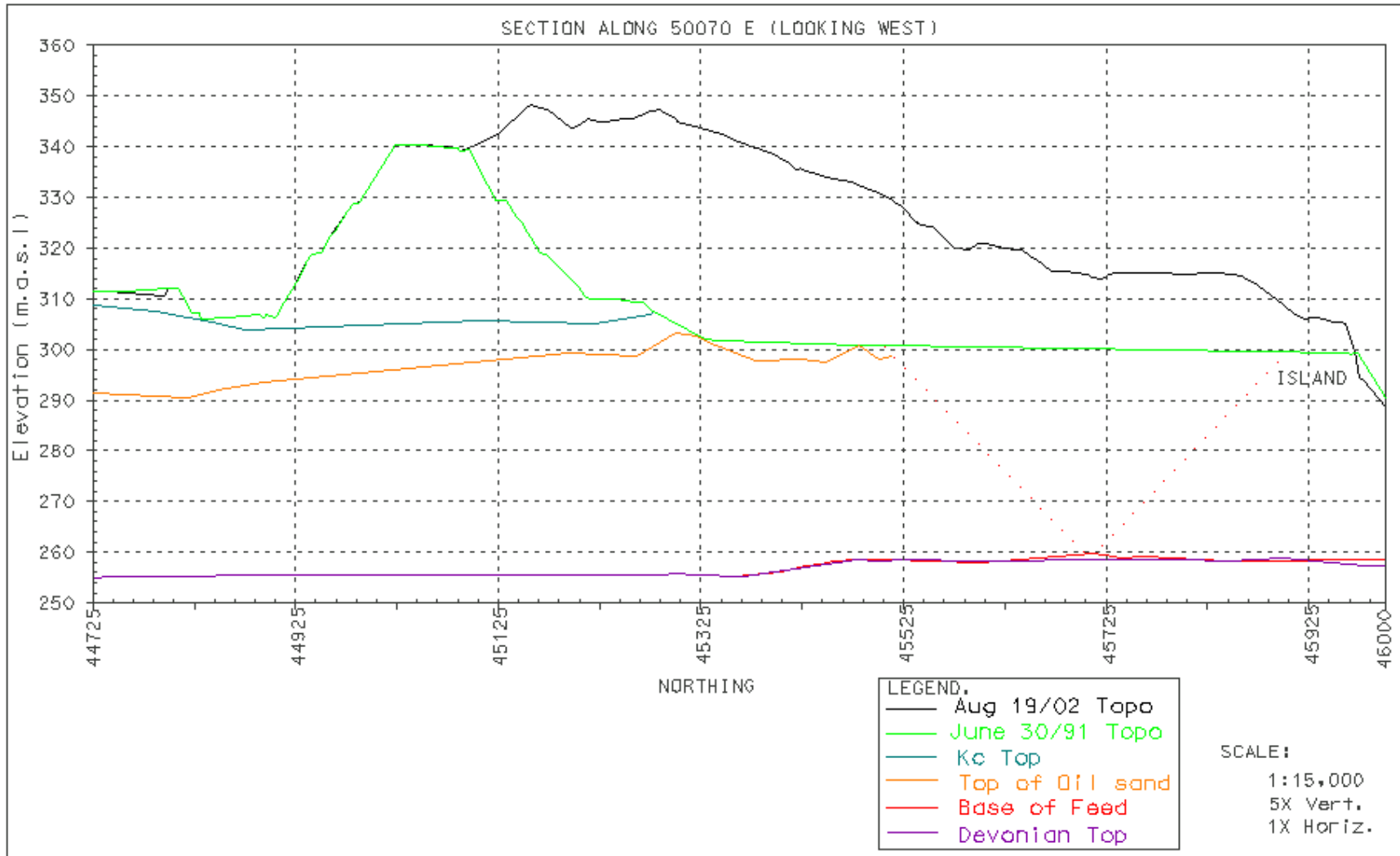


Figure B8 August 2002 topographic map showing section 50070 E looking west.

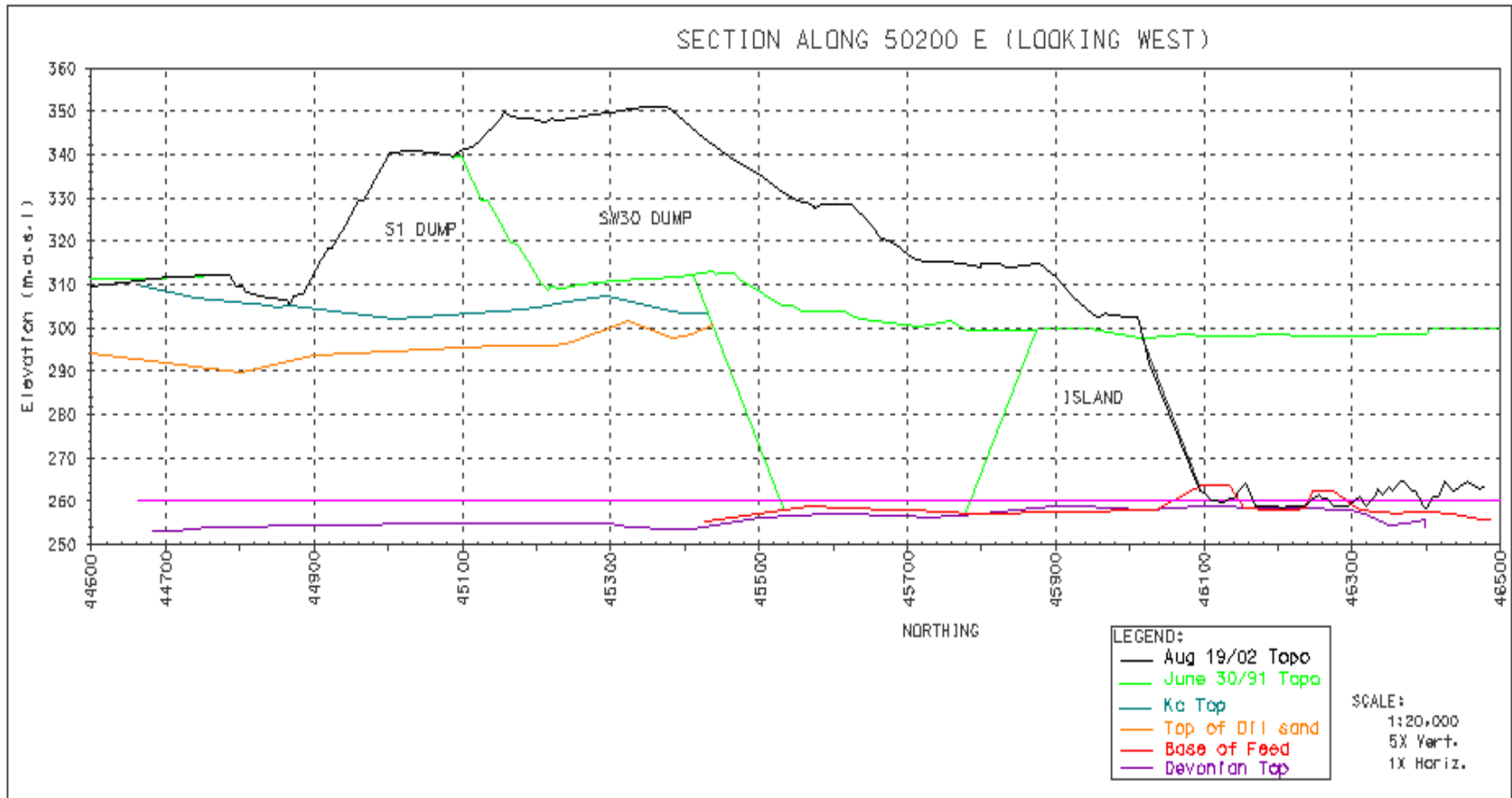


Figure B9 August 2002 topographic map showing section 50200 E looking west.

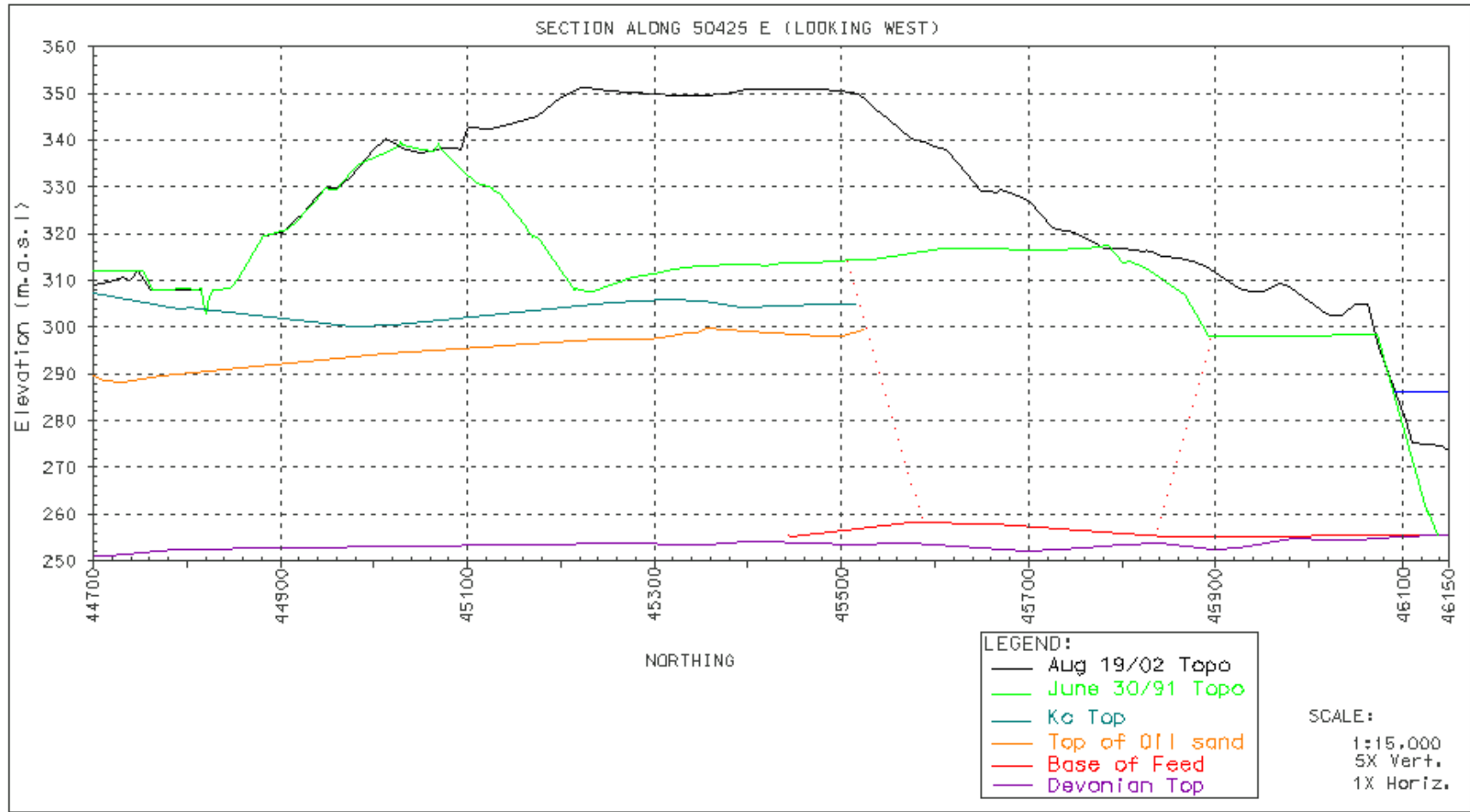


Figure B10 August 2002 topographic map showing section 50425 E looking west.

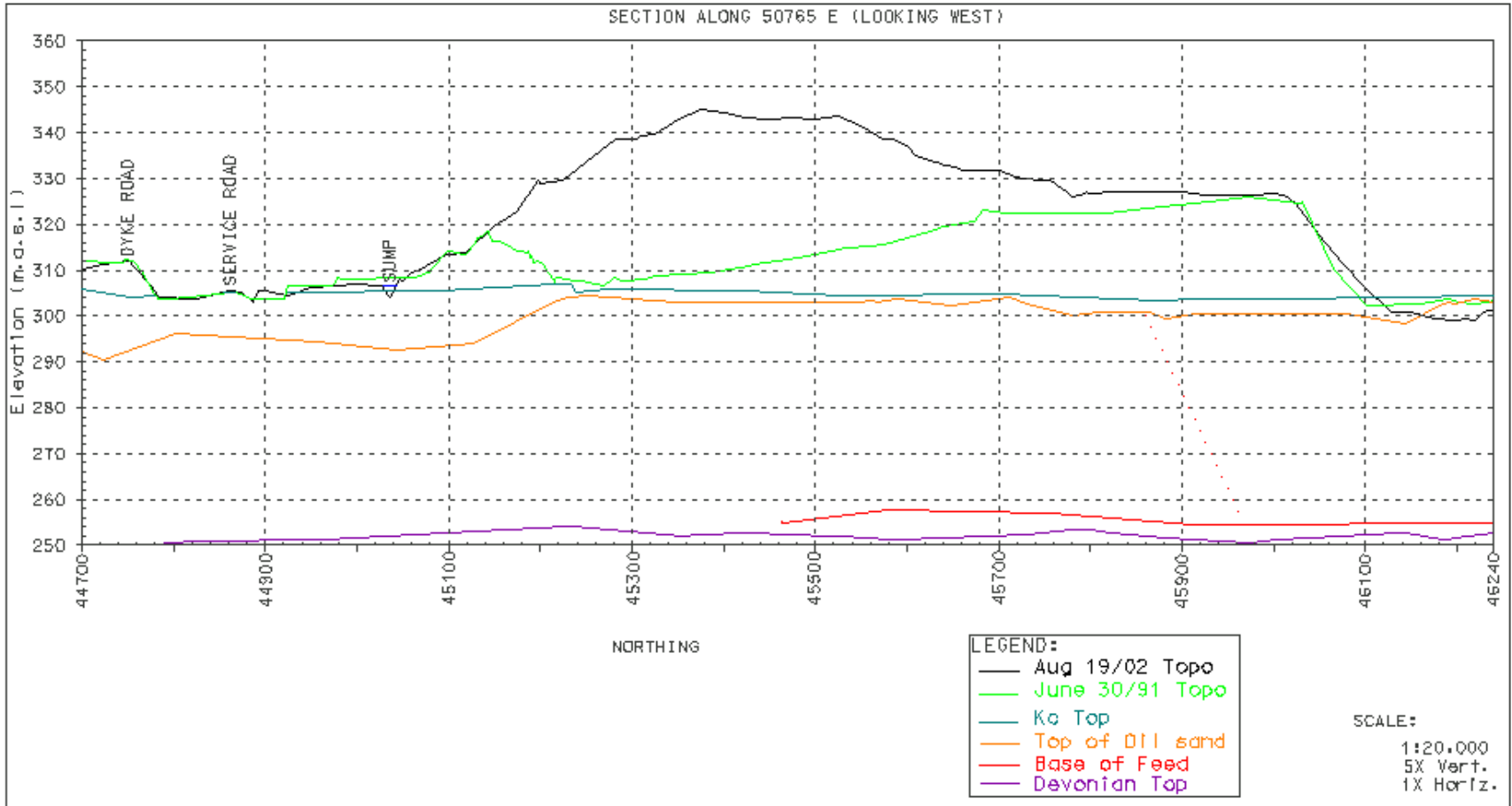


Figure B11 August 2002 topographic map showing section 50765 E looking west.

APPENDIX C

Raw Geochemistry Data

Table B.1
Major ion chemistry from South Bison Hill piezometers in 2002

Standpipe ID	Northing	Easting	Midpt Screen (masl)	Date	pH	Cond ($\mu\text{S}/\text{cm}$)	(Concentration in mg/L)						
							Na	K	Mg	Ca	Cl	SO ₄	HCO ₃
SP011730-02	45153.5	50236.1	339	9-Aug-02	7.1	7380	1870.0	15.0	75.1	231.0	270.0	3510.0	1230.0
SP011730-04	45154.1	50240.6	314	11-Aug-02	6.9	2250	250.0	11.0	75.3	137.0	180.0	215.0	1110.0
SP011730-07	45383.2	50218.8	335	11-Aug-02	7.1	13400	3580.0	27.8	151.0	162.0	690.0	6700.0	1310.0
SP011730-08	45381.5	50219.7	325	11-Aug-02	7.5	8730	2330.0	19.3	57.6	87.0	365.0	4210.0	866.0
SP011730-08a	45375.5	50222.7	260	15-Aug-02	7.6	1468	458.0	30.2	21.6	62.7	170.0	420.0	761.0
SP011730-09	45035.4	50233.5	336	9-Aug-02	7.1	3120	368.0	5.9	94.7	150.0	360.0	160.0	1370.0
SP011730-10	45035.6	50234.8	332	9-Aug-02	7.0	1570	84.8	BDL*	78.6	210.0	53.0	26.0	1050.0
SP011730-11	45597.9	49875.8	310	13-Aug-02	7.2	10970	3980.0	35.9	163.0	138.0	250.0	8400.0	1310.0
SP011730-12	45596.6	49878.3	304	13-Aug-02	7.2	9207	3100.0	38.6	321.0	364.0	140.0	7500.0	1330.0
SP011730-14	45594.3	49881.6	259	16-Aug-02	7.0	2430	916.0	11.9	32.8	71.0	350.0	530.0	1620.0
SP011730-15	45602.9	50195.9	314	12-Aug-02	7.4	4320	1580.0	12.1	42.8	80.4	505.0	850.0	2970.0
SP011730-16	45596.8	50199.8	259	14-Aug-02	7.2	2582	980.0	12.2	44.5	105.0	220.0	515.0	2100.0
SP011730-19	45269.7	49893.4	288	16-Aug-02	6.9	2730	651.0	36.5	140.0	341.0	74.0	2180.0	487.0
SP011730-20	45284.2	49890.1	323	19-Aug-02	7.4	11600	2910.0	20.0	57.7	82.6	1980.0	2850.0	1960.0
SP990145	45281.4	49890.8	317	19-Aug-02	7.3	11810	3220.0	34.5	127.0	197.0	590.0	6200.0	917.0
SP990124	45649.6	50756.2	311	20-Aug-02	7.4	2991	929.0	14.1	120.0	245.0	60.0	1870.0	1300.0
SP990125	45654.6	50756.1	322	20-Aug-02	7.0	2790	818.0	17.0	138.0	288.0	18.0	1890.0	1160.0
SP990126	45652.1	50756.7	316	20-Aug-02	7.3	748	951.0	17.1	68.6	169.0	34.0	1150.0	1920.0
SP990127	45153.5	50236.1	339	9-Aug-02	7.1	7380	1870.0	15.0	75.1	231.0	270.0	3510.0	1230.0
SP990128	45154.1	50240.6	314	11-Aug-02	6.9	2250	250.0	11.0	75.3	137.0	180.0	215.0	1110.0

*BDL – Below detection limit

Table B.2
Major ion chemistry from South Bison Hill piezometers in 2003

Standpipe ID	Northing	Easting	Midpt Screen (masl)	Date	pH	Cond ($\mu\text{S}/\text{cm}$)	Concentration in (mg/L)							
							Na	K	Mg	Ca	Cl	SO ₄	HCO ₃	Ion Balance
SP011730-02	45153.5	50236.1	339	8-May-03	7.1	6850.0	1580.0	13.5	78.8	105.0	380.0	2990.0	597.0	1.0
SP011730-04	45154.1	50240.6	314	8-May-03	7.0	2220.0	294.0	11.3	74.1	104.0	170.0	223.0	926.0	1.0
SP011730-07	45383.2	50218.8	335	6-Jul-03	7.0	10070.0	2350.0	37.0	186.0	117.0	13.0	4800.0	1060.0	1.1
SP011730-08a	45375.5	50222.7	260	8-May-03	7.2	2450.0	481.0	11.8	44.6	103.0	100.0	1010.0	425.0	1.0
SP011730-09	45035.4	50233.5	336	3-Jun-03	7.2	3060.0	373.0	0.1	89.3	178.0	340.0	136.0	1090.0	0.9
SP011730-10	45035.6	50234.8	332	6-Jul-03	7.2	1770.0	86.6	0.1	80.9	217.0	220.0	94.5	867.0	1.0
SP011730-12	45035.4	50241.8	278	8-May-03	7.4	136.0	205.0	15.8	34.7	83.0	45.0	561.0	227.0	1.0
SP011730-14	45597.9	49875.8	310	26-Aug-03	7.7	15100.0	4250.0	30.4	145.0	324.0	200.0	9230.0	1020.0	1.0
SP011730-15	45596.6	49878.3	304	3-Jun-03	7.0	12240.0	2990.0	31.4	286.0	98.0	140.0	7600.0	769.0	0.9
SP011730-16	45594.3	49881.6	259	3-Jun-03	7.4	4450.0	1200.0	11.9	37.5	59.2	380.0	676.0	1730.0	1.1
SP011730-19	45602.9	50195.9	314	19-Jun-03	7.4	6020.0	1560.0	9.2	32.8	57.6	440.0	621.0	3030.0	1.0
SP011730-20	45596.8	50199.8	259	8-May-03	7.2	3960.0	972.0	7.6	41.0	92.0	230.0	500.0	2010.0	1.0
SP990145	45269.7	49893.4	288	8-May-03	7.2	8660.0	1900.0	37.5	173.0	280.0	450.0	4260.0	988.0	1.0
SP990124	45284.2	49890.1	323	4-Jun-03	7.6	11440.0	2950.0	16.9	50.9	65.3	1800.0	2830.0	2000.0	1.0
SP990125	45281.4	49890.8	317	19-Jun-03	7.4	6210.0	1430.0	10.6	48.7	110.0	280.0	2460.0	704.0	1.0
SP990126	45649.6	50756.2	311	7-Jul-03	7.0	5280.0	999.0	14.2	142.0	118.0	53.0	1880.0	1680.0	0.9
SP990127	45654.6	50756.1	322	4-Jun-03	7.1	4150.0	846.0	14.0	118.0	98.7	25.0	1810.0	1150.0	0.9
SP990128	45652.1	50756.7	316	5-Jul-03	7.1	5100.0	1180.0	23.3	82.8	117.0	44.0	1260.0	2090.0	1.0

Table B.3
Major ion chemistry from Syncrude Lease Formations (Reszat, 2002)

		pH	Temp	(ppm)							
				Na	K	Ca	Mg	Cl	Alk.	SO4	
Cretaceous McMurray	BML97-08	7.04	11.6	3690	32.3	12	63.7	3190	3330	269	
	BML97-09	6.98	12.4	10500	58.2	45	201	10900	2630	0	
(Kca/Kcb) OW92-04	05/20/92	6.83		25	1.1	26	5.5	10	142	14	
	05/25/93	7.73		142	4.4	109	17.4	51	582	94	
	09/20/93	6.38		70	3.1	121	18.1	14	534	110	
	05/25/94	6.67		63	2.9	157	21.1	8	510	163	
	06/05/97	6.84		62	3.4	145	20.6	6	527	152	
	06/26/96	6.99		67	1.5	130	15.4	7	397	158	
	07/10/97	7.18		53	1.5	135	15.3	5	464	103	
(Kca/Kcb) OW96-06	06/13/96	7.64		189	2.1	8	1.9	3	514	9	
	07/02/97	8.55		206	2.3	2	1.1	0	542	1	
(Kcc) OW92-06		7.59		2324	18.5	53	29.6	2800	1277	4	
		7.61		1949	14.6	34	24.3	2629	1236	0	
		7.57		1030	9	25	15.8	2	1202	1468	
		7.32		1244	10.3	26	15.6	1324	1194	0	
		7.45		2235	13.4	36	25.4	2727	1269	1	
		7.76		1960	16.9	42	30.6	2450	1210	0	
		7.74		2284	15	41	29.5	2742	1285	0	
		7.39	13.3	2062	11.7	39	26	2765	1297	0	
		7.15	6.5	2140	12.1	40	27.3	2894	1266	0	
		7.77	7.4	2258	12.3	33	24.1	3030	1283	4	
		7.77	7.4	2059	12.7	38	25.8	2715	1271	7	
		7.46	7.6	2390	12.9	25	26	2720	1260	0	
(Kcc) OW92-05	05/20/92	7.63		297	10.3	64	30.1	104	732	144	
	05/25/93	7.39		249	5.1	55	31.8	88	702	122	
	09/20/93	7.3		241	4.7	95	31.8	79	699	125	
	05/25/94	7.2		320	6.1	51	27.9	146	747	140	
	06/05/97	6.89		359	61	34	20	153	773	138	
	06/26/96	7.35		376	6.4	27	17.7	149	750	130	
	06/12/97	7.4		340	6	41	24.5	131	758	134	
	06/08/98	7.46		325	5.5	32	19.5	110	763	135	
	06/01/99	7.98		509	6.8	36	19.5	340	876	154	
	06/15/00	7.83		623	7.7	40	22.4	514	966	163	
	07/09/01	7.34		880	8	27	26.1	595	975	150	
(Kcc/Kcd) OW92-08	05/20/92	7.31		182	4.4	55	25.6	23	602	103	
	05/25/93	7.14		170	2.8	87	42.5	14	799	100	
	09/20/93	6.98		172	3.8	109	51.8	107	908	9	
	05/25/94	6.93		176	4.1	168	81	9	1181	137	
	06/05/97	7.57		1558	8.9	19	14.4	30	1556	1941	
	06/27/96	6.88		162	3.1	228	105	15	1140	314	
	06/17/97	7.41		185	3.2	289	133.2	94	1254	424	
	06/08/98	6.92		248	2.4	182	76.6	77	1137	277	
	06/01/99	6.55		246	2.8	208	89.6	60	1198	307	
	05/25/00	7.31		480	4	162	10.6	52	1252	616	
	07/12/01	7.27		541	3.7	97	87.8	75	1280	568	

Table B.4

Major ion chemistry anerobic solids chemistry from South Bison Hill neutron access tube installation (Wall, 2004)

	Average depth (m)	mass soil	wet mass	mass H2O added	Na mg/L	NH4 mg/L	K mg/L	Mg mg/L	Ca mg/L	Cl mg/L	NO3 mg/L	SO4 mg/L	TDS mg/L
SB13C	0.6	102.0	153.7	51.7	164.1	13.1	28.7	58.3	282.3	45.0	22.4	305.3	919.2
SB14C	1.0	101.4	150.3	48.9	316.3	n.a.	24.3	90.4	447.9	25.8	n.a.	1,016.7	1,921.3
SB16C	1.4	101.1	193.3	92.2	2,399.6	28.6	75.1	301.2	470.8	83.3	n.a.	4,989.1	8,347.7
SB17C	2.5	100.3	193.2	92.9	1,978.2	n.a.	56.7	43.4	121.6	102.2	43.1	2,427.4	4,772.6
SB18C	2.9	100.3	214.9	114.6	1,230.4	n.a.	42.5	8.9	24.5	102.0	49.2	980.0	2,437.5
SB19C	4.2	100.6	250.3	149.7	890.9	n.a.	40.4	6.7	38.1	83.3	29.1	418.7	1,507.3
SB20C	4.8	101.0	232.2	131.3	969.3	n.a.	37.4	5.1	14.9	61.9	n.a.	347.1	1,435.7
SB24C	7.9	100.5	231.3	130.9	808.4	15.7	32.5	6.5	19.8	67.6	n.a.	264.1	1,214.5
SB25C	9.2	101.6	235.4	133.8	969.2	18.3	42.0	n.a.	4.1	58.0	14.4	629.8	1,735.7
SB26C	11.2	101.7	273.0	171.3	898.0	n.a.	26.8	5.4	14.7	64.0	n.a.	538.9	1,547.8
SB35C	12.0	101.4		142.5	701.2	n.a.	22.2	12.9	29.0	63.2	n.a.	148.1	976.6
SB34C	14.7	102.1	242.8	140.7	857.4	n.a.	65.1	12.6	33.4	123.2	85.7	366.0	1,543.5
SB32C	15.2	100.5	234.0	133.5	1,110.6	n.a.	25.8	12.7	44.0	68.2	n.a.	1,074.9	2,336.2
SB33C	16.8	100.9	246.1	145.3	646.5	n.a.	16.4	3.3	10.1	73.4	n.a.	79.4	829.2
SB31C	19.2	101.9	254.6	152.6	2,123.8	54.3	73.5	104.2	181.5	53.2	n.a.	3,437.9	6,028.3
SB30C	20.6	101.0	210.7	109.7	1,393.9	28.5	44.7	22.8	70.0	32.4	n.a.	1,734.3	3,326.7
SB28C	21.3	101.0	229.6	128.6	1,001.6	30.9	37.7	9.5	33.5	56.6	90.6	793.8	2,054.1
SB29C	21.9	100.9	222.7	121.8	1,193.2	n.a.	39.0	17.3	38.3	50.9	n.a.	1,202.8	2,541.5
SB27C	24.4	100.2	222.1	122.0	865.9	n.a.	58.8	11.4	30.1	55.3	32.0	349.3	1,402.8

Table B.5
Major ion chemistry oxidized solids chemistry from South Bison Hill neutron access tube installation (Wall, 2004)

Sample	Average depth (m)	Ca mg/L	Mg mg/L	Na mg/L	K mg/L	SO4 mg/L	Cl mg/L	N03 mg/L	TDS mg/L
1	1.7	677.8	328.19	1901.58	48.47	6408.16	186.18	42.13	9592.55
3	4.8	117.8	45.52	2522.65	88.10	5239.82	133.15	<10ppb	8147.05
5	9.4	47.0	33.06	1954.50	56.97	4354.83	128.10	<10ppb	6574.40
6	10.9	336.0	101.05	2034.55	51.27	3982.94	97.54	<10ppb	6603.35
7	12.4	359.5	264.92	2240.27	54.05	4589.50	1046.75	<10ppb	8554.97
8	13.9	12.7	17.14	1666.00	35.24	2888.33	173.04	<10ppb	4792.48
9	15.5	207.7	158.77	3562.42	103.38	8147.02	267.33	<10ppb	12446.62
10	17.0	461.7	214.14	1625.21	71.27	4910.43	73.26	4.88	7360.90
11	18.3	207.4	128.69	2834.91	83.53	6527.71	132.12	<10ppb	9914.38
12	19.8	129.8	87.07	2673.50	87.95	5416.97	109.43	<10ppb	8504.71
13	21.3	395.4	217.31	2823.18	98.13	7758.79	91.80	<10ppb	11384.56
14	22.8	103.1	66.24	2716.49	73.71	5532.28	180.64	<10ppb	8672.41
15	24.3	21.9	14.90	1484.05	24.74	2676.63	43.25	<10ppb	4265.48

APPENDIX D

Hydraulic Conductivity Plots using Hvorslev Analysis

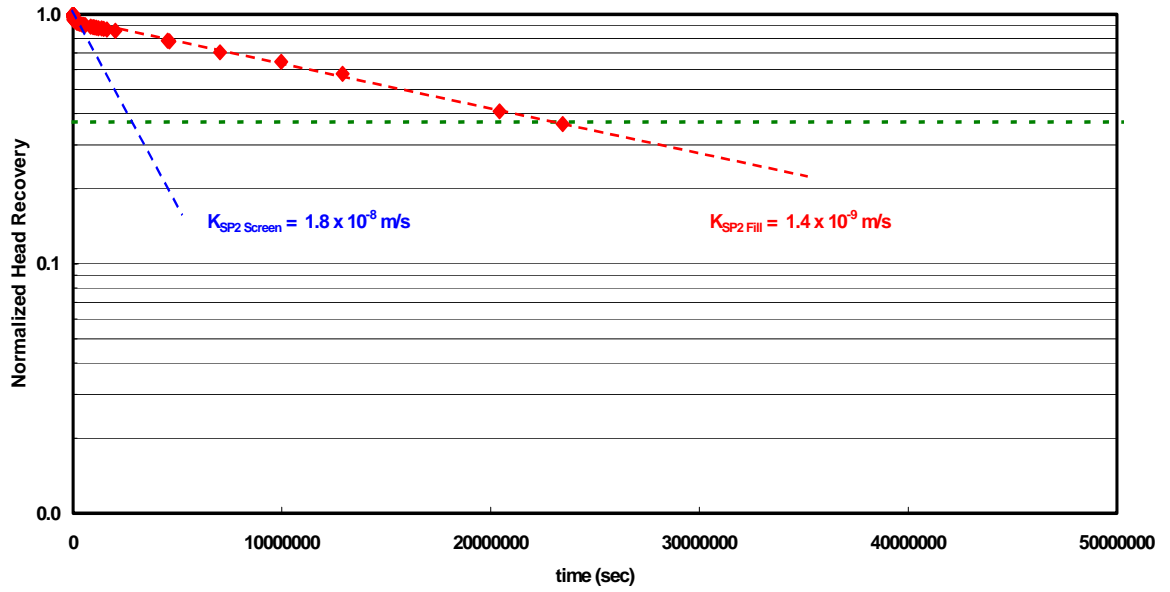


Figure D1 Permeability test for SP999902 in 2002 (Location D)

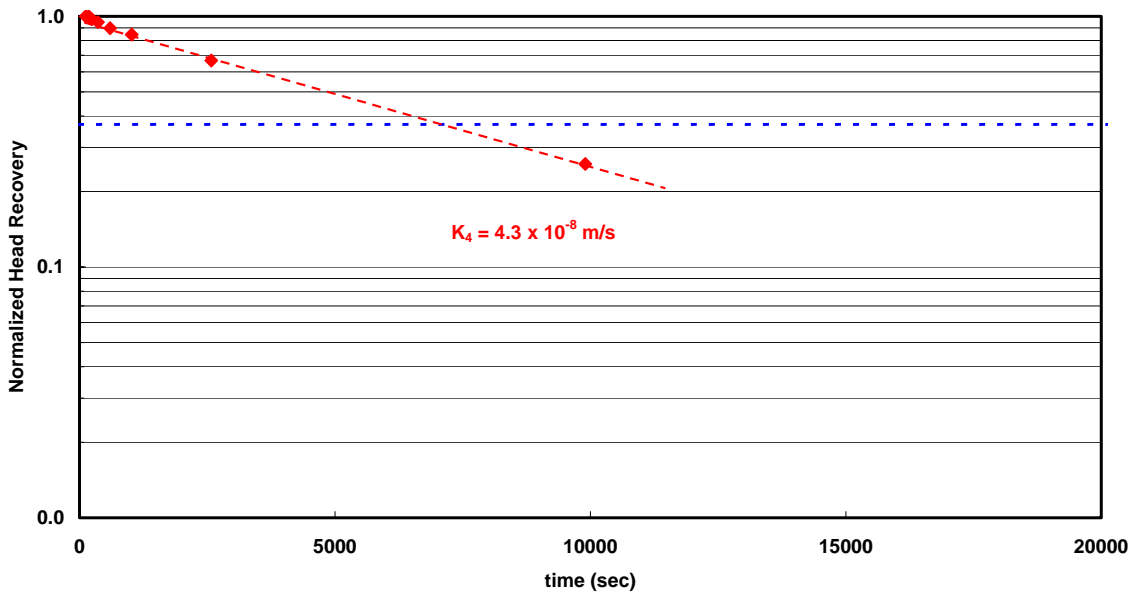


Figure D2 Permeability test for SP999904 in 2002 (Location D)

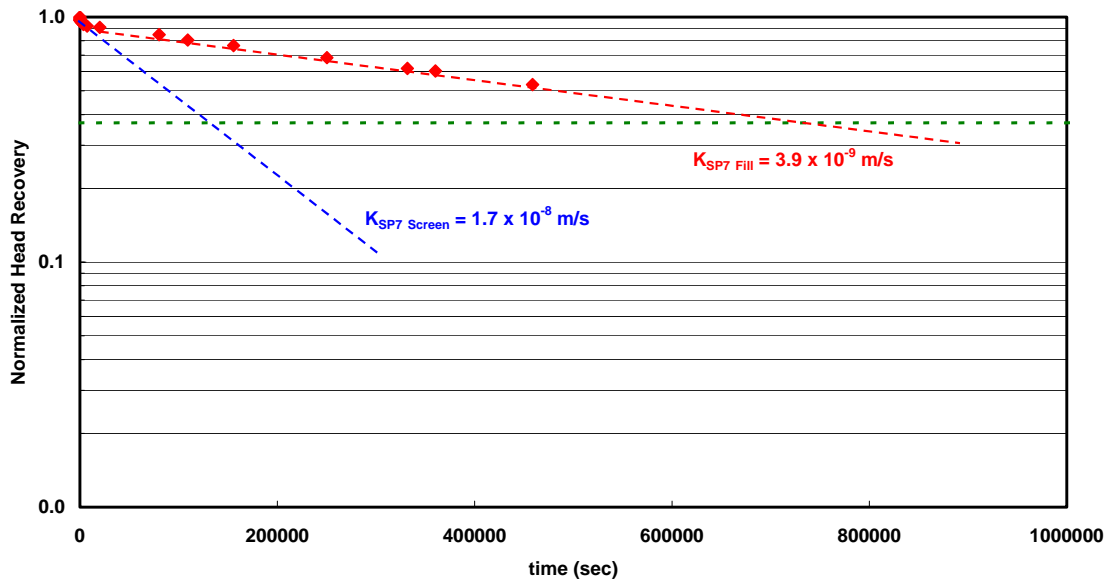


Figure D3 Permeability test for SP999904 in 2003 (Location D)

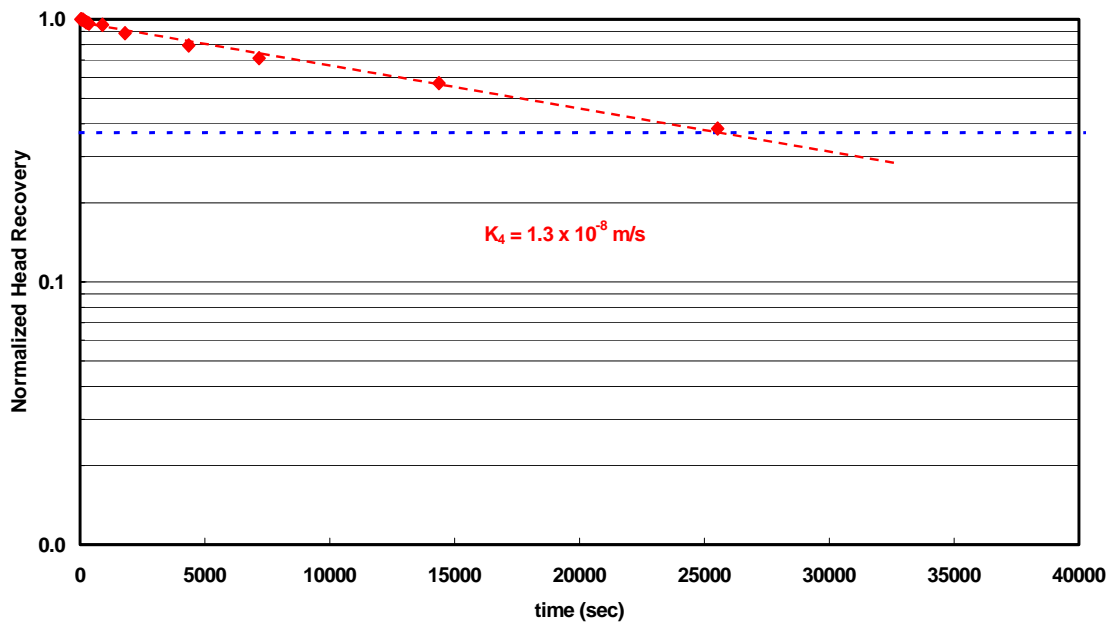


Figure D4 Permeability test for SP999907 in 2002 (Location E)

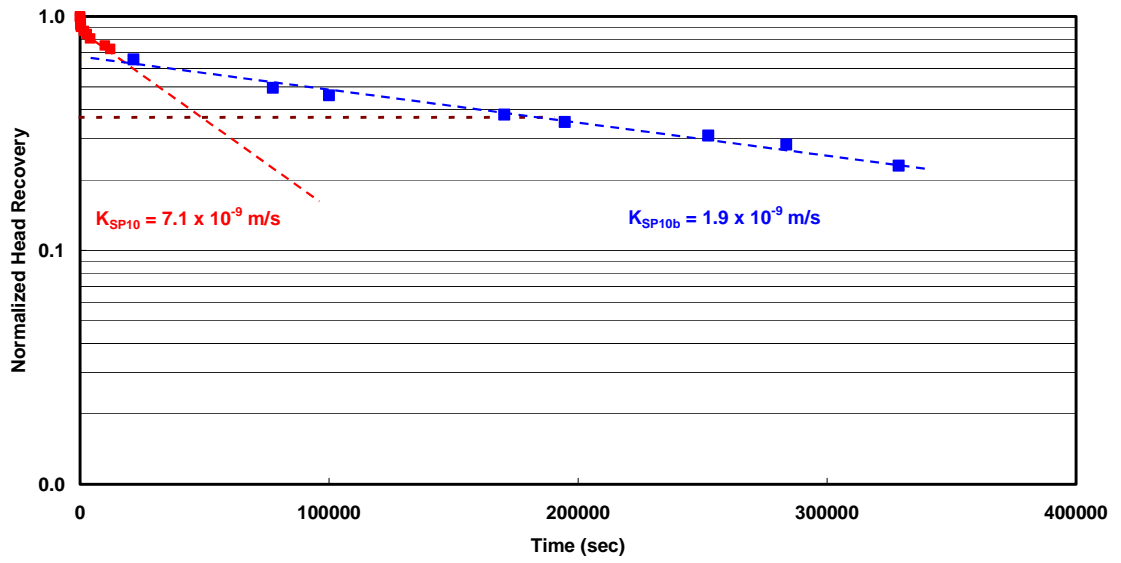


Figure D5 Permeability test for SP011730-10 in 2002 (Location C)

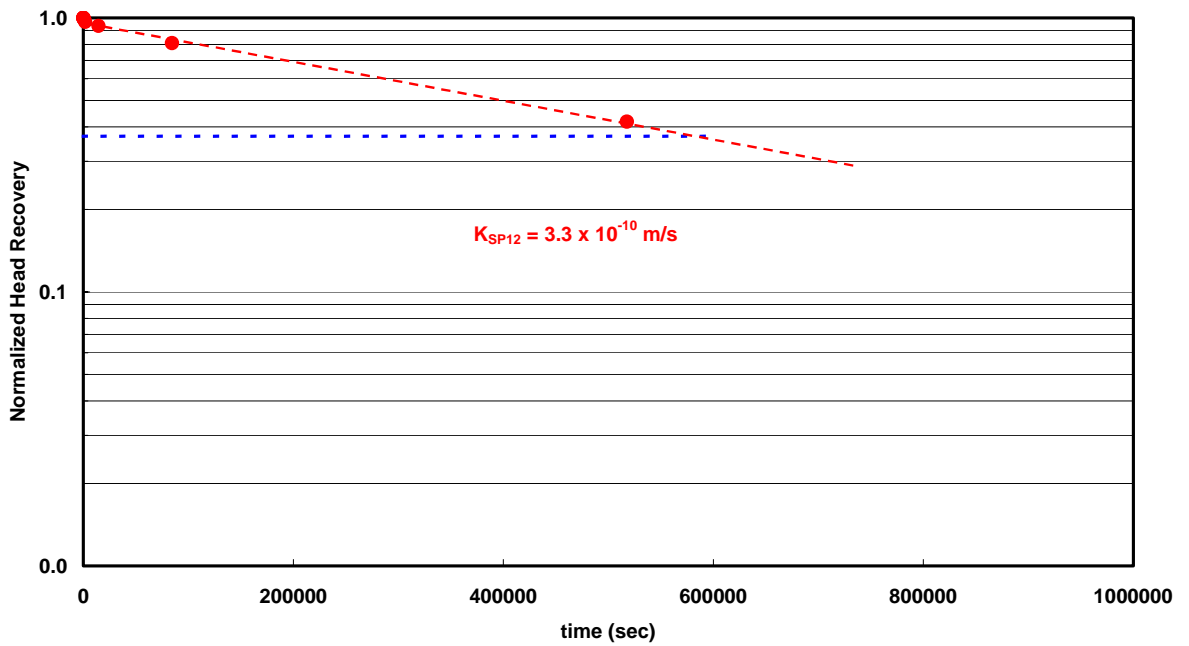


Figure D6 Permeability test for SP011730-12 in 2003 (Location C)

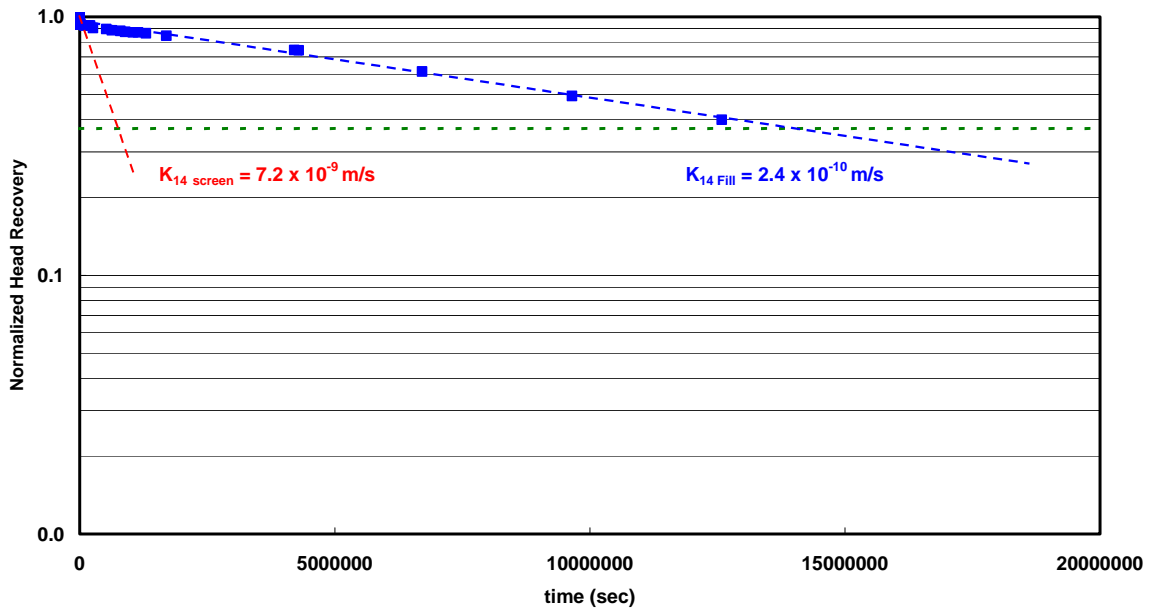


Figure D7 Permeability test for SP11730-14 in 2002 (Location G)

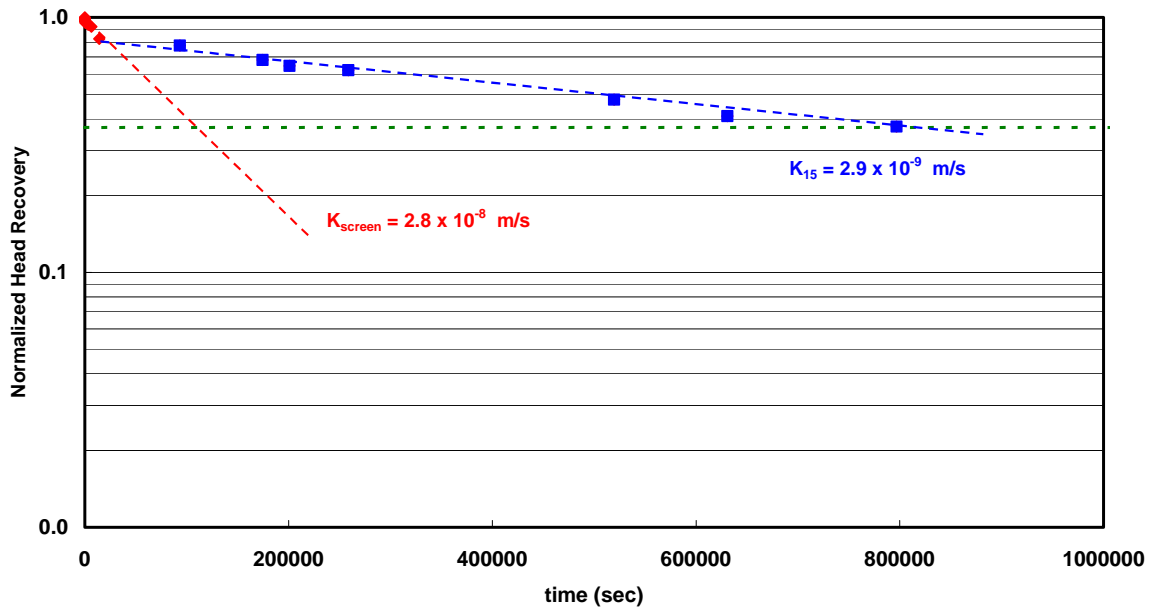


Figure D8 Permeability test for SP11730-15 in 2002 (Location G)

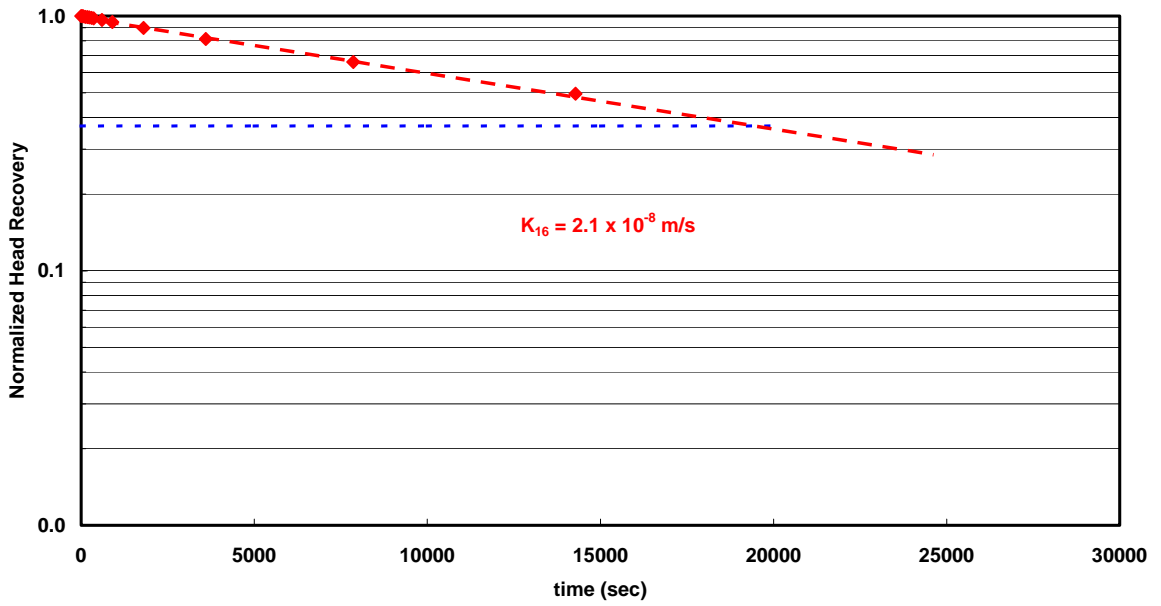


Figure D9 Permeability test for SP011730-16 in 2002 (Location G)

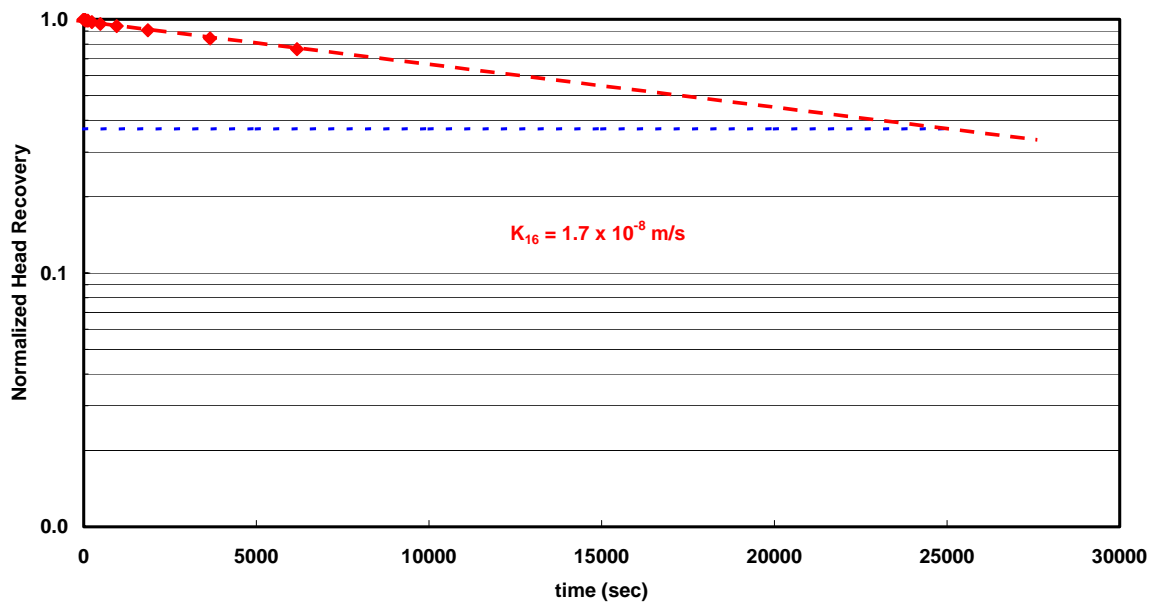


Figure D10 Permeability test for SP011730-16 in 2003 (Location G)

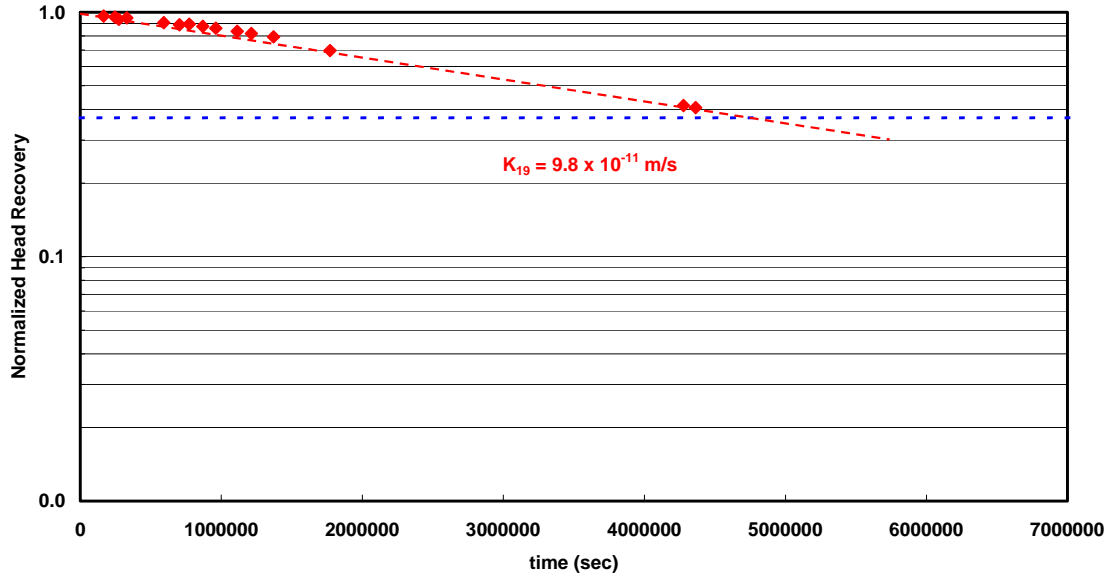


Figure D11 Permeability test for SP9999019 in 2003 (Location F)

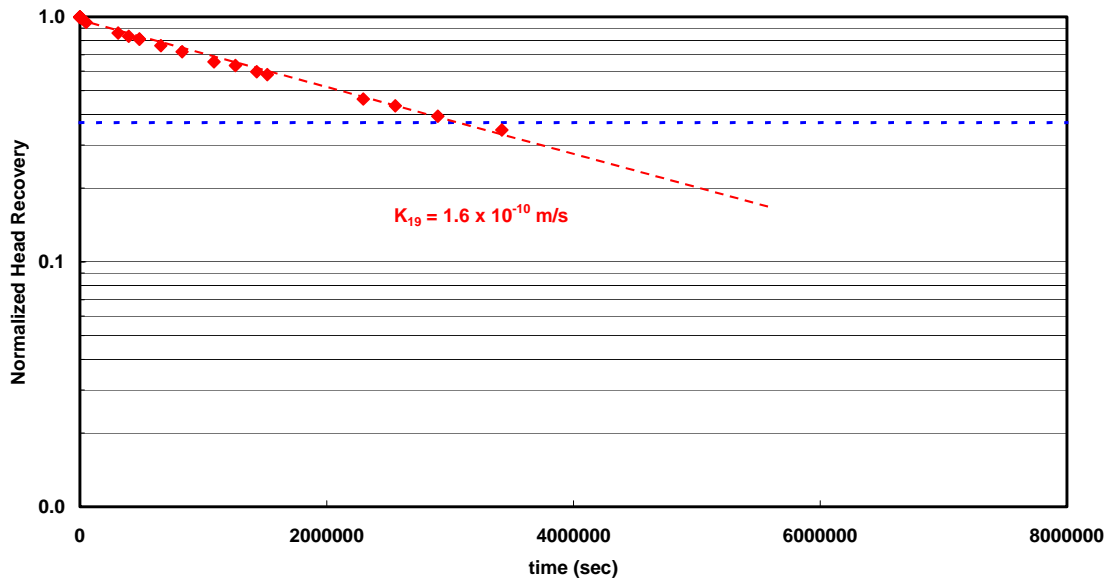


Figure D12 Permeability test for SP9999019 in 2003 (Location F)

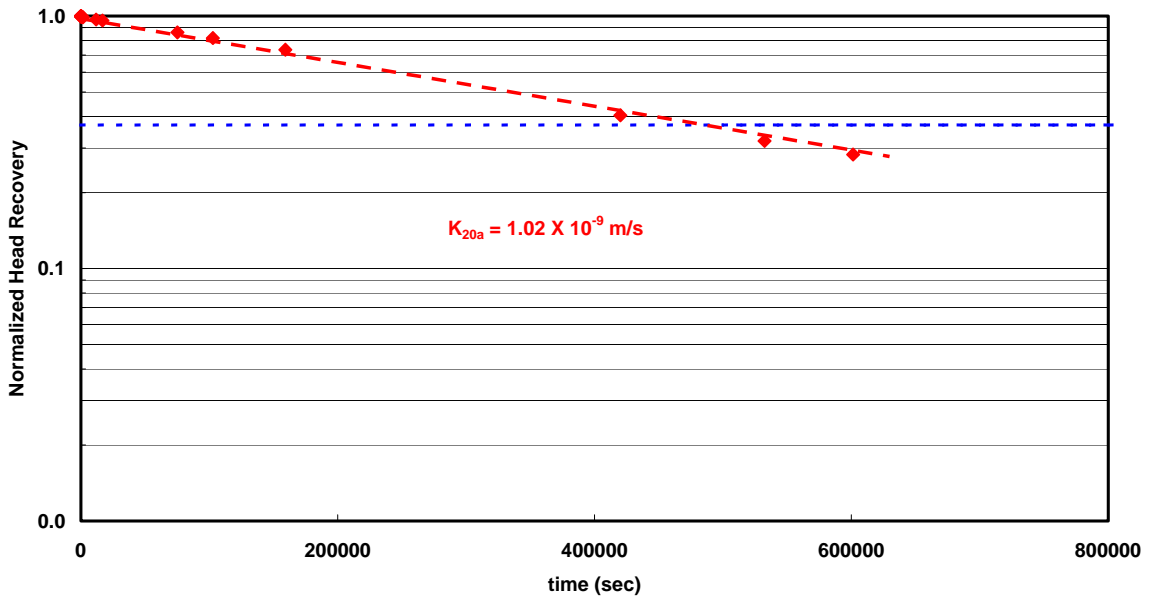


Figure D13 Permeability test for SP011730-20 in 2002 (Location F)

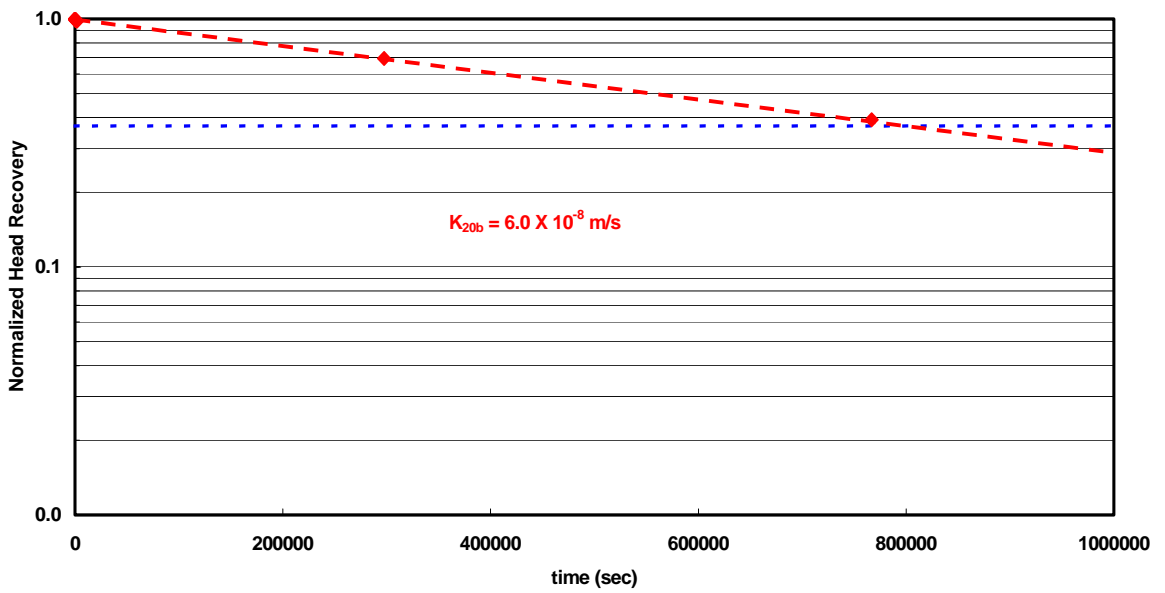


Figure D14 Permeability test for SP011730-20 in 2003 (Location F)

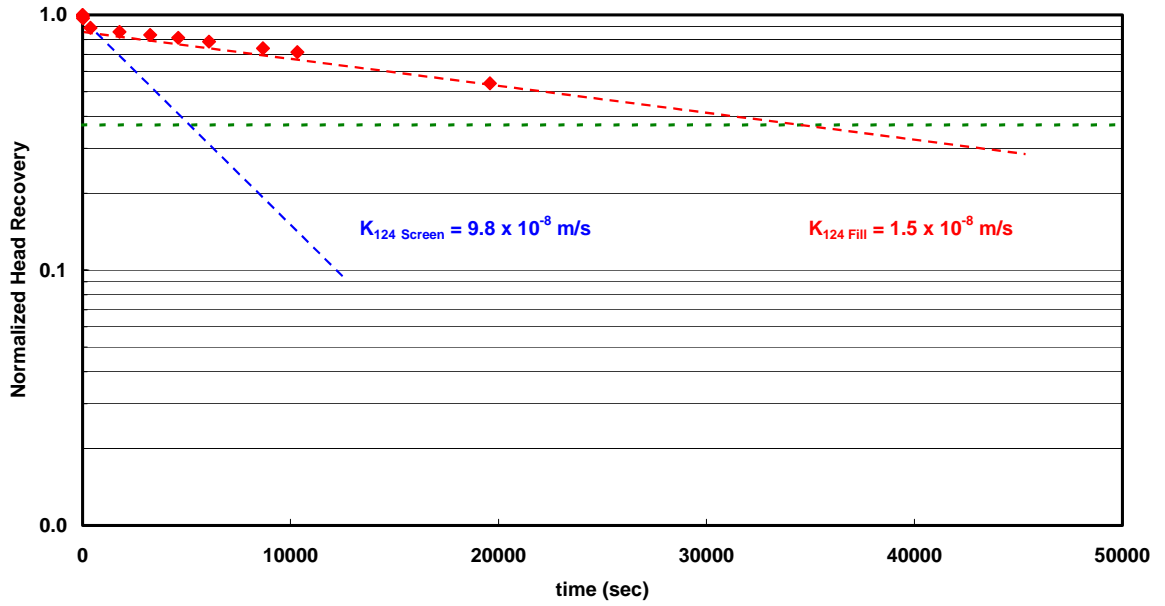


Figure D15 Permeability test for SP9999124 in 2002 (Location B)

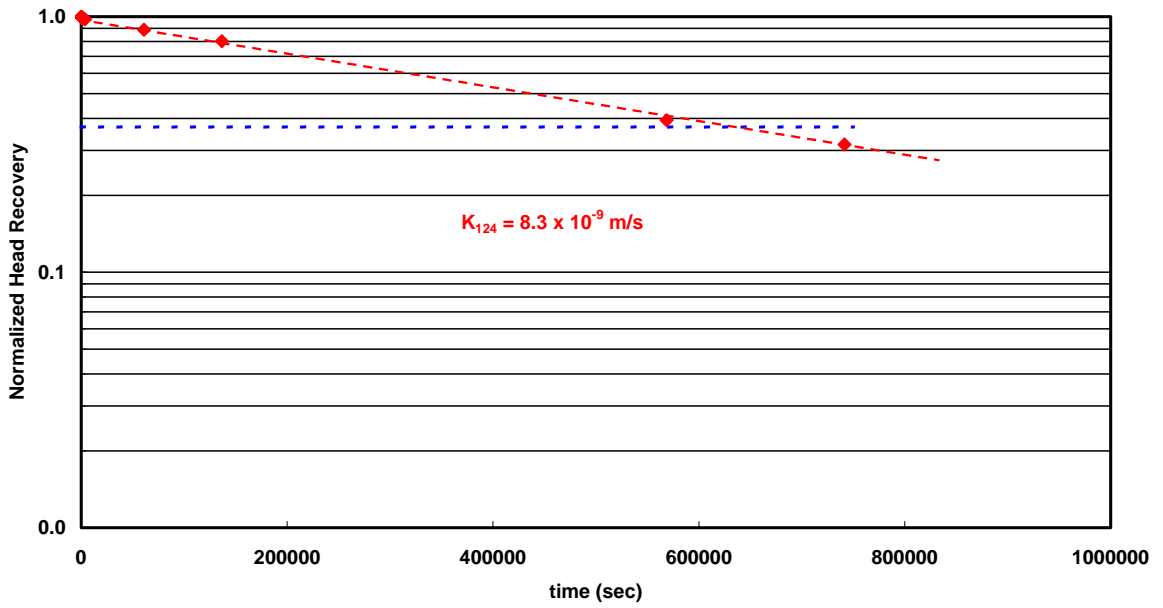


Figure D16 Permeability test for SP9999124 in 2003 (Location B)

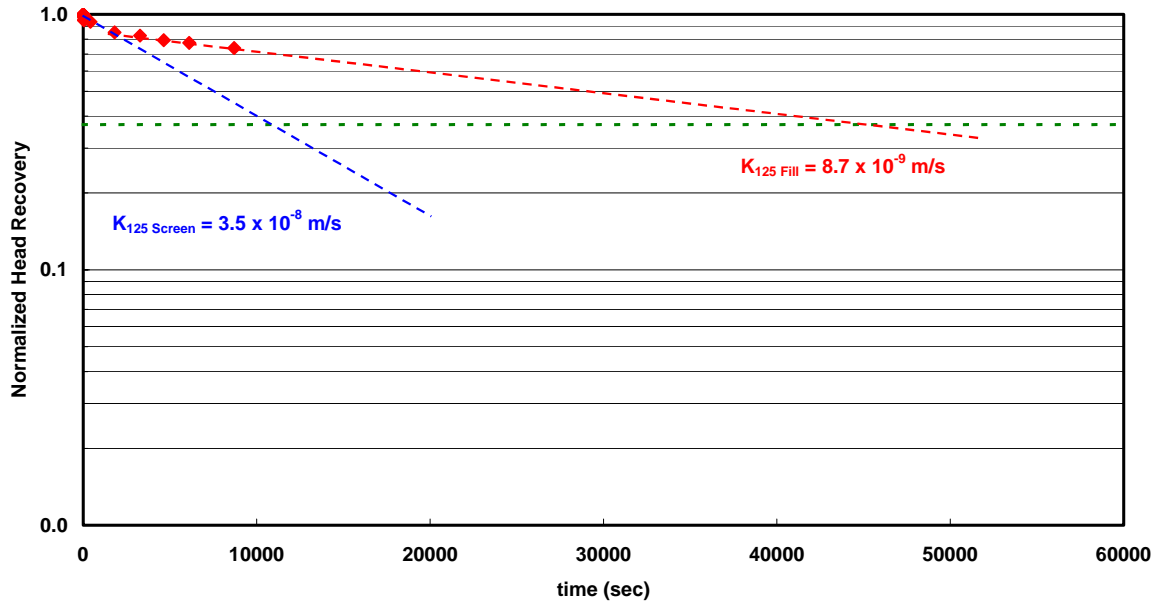


Figure D17 Permeability test for SP9999125 in 2002 (Location B)

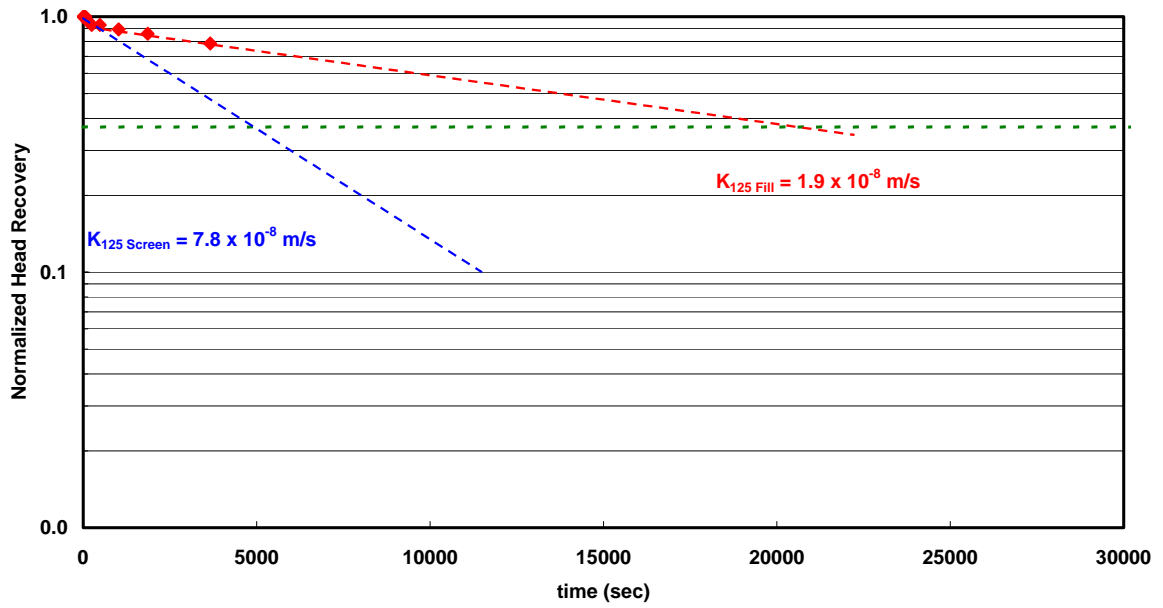


Figure D18 Permeability test for SP9999125 in 2003 (Location B)

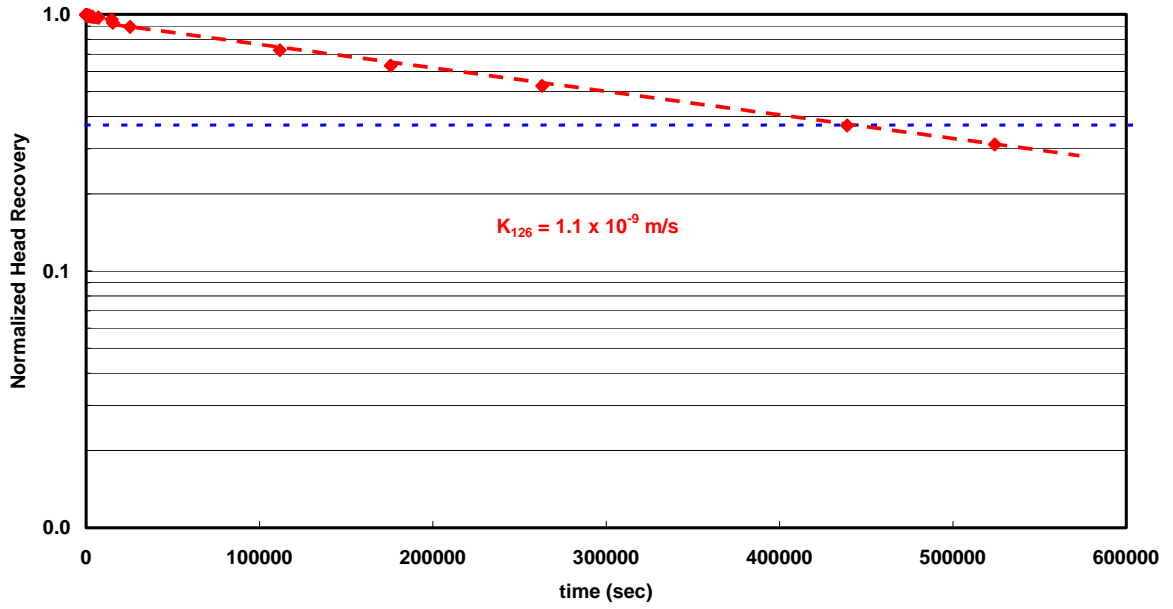


Figure D19 Permeability test for SP99990126 in 2002 (Location A)

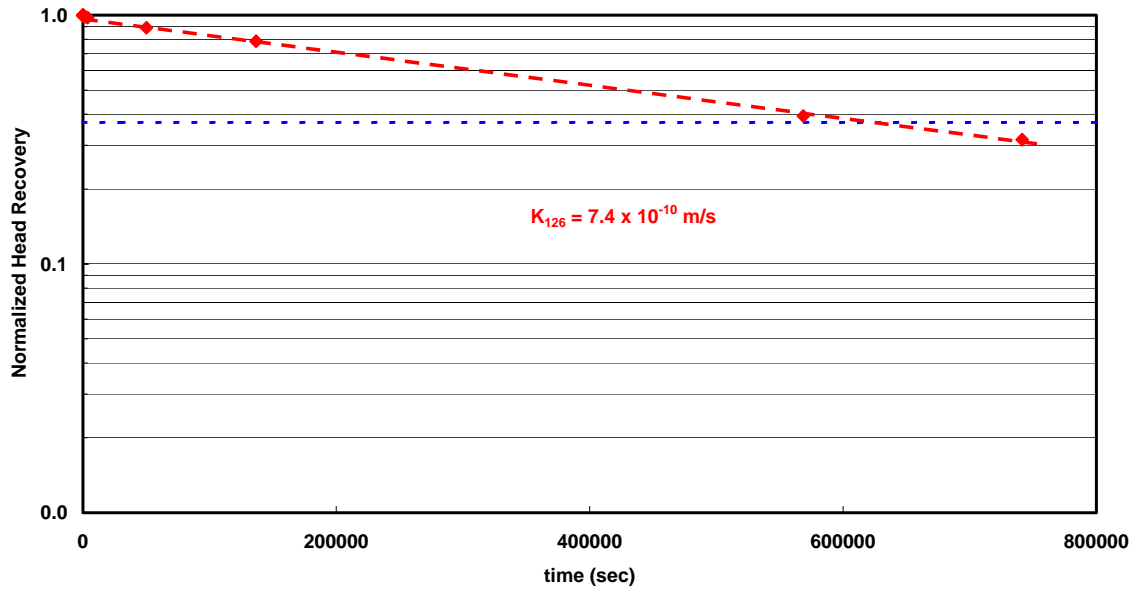


Figure D20 Permeability test for SP99990126 in 2003 (Location A)

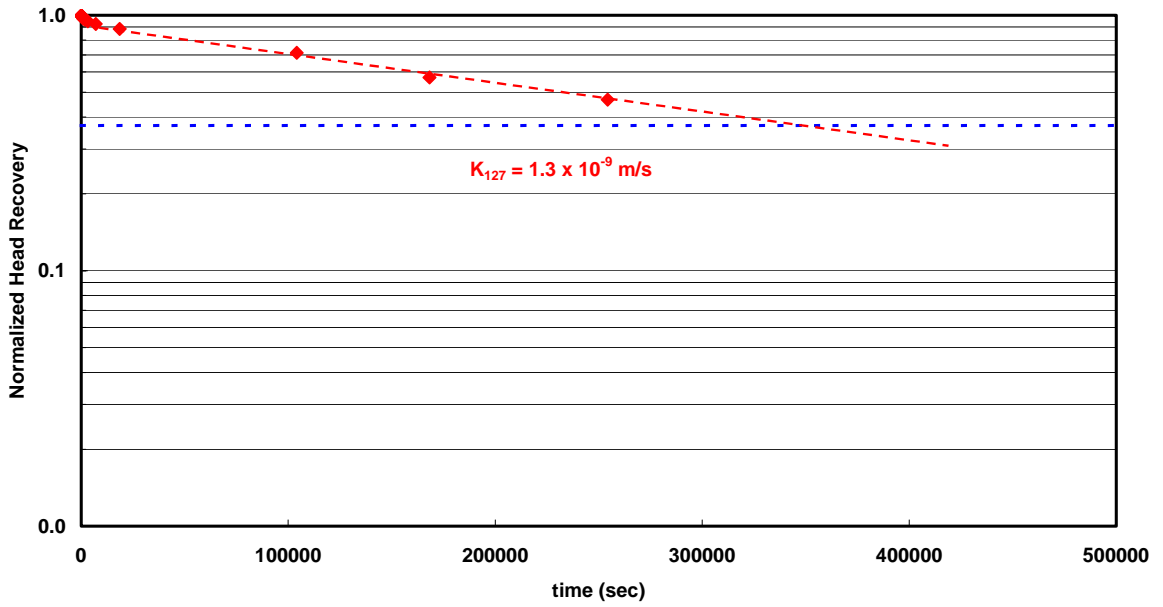


Figure D21 Permeability test for SP9999127 in 2002 (Location A)

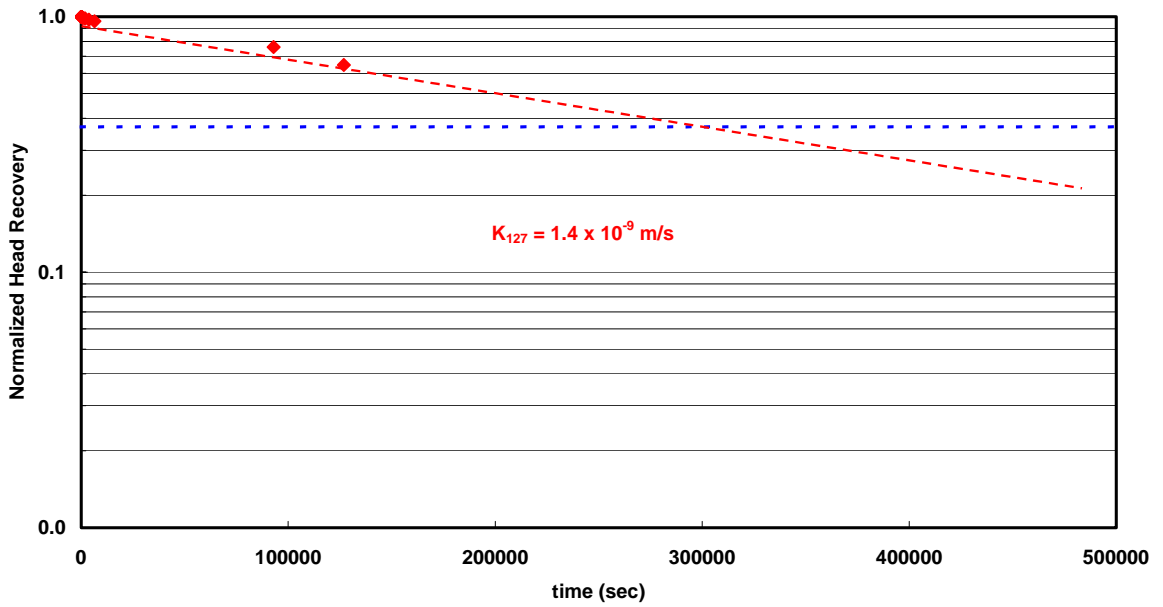


Figure D22 Permeability test for SP9999127 in 2003 (Location A)

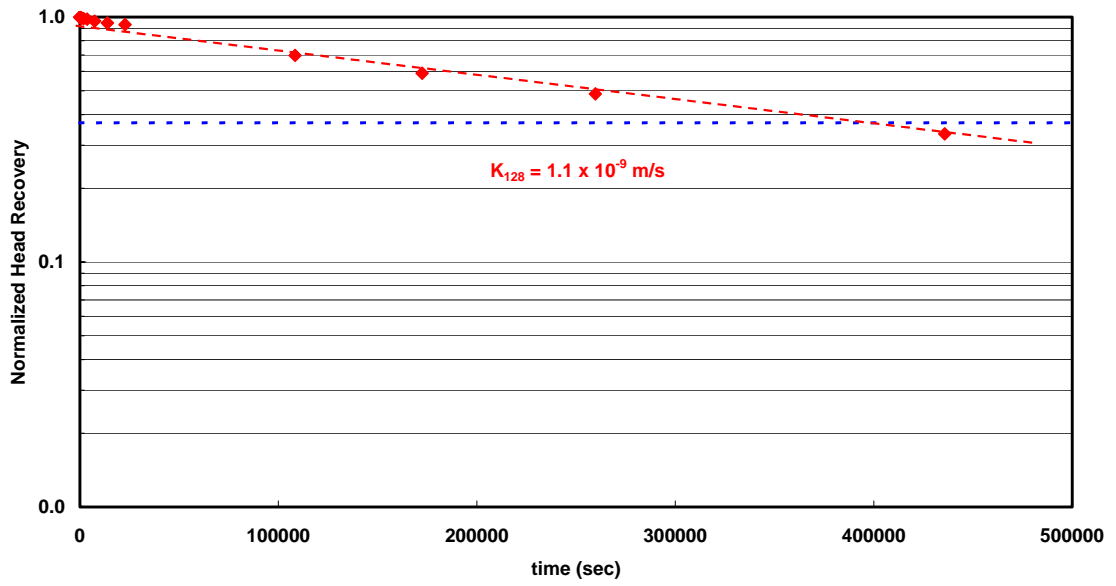


Figure D23 Permeability test for SP9999128 in 2002 (Location A)

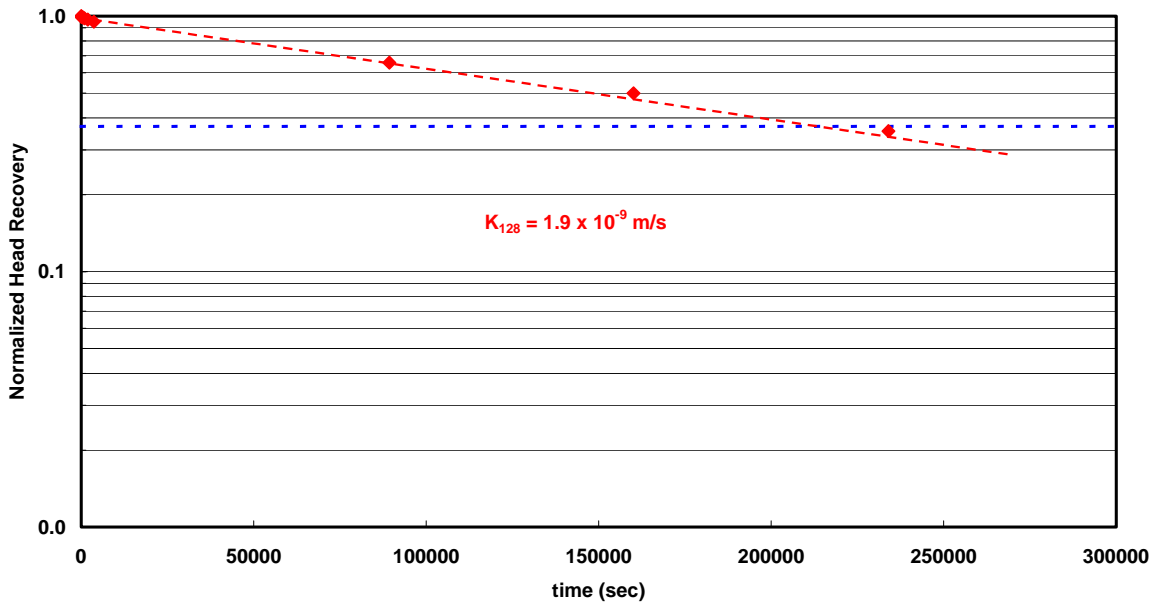


Figure D24 Permeability test for SP9999128 in 2003 (Location A)

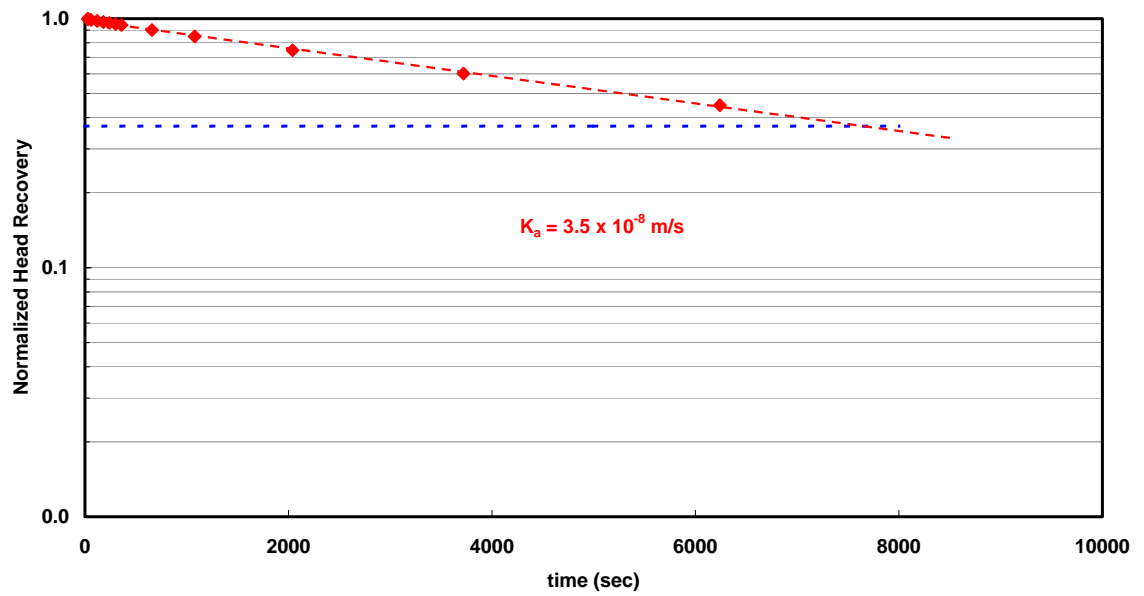


Figure D25 Permeability test for SP99990145 in 2002 (Location B)

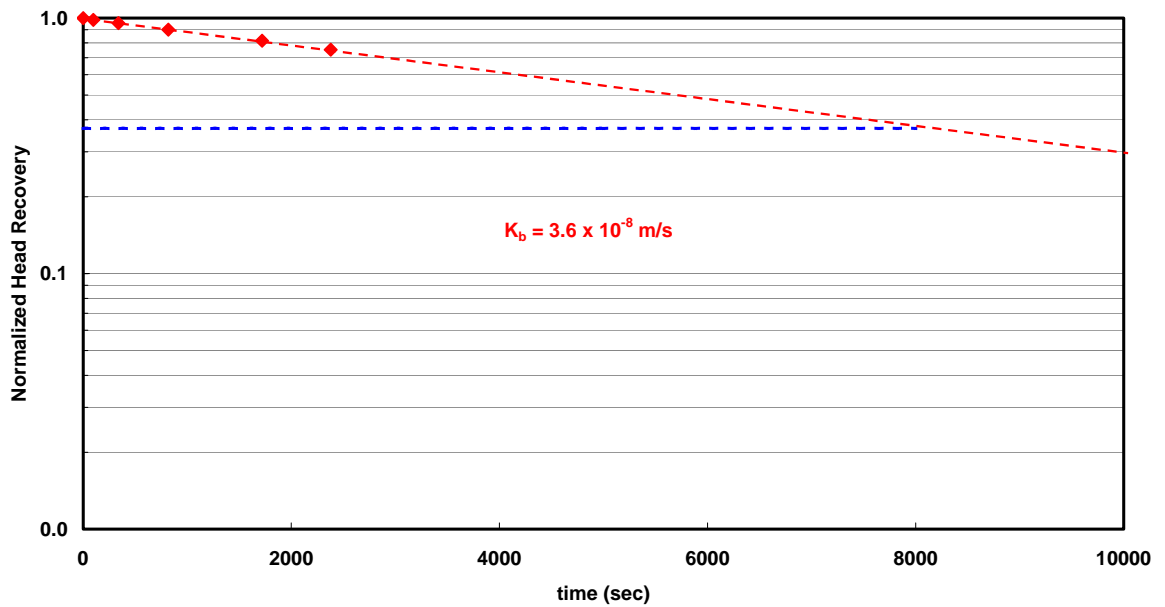


Figure D26 Permeability test for SP99990145 in 2003 (Location B)